Geo 511

Master thesis

Home range analyses and kill site detection of lions and leopards in the Kalahari, Botswana

Author:

André Zehnder
09-708-306

Supervisor and faculty member:

Prof. Dr. Robert Weibel

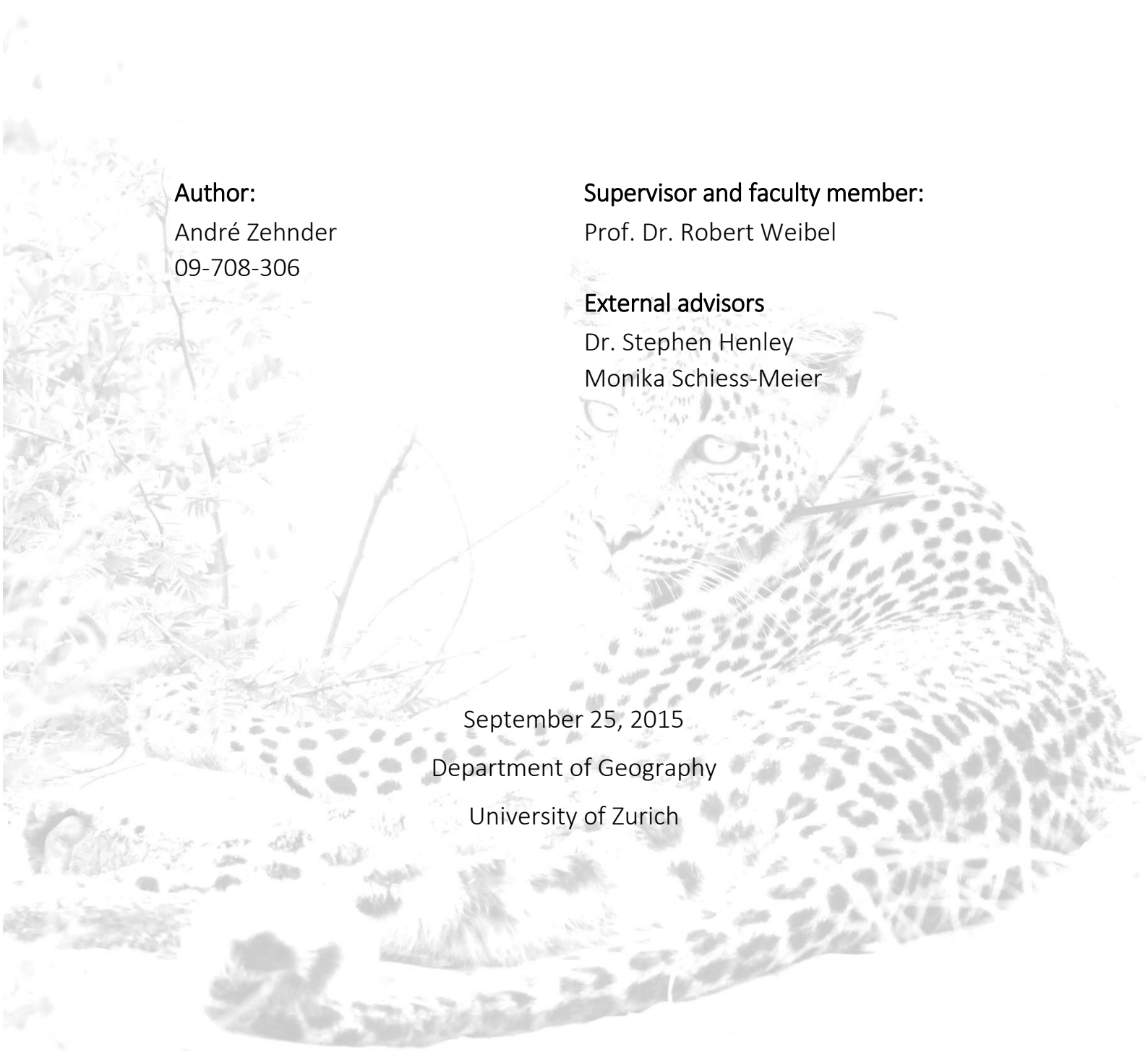**External advisors**

Dr. Stephen Henley
Monika Schiess-Meier

September 25, 2015

Department of Geography

University of Zurich

Contact

Prof Dr. Robert Weibel

University of Zurich

Department of Geography

Winterthurerstrasse 190

CH-8057 Zurich

Dr. Stephen Henley

Leopard Ecology & Conservation

Private Bag BR 7

Gaborone, Botswana

leopardecology@gmail.com

Monika Schiess-Meier

University of Zurich

Institute of Evolutionary Biology and Environmental Studies

Winterthurerstrasse 190

CH-8057 Zurich

monika.schiess@ieu.uzh.ch

André Zehnder

andre.zehnder@uzh.ch

Summary

Due to losses of habitat and reduced prey abundances for predators such as leopards and lions, conflicts between them and humans are widespread in Africa. As a consequence, predators feed on livestock of local farmers and thus risk to be shot. To enable effective management strategies that mitigate such conflicts, a comprehensive understanding of the spatial ecology of predators is critical. By analyzing home ranges and kill sites, this study addressed two major aspects of the ecology of leopards and lions in the Khutse and Central Kalahari Game Reserve, Botswana.

Regarding home ranges, four methods were selected to investigate the effect of their parameterization: MCP, KDE, t-LCH and BRB. First, the effect of the parameters was analyzed for each method. Then, systematic trends of the methods were analyzed. The most appropriate versions of each method were used to analyze the home ranges of the individual leopards and lions in an ecological context. An emphasis thereby was to examine the temporal variability of the results in terms of their area and shape. It was found that the k-rule of t-LCH performed markedly better than the a-rule. The inclusion of time scaling factors yielded more interconnected isopleths whose shape indicated moving pathways. For BRB, the ecological model used to set the smoothing parameter turned out to be critical and to cause problems in conjunction with heterogeneous sampling intervals. On average, MCP produced home ranges whose areas and shapes differed significantly from those of the other methods. The areas of KDE, t-LCH and BRB were similar whereas their shapes allowed for a better differentiation. The observed individuals have home ranges that are among the largest worldwide and mostly within the protected area. Particularly the home ranges of the lions varied markedly over time, emphasizing the need to consider different temporal aggregations. Despite their largely overlapping home ranges, the leopards rarely encountered and thus indicate a strong active avoidance behavior.

Regarding kill sites, the performance of a clustering approach was analyzed by using different variables to indicate the probability of a cluster to be an actual kill site through weights. The sets of variables that yielded the lowest errors were used to determine the spatial distribution of kill sites in terms of their proportion inside the core area, home range and game reserves. The combination of the cluster duration and ratio of distances moved before and after a cluster proved to yield the lowest errors, while the time of day had hardly any impact. The incorporation of additional variables consistently led to higher success rates regarding the detection of kill sites. Irrespectively of the criterion used to set the weight threshold, the ratios of kill sites within the core area and home range remained stable. Almost all detected kill sites were within the home range. Two lions that were shot because of livestock predation proved to have small proportions of kill sites outside the game reserves. However, these ratios seemed to be too low to justify their killing. It is thus likely that spatiotemporal clustering approaches cannot detect such clusters reliably.

Acknowledgments

This thesis would not have been possible without the invaluable support of various people that accompanied its formation process. I would like to thank particularly:

- Prof. Dr. Robert Weibel, for his engagement, valuable feedback and suggestion of this interesting but so far unknown research topic. Meetings with him were constantly a source of motivation to carry on and refine every little detail.

- Monika Schiess-Meier, for being so dedicated and responsive. Whenever I needed another information or dataset, she managed to dig it out – even when it was located in the dry sand of the Kalahari.

- Stephen Henley, who shared his ecological expertise with me. Thanks to him, a more comprehensive ecological understanding of these interesting species could be obtained.

- Leopard Ecology & Conservation, which provided all the laboriously collected movement data. Without this data, none of the analyses could have been carried out.

- Nicole Gusset-Burgener, for being so kind to read through the numerous pages of this thesis and detect every single mistake and inconsistency.

- Georgios Technitis, for his excellent *R* programming support and methodological advices.

- Christian Gschwend, who accompanied me during the first burdensome months of orienting myself in a completely new subject area.

- My whole family and particularly my mother, for their moral support and endurance.

Table of contents

List of abbreviations

BCV	Biased cross-validation
BRB	Biased random bridge
CKGR	Central Kalahari Game Reserve
CV	Coefficient of variation
DOP	Dilution of precision
HR	Home range
HRE	Home range estimator
KDE	Kernel density estimator
KGR	Khutse Game Reserve
LCH	Local convex hull
LEC	Leopard Ecology & Conservation
LSCV	Least square cross-validation
MCP	Minimal convex polygon
MISE	Mean integrated squared error
MSHC	Minimum spurious hole covering
REF	Reference bandwidth
SCV	Smoothed cross-validation
SI	Sampling interval
PI	Solve the equation plug-in
t-LCH	Time local convex hull
TK	time to kill
TSD	Time-scaled distance
UD	Utilization distribution

I   General introduction

1   Motivation

Large cats, such as leopards and lions, are not only critical for healthy ecosystems, but also contribute to the economic welfare of a country by means of ecotourism (Bauer & de Iongh 2005; Pitman et al. 2012). However, their presence also leads to conflicts with local farmers in many African countries, since their livestock gets attacked and killed by feline predators (Bauer & de Iongh 2005; Patterson et al. 2004; Schiess-Meier et al. 2007). A major driver of this conflict is the spreading of the area used by humans for living and agriculture, which leads to a fragmentation and loss of habitat of large cats as well as decreasing abundances of their natural prey (Pitman et al. 2012; Ramsauer 2006; Swanepoel et al. 2013; Winterbach et al. 2014). In order to mitigate the issue of livestock predation, typical strategies of public authorities include translocating problem animals and constructing fences around the borders of game reserves. Fences, however, rarely forms an obstacle for predators due to insufficient maintenance and construction types (Kesch et al. 2014). Translocations, on the other hand, can only be successful when being based on a profound knowledge of the demands of the predators in the respective area (Fontúrbel & Simonetti 2011; Tumenta et al. 2013; Weilenmann et al. 2010). When such strategies fail, predators are shot by the government or killed by local farmers (Bauer et al. 2014; Patterson et al. 2004). As a consequence, the African populations of leopards and lions have been rapidly decreasing during the last decades (Bauer et al. 2014; Marker & Dickman 2005; Swanepoel et al. 2013).

2   Goals of this study

In order to develop effective conservation strategies for these species, it is critical to enhance the knowledge about their spatial ecology. Two major aspects in this context are to determine the area that offers the resources required by an animal to live and to investigate its interactions with prey species (Downs & Horner 2008; Pitman et al. 2014; Swanepoel et al. 2013; Tambling et al. 2010; Tumenta et al. 2013). This thesis addresses these two aspects for leopards and lions in the Kalahari by analyzing their home ranges and kill sites.

Numerous papers are available concerning the analysis of home ranges. However, only few of them used more than one or two home range estimators to compute the results of free-ranging animals while the majority concentrated on simulated data (such as Getz et al. (2007), Lichti & Swihart (2011) or Wall et al. (2014)). Since the performance of a home range estimator depends on the used simulation, the findings of such studies often differ markedly from each other and analyses that used data of free-ranging animals (Downs & Horner 2008; Horne & Garton 2006). Another feature shared by most studies is the implicit assumption of temporally invariable home

ranges. This issue arises when home ranges are computed on data from only one single time period (typically one year). Although there are papers that investigated temporal variations of home ranges, they concentrated only on the presence of seasonal patterns of their area sizes but neglected their shape (e.g. Loveridge et al. (2009), Marker & Dickman (2005) or Tumenta et al. (2013)).

An objective quantification of kill sites is critical since those occurring within grazing areas indicate potential livestock predation and can ultimately cause the predator to be killed. The only data source to determine the extent of livestock predation, however, are usually reports of affected local farmers. In order to get rid of problem animals that cause financial losses and to receive higher financial compensations, farmers are tempted to exaggerate the actual extent of livestock predation and accordingly may be not an objective data source (Bauer & de Iongh 2005; Schiess-Meier et al. 2007). An inherent step in independently quantifying kill sites and analyzing them from an ecological perspective it to locate them first. Even if machine learning techniques are intended to locate and predict kill sites in the end, they first require large amounts of validation data to be trained (Pitman et al. 2012; Tambling et al. 2010). Such validation data can be ideally obtained by locating kill sites through spoor-tracking or continuous observation. However, both of them are time-consuming and may be infeasible, depending on the predator species and habitat. Spatiotemporal clustering approaches provide a time-saving means of automatically detecting potential kill sites and subsequently visiting only promising candidates in the field (Tambling et al. 2012). The amount of time savings, however, depends on the predator species and the clustering rules of the algorithm. Particularly for lions, only a relatively simple algorithm was used so far that resulted in many false alarms (Tambling & Belton 2009; Tambling et al. 2010; Tambling et al. 2012).

This thesis addresses the above-mentioned research gaps by investigating the following points:

- Quantification of the effect of different home range estimators and their parameterizations on the result when being applied to data of free-ranging animals
- Computation of the home range sizes of leopards and lions in the Kalahari by using different home range estimators
- Analysis of the temporal variability of the area size and shape of home ranges
- Development of an enhanced clustering approach that yields lower errors
- Analysis of the spatial distributions of kill sites with regard to ratios inside home range boundaries and the protected game reserves

3   Thesis structure

Part I and II of this thesis provide basic knowledge about the ecology of the analyzed species and their environment. In addition, detailed information is provided about the data and its preprocessing. Part III refers specifically to the home range analyses. The first chapter of this part,

Chapter 7, introduces the concept of home ranges and discusses temporal autocorrelation as one of its major issues. Detailed information is given on the functionality and parameters of the home range estimators used in this study and further methods are briefly reviewed. Chapter 8 informs about all selected parameters and conducted analyses, whose results are presented in Chapter 9. The discussion of the results in Chapter 10 incorporates ecological information from the literature and the organization whose data was used (Leopard Ecology & Conservation), to put it in a wider context. Chapters 11 to 14 belong to part IV and refer to the detection of kill sites. Chapter 11 thereby introduces the concept of spatiotemporal clustering and reviews findings of previous studies. Chapter 12 informs about how the enhanced clustering approach developed in this study works and how its results were validated and used to estimate the spatial distribution of kill sites. The results are shown in Chapter 13 and discussed in Chapter 14. Part V discusses the main achievements of the home range and kill site analyses and their implications. Finally, an outlook is given on potential research questions, which arose from the results of this theses.

4   Cat ecology

Leopards (*Panthera pardus*) and lions (*Panthera leo*) are phylogenetically closely related animals since both of them belong to the same lineage of the family Felidae (Macdonald & Loveridge 2010). This phylogenetic family comprises all cats and is subdivided into several different lineages. Except for a highly similar structure of the skeleton, another characteristic shared by all felids (cats) is that they are carnivorous (Hunter & Hinde 2005). However, despite of their kinship, leopards and lions differ in some points distinctively.

4.1   Lion

Apart from the tiger, which does not live on the African continent, the lion is the largest member of the family *felidae* in Africa (Haas et al. 2005). For males, the shoulder height usually ranges between 1.1 and 1.2 meters, whereas the body length (without the tail) lies between 1.7 and 2.5 meters. This results in body masses of 160 to 200 kg, although this range may be exceeded or undercut massively in rare cases. Female lions are roughly 20–27 percent smaller and lighter than males, even though their shoulder height is almost the same (Figure 1) (Haas et al. 2005; Hunter & Hinde 2005). In captivity, lions may reach an age of up to 30 years, whereas this life span is roughly reduced by half, meaning 12 to 15 years, in the wild (Hunter & Hinde 2005). Today, lions are mainly found in sub-Saharan African countries, especially in the eastern and southern parts of the continent. However, a small and isolated population lives in the *Gir Forest* region of India, which is a relic of the formerly much larger dispersal of lions over parts of Europe and Southwest Asia (Bauer et al. 2012; Ramsauer 2006). No precise counts are available for the overall population size. Extrapolations of known small populations and educated guesses resulted in African population sizes of 39'000 (range from 29'000 to 47'000) and 23'000 (16'500 to 30'000) for the year 2002 (Bauer et al. 2012; Bauer & Van Der Merwe, S. 2004). Despite the high

uncertainty, it is clearly evident that the number of lions has been decreasing for a long time and still does. Accordingly, the International Union for Conservation of Nature (IUCN) classes this species as *vulnerable* on their Red List of threatened species (Bauer et al. 2012).

Figure 1. A female lion located in the study area. Photography by Monika Schiess-Meier.

Unlike most members of the family Felidae, lions live in prides (Eloff 1998). The size of such prides is highly variable due to their dependency on the environmental conditions. Typically, a pride consists of 5–9 adult females and 2–6 adult males (Haas et al. 2005). In arid habitats with a scarcity of prey, prides may be much smaller with up to two members (Eloff 1998; Haas et al. 2005). Whereas in the majority of cases a lioness stays with the pride in which she was born, males have to leave their pride when reaching sexual maturity (at approximately 2–2.5 years) or some months thereafter to find a new pride or live with other males in a coalition (Funston 2011; Haas et al. 2005; Hunter & Hinde 2005; Macdonald & Loveridge 2010). Although a pride membership is stable, it is common that, especially under difficult conditions like droughts, its members form subgroups that live spatially separated for hours to months. This social structure of repeated splitting and merging is called as *fission-fusion* (Ramsauer 2006; Spong 2002).

Several tasks are undertaken together within the pride, such as the breeding of cubs, the defense of the territory, or hunting (Hunter & Hinde 2005; Macdonald & Loveridge 2010). The latter usually involves several members of the pride, which cooperate by adopting different roles (Haas et al. 2005). In this cooperative hunting strategy, some of the lions sneak to the flank of their

potential prey and start to leap towards it and thereby direct it towards the second, waiting group (Hunter & Hinde 2005). However, lions do not strictly follow this pattern but occasionally exhibit deviating behaviors in which single lions participate in the hunt not at all or only partly ((Haas et al. 2005; Scheel & Packer 1991). When lions hunt individually or in small groups, their success strongly depends on how closely they can sneak to their victim, since they lack the stamina for extended chases. They usually begin their sprint when they are not further than 5–15 meter away and thereby reach top velocities of 50–60 km/h (Haas et al. 2005; Hunter & Hinde 2005). Lions are not picky about their nutrition and consume everything from larger insects up to adult elephants and also scavenge carcasses. Their preferred prey, though, weights around 150 kg and includes animals such as gemsboks, buffalos, giraffes or zebras (Haas et al. 2005; Macdonald & Loveridge 2010). Hunting takes place due to the reduced visibility of the predators and the reduced heat in some areas mainly during dusk, night and dawn (Hunter & Hinde 2005, Macdonald & Loveridge 2010; Ramsauer 2006).

Territoriality is an important aspect of the ecology of lions (Spong 2002). Because a territory of a pride usually persists for many generations and the reproduction success of expelled adult lions that need to find a new territory is significantly lower, its defense is of high importance and involves the whole pride (Hunter & Hinde 2005; Spong 2002). While lionesses primarily want to protect their cubs, denning sites, water sources and hunting grounds, the main objective of males is to preserve their exclusive mating privileges (Haas et al. 2005). The size and shape of such a territory is represented by the concept of *home ranges* in ecology, which is the "[…] area routinely used by an animal to meet its daily needs" (Fieberg & Börger 2012: 890). This concept will be introduced in more detail in Chapter 7.1. A home range is shared by all members of a pride and its size depends highly on the environmental conditions. Thus, depending on the availability of resources such as prey or water, the size of home ranges may vary between a few dozen and more than thousand square kilometers (Hayward et al. 2009). Apart from a few areas with high prey abundances such as in central Kenya, territories of prides of lions often overlap to a considerable degree (Hunter & Hinde 2005; Spong 2002). Especially in arid areas such as the Kalahari, where home ranges are among the biggest worldwide, it appears reasonable to allow a shared usage of parts of the territory since they could hardly be defended effectively anyway (Hunter & Hinde 2005). In fact, the members of adjacent prides are thoroughly aware of the presence of the intruders because they use a variety of techniques to proclaim their presence, such as roaring, scent marks and scraping (Eloff 1998; Hunter & Hinde 2005). This active avoidance behavior prevents that members of the different prides are at the same time in the overlapping region and accordingly get in conflict. In most cases, only peripheral areas of the home range overlap each other while the core areas are used exclusively (Haas et al. 2005; Spong 2002).

4.2   Leopard

The leopard belongs together with the lion and cheetah to the group of the three big African cats (Hunter & Hinde 2005). However, it is considerably smaller than the lion with a shoulder height of 50–70 cm and a body length of 90–170 cm (without tail) for adult males. This results in a weight of typically 40–75 kg, compared to 160–200 kg for a male lion (depending on the habitat, more extreme weight may exist). Female leopards are roughly 10 % smaller and up to 40 % lighter (Bailey 1993; Hagen et al. 1995; Stein & Hayssen 2013). In captivity, a leopard can reach an age of more than 20 years. Due to injuries, starvation, trophy-hunting, and so on, its lifespan in the wild is substantially reduced and lasts only 10–12 years on average (Bailey 1993; Hunter & Hinde 2005; Stein & Hayssen 2013). Because of its high adaptability and habitat tolerance, the leopard is the most widely distributed wild cat (Marker & Dickman 2005; Pitman et al. 2013). It can survive in forests, savannahs, mountain areas, and even semi-deserts and, thus, can be found nearly in all of sub-Saharan Africa and large parts of southern Asia such as Iran, India, China, or Thailand (Macdonald & Loveridge 2010; Marker & Dickman 2005; Stein & Hayssen 2013). No precise numbers of the worldwide population size are available and the latest large-scale census from Martin & de Meulenaer (1988 in Marker & Dickman 2005) estimating 714'000 individuals for sub-Saharan Africa dates back to 1988 and is known to be flawed (Henschel et al. 2008; Marker & Dickman 2005). Due to its decreasing trend (Henschel et al. 2008) and the fact, that this estimate is 27 years old, the current African population size will be considerably smaller. The leopard is currently labeled as *near threatened* by the IUCN but this classification could change to *vulnerable* soon (Henschel et al. 2008).

Like the majority of cats, leopards are solitary and, thus, have no social constructs such as a pride (Bailey 1993; Stein & Hayssen 2013). As already discussed for the lions, food efficiency for cats is assumed to be optimal for solitary individuals or groups of two. Due to their smaller body size and reduced physical strength compared to lions, leopards prefer smaller prey which can be dragged away from potential rivals to a safe place (Hunter & Hinde 2005; Stein & Hayssen 2013). Accordingly, living in a pride to defend the prey is not necessary. As a consequence, leopards meet each other only for a few days for reproduction (Hagen et al. 1995; Hunter & Hinde 2005). An exception are female leopards which live temporarily in small groups with their cubs during upbringing. As soon as the cubs are able to take care of themselves, what happens after 12 to 20 months, they leave their mother and look for their own home range (Bailey 1993; Hagen et al. 1995; Mizutani & Jewell 1998).

Figure 2. A leopard lying on the ground surrounded by shrubs. Photograph by Monika Schiess-Meier.

Because leopards occur in many parts of the world, their prey is versatile and requires flexible hunting strategies (Hagen et al. 1995). One approach is to hide behind cover and sneak in the direction of the potential prey. As soon as the distance is within 5 to 15 meters, a short sprint with velocities of up to 60 km/h begins (Hunter & Hinde 2005). Another strategy is to ambush prey on a tree and let oneself drop upon the prey or climb down the tree unseen and start a sprint (Hagen et al. 1995). Just as lions, leopards are tolerant in terms of feeding and eat everything from a buck to a zebra or steal remains of prey hunted down by other predators (Bailey 1993; Hagen et al. 1995). Their preferred prey size is around 50 kg, ranging from 20 to 80 kilograms and including the bushbuck, impala, antelope, or duiker (Hunter & Hinde 2005; Macdonald & Loveridge 2010). In order to protect their prey from scavengers, leopards drag it on a tree or, if trees are unavailable, hide it in a cave or thick bush (Bailey 1993; Hagen et al. 1995). The hunting behavior of leopards depends strongly on the available prey and its customs and other factors such as human disturbances (Hagen et al. 1995). For these reasons, the leopard hunts during the day instead of the night in some parts of its distribution area (Bailey 1993).

Just as lions, leopards are territorial and, therefore, have home ranges that they will defend against other leopards (Hunter & Hinde 2005). The prevailing goal of females in this regard is to obtain and secure access to resources required for survival and reproduction, while males primarily want to have access to as many females as possible. Hence, male leopards have significantly larger

home ranges than females have (Bailey 1993). Except for differences due to sex, differences due to the extensive global distribution area with strongly varying environmental conditions lead to diverging home range sizes. In Thailand, where resources are abundant, leopards occupy areas as small as 2.5–7.5 km^2 (Macdonald & Loveridge 2010). For many parts of Africa, home ranges are within 30 and a few hundred square kilometers (Hagen et al. 1995; Hayward et al. 2009; Marker & Dickman 2005), although they may be expanded up to 500 km^2 for females and 2'500 km^2 for males in the arid Kalahari region (Hunter & Hinde 2005). Depending on the average size of the home ranges in an area, the degree of overlap varies substantially. While there are no or only minimal overlaps in habitats such as Thailand, they may exceed a quarter of a leopard's entire home range in dry African habitats (Hunter & Hinde 2005). Home ranges of females show generally a higher proportion of overlaps because their cubs usually settle down nearby (Hagen et al. 1995). In order to avoid confrontations within the shared areas, leopards actively avoid each other just as the lions do (active avoidance behavior). This means that each leopard knows the position of its neighbors because of scent marking and vocal communication and thereby avoids clashes (Bailey 1993; Hunter & Hinde 2005; Marker & Dickman 2005). Ecologists presume that leopards (and lions) tolerate such shared areas because it is better than risking injuries during a fight and possibly get a new, more powerful neighbor which insists on an exclusive use of its territory (Hunter & Hinde 2005).

4.3   Cross-species interactions between lions, leopards and humans

By nature, leopards are cautious and avoid encounters with other predators. This is particularly true for clashes with lions, which can easily kill an adult leopard due to their inferior physical strength. Therefore, when a leopard detects a nearby lion, it usually seeks shelter in a thicket, crevice, or on a large tree (Hagen et al. 1995). If an adult leopard stumbles upon an unattended lion cub, however, it will kill it. The same is true for adult lions and in fact, they are the main source of mortality to juvenile leopards (Hunter & Hinde 2005). Another, quite one-sided interaction concerns *kleptoparasitism*, which means the stealing and consuming of prey that another animal has hunted down. Thereby, lions play the role of the thieves and steal prey from a broad variety of other predators, such as the leopard or cheetah (Bailey 1993; Hunter & Hinde 2005).

Both lions and leopards show a decreasing population trend, as mentioned before. The main reason for this is the loss of habitat due to the increasing human population and subsequently the expanding agriculture (Bailey 1993; Macdonald & Loveridge 2010; Schiess-Meier et al. 2007). As a consequence, there is less natural prey available for predators. In order to compensate this, predators raid the farmer's livestock (Hagen et al. 1995; Hunter & Hinde 2005). Although significantly more livestock is lost annually due to other causes such as diseases, injuries or starvation, particularly lions and leopards induce considerable economic losses and are therefore

frequently killed by farmers (Hunter & Hinde 2005; Macdonald & Loveridge 2010; Patterson et al. 2004). In addition, some leopards and lions die each year because of trophy-hunting (Macdonald & Loveridge 2010). Because of the growing wildlife-tourism, however, which generates income for the local residents, the protection of these animals has improved during the last decades (Hagen et al. 1995; Hunter & Hinde 2005).

II Data and study area

5 Available data

All telemetry data on the leopards and lions were collected and provided by the organization *Leopard Ecology & Conservation*. The data, provided as Excel worksheets, encompasses recorded positions of 16 leopards and 21 lions. The time spans of the datasets vary between a few months and several years. Since the quality and quantity of the data is heterogeneous, the datasets needed to be preprocessed before the ones appropriate for the scheduled analyses were selected.

5.1 Preprocessing

In a first step, the attributes containing the date and time were transformed to a consistent format for all datasets. In addition, records with an invalid or missing value for one of these two attributes or the geographic coordinates were deleted. In order to remove spurious records, the datasets were further filtered according to their coordinates, notes-attribute and dilution of precision (DOP) values. This included the removal of records with a longitude or latitude value distinctively different from all the other values of the dataset (i.e. outliers). If the coordinates of an animal did not change beyond the scope of spatial uncertainty between the records in a dataset and the notes revealed that the collar had to be changed, broke off or the animal died, these records were considered as spurious and were deleted. The DOP informs about the spatial configuration of the satellites used to obtain a positional measurement. Although other factors play a role as well and the relationship is nonlinear, a large DOP indicates imprecise and possibly defective measurements (Frair et al. 2010; Lewis et al. 2007). Thus, these records were removed. Because this accompanied by a loss of information, a cut-off value of 10.0 was used, as proposed by Lewis et al. (2007). Less than 1 % of the records of each animal were lost due to the threshold of 10.0. Because different kinds of collars were used, some of the datasets include Argos measurements in addition to the GPS measurements. They occur, however, only as irregularly distributed short bursts and are quantitatively negligible. For reasons of consistency, these Argos measurements were deleted.

5.2 Selection criteria

5.2.1 Home range analysis

In order to be considered for the analysis of the home ranges, the position data of each leopard and lion had to fulfill three criteria:

- The dataset records measurements over at least one entire year.
- No gap (i.e. a period of missing fixes) longer than one week occurs.
- The period over which fixes were recorded matches the one of the other leopards and lions so that the temporal intersection of all animals is at least half a year.

The first criterion ensures that the home range constructed from the point data includes all ecologically important regions for the animal. It also allows to investigate effects of seasonality, if present. This is also a goal of the second criterion, since an investigation of seasonal differences requires all seasons to be included in the data. Additionally, long gaps could cause certain regions to be over- or underemphasized in the home range estimation. The specific threshold of one week was selected following an initial investigation of the datasets. The vast majority of occurring gaps was shown to last less than one week, while a few datasets had gaps of several weeks or months. The third criterion ensures that the comparison of the results of different individuals is significant. The time period over which fixes are available for all of the leopards and lions is half a year. However, the shared time period for all of the individuals except for a few ones can be much longer.

5.2.2   Kill site detection

For the detection of kill sites, the same criteria were used as for the home range analysis. However, only datasets of lions were considered due to their finer sampling intervals (Table 1). The lion datasets were further filtered according to the number of validated kill sites for the respective individual, with a lower boundary of 15 validated kill sites.

5.3   Harmonization of the sampling intervals

A closer look at the selected datasets revealed, that different sampling intervals occur within most of them. For example, the majority of the lion's datasets mix main sampling intervals of 5, 30 and 60 min (Table 1). This means a factor of 6 or 12 between the lowest and highest SI. For the leopards, the range of SI is smaller with factors of 1 to 3.3.

Table 1. Range of sampling intervals of each selected leopard and lion. Only frequent sampling intervals are listed. The order in which the SI are presented corresponds to their incidence.

Individual	Species	Main SI [min]	Factor
Verity	Lion	30, 5	6.0
Ella	Lion	30, 5, 60	12.0
Jane	Lion	30, 60, 5	12.0
Hitchcock	Lion	30, 60, 5	12.0
Mexico	Lion	30	1.0
Madge	Lion	30, 60, 5	12.0
Orange	Lion	30, 60	2.0
Getika	Lion	30, 5	6.0
Ronja	Leopard	300, 180, 120	2.5
Mothamongwe	Leopard	300, 90	3.3
Bogarigka	Leopard	60	1.0
Gham	Leopard	60	1.0

Irregular sampling intervals can, depending on the method used for home range estimation, result in biased results (Calenge et al. 2009; Katajisto & Moilanen 2006; Kranstauber et al. 2012). In order to avoid this bias, one can remove all records that have been recorded more frequently than those with the coarsest sampling interval. Another approach would be to include a lot of interpolated records so that the SI of all fixes orient themselves towards the highest sampling interval. While the first approach reduces the number of records, the second one includes points that are only estimated and may deviate from the true position distinctively.

In order to decrease the potential bias of the home range results, the range of sampling intervals was reduced by removing points that have been sampled too frequently. However, this was carried out only for the lion datasets that include a 5 min SI (Verity, Ella, Jane, Hitchcock, Madge and Getika). There are two reasons for this decision: Firstly, the factors of these individuals are markedly higher than the factors of the others. Secondly, there is hardly a benefit in measuring the position every 5 instead of 30 minutes. Thus, the loss of ecological information for the purpose of home range estimation should be minimal. In addition, the shrinkage of the affected datasets to 73.6 % – 95.6 % of their previous size is acceptable. This solution is a compromise between the loss of data, the reduction of potential biases and the conservation of biological information.

It needs to be emphasized that this partial reduction of the SI does not seek to eliminate the temporal autocorrelation (see discussion in Chapter 7.2). Table 12 and Table 13 of Section 9.1 clearly show that the datasets are still temporally autocorrelated.

5.4   Final data

5.4.1   Home range analysis

Six lions and four leopards fulfilled all criteria mentioned in Section 5.2 and thus constitute the basis for the analyses (Table 2). Additionally, two more lions are listed in Table 2 (Orange and Getika). Although they fulfill criteria 1 and 2, the shared time period required by criterion 3 will get too narrow if these two lions are included. Because their datasets nonetheless carry significant ecological information, they are incorporated into selected analyses.

Figure 3 shows the time spans over which positions have been recorded for the selected animals. The datasets roughly cover the period from the second half of 2011 to the end of 2014, whereby the time periods of the lion datasets tend to be longer than those of the leopards. One exception is the leopard named Ronja, who has the longest time series of all animals. Because Ronja is the only animal of the selection that has records from the years 2009 and 2010, her movements cannot be compared to any of the other individuals during this time period. Therefore, the records of Ronja from 2009 and 2010 were removed for the analyses. Figure 4 presents the sampling intervals of the lion and leopard datasets. While the most frequent intervals of the lions after the

harmonization are 30, 60 and rarely 270 minutes, the positions of the leopards had been recorded at much coarser intervals of 5, 1, 3 and sometimes 2 or 1.5 hours. Thus, the sampling interval varies not only between the animals (of the same and different species), but also within a single dataset. Due to these differences, the lion-datasets contain much more records than those of the leopards (Table 2)

Table 2. List of individuals used for the home range analysis. Two of the animals (Orange and Getika) are highlighted (*) because their comparability to other individuals was limited in some of the analyses. The number of records after the harmonization of the SI for some of the lions are presented in the outer right column.

Name	Species	Sex	No. of records
Verity	Lion	F	23'369
Ella	Lion	F	31'039
Jane	Lion	F	21'944
Hitchcock	Lion	M	20'246
Mexico	Lion	M	22'520
Madge	Lion	F	28'277
Orange *	Lion	M	17'787
Getika *	Lion	F	20'711
Ronja	Leopard	F	9'447
Mothamongwe	Leopard	M	6'130
Bogarigka	Leopard	M	7'474
Gham	Leopard	M	5'088

Whereas all lions were equipped with the same collar type designated *GPS Plus Iridium* (Vectronic Aerospace GmbH, Berlin, Germany), three different types of two manufacturers were used for the leopards. Except for the types *GPS Plus Globalstar* and *Vertex Survey Iridium* (Vectronic Aerospace GmbH, Berlin, Germany), the model *G3C 275A* of the manufacturer *SirTrack* (SirTrack Limited, Havelock North, New Zealand) were used for the leopards. All of these collars determine their position by using a satellite navigation system, although the *SirTrack* collar also records a few fixes based on Argos Doppler shift measurement at episodic intervals.
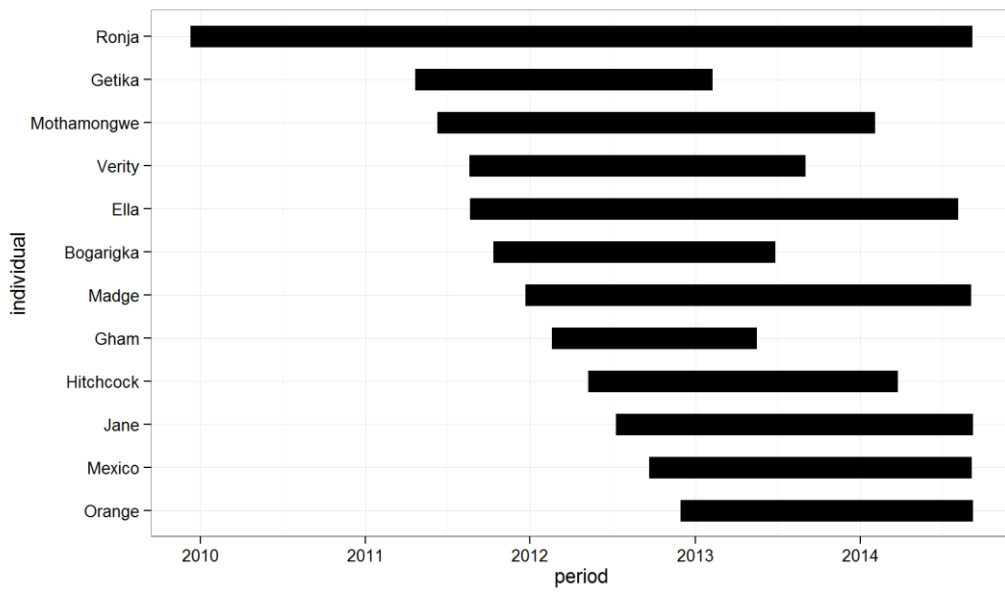
Figure 3: Time periods covered by the datasets of the selected animals. Except for Ronja, the datasets of the leopards tend to contain data over a shorter period than those of the lions. Considering only the 10 regular animals (without Getika and Orange), the period shared by all of them lies between September 2012 and May 2013.
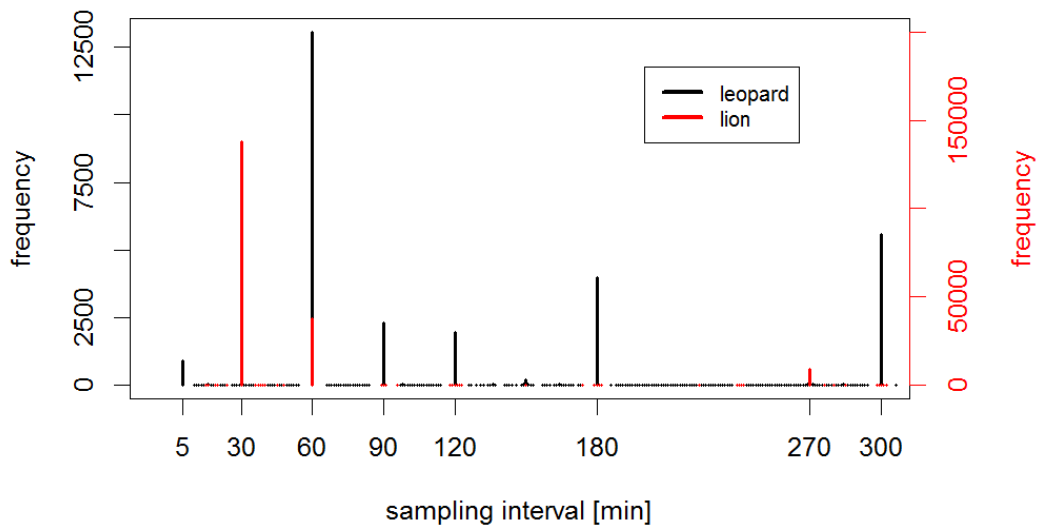

Figure 4. Sampling intervals of the eight lions (red) and four leopards (black). The main SI of the lions (after the harmonization) are 30 and 60 minutes. The intervals of the leopards are much coarser with values of 5, 1, 3 and sometimes 2 or 1.5 hours. Values that differ up to 5 minutes from these most frequent sampling intervals have been rounded to the nearest interval for this diagram.

5.4.2   Kill site detection

Four lions, which are listed in Table 3, fulfilled all criteria and were used for the kill site detection part. Since the datasets have not been altered for the kill site detection, the information about these lions presented in section 5.2.1 is valid here as well.

Table 3. Four lions met all criteria for the kill site detection part. The number of validated non-kill sites was not a selection criterion. Due to the low numbers for the other lions, only the non-kill sites of Madge was included in the validation.

Name	Species	Sex	No. of validated kill sites	No. of validated non-kill sites
Verity	Lion	F	23	2
Ella	Lion	F	29	1
Madge	Lion	F	18	14
Getika	Lion	F	22	4

6   Study area description

The study area is situated in the central Kalahari region in Botswana, between 22.5–24.5° S and 23.0–26.0° E. It includes both the Khutse Game Reserve (KGR, 2'600 km^2) and the much bigger Central Kalahari Game Reserve (CKGR, 54'000 km^2) just north of KGR (Figure 5), where animals are being protected (Weilenmann et al. 2010). The only artificial barrier that separates the game reserves from the adjacent regions is a fence at their southeastern border. However, since various species are known to dig holes under fences in the Kalahari, it is permeable to a certain degree for animals such as leopards, lions or hyenas (Kesch et al. 2014). In particular the regions in the Southeast of the study area are used by many farmers (Mishra et al. 2015). The grazing land for their livestock is in some cases located directly at the border of the game reserves or may even overlap them (Mills & Schiess-Meier 2009; Schiess-Meier et al. 2007).

The climate of the study area can be described as semi-arid, having a cold and dry season during the hemispherical winter (June–September) and a warm and wet season during summer (November–April) (Department of Meteorological Services, Leopard Ecology & Conservation 2014; Weilenmann et al. 2010). As observable in Figure 6, the mean monthly precipitation lies between 0 and 10 mm during winter and increases to 60–80 mm during summer months. The mean monthly temperature also shows seasonality and varies between 12° C and 25° C. The vertical bars, which show the averaged daily minimum and maximum values, reveal that the diurnal variances are quite pronounced and often higher than the seasonal differences (Department of Meteorological Services).
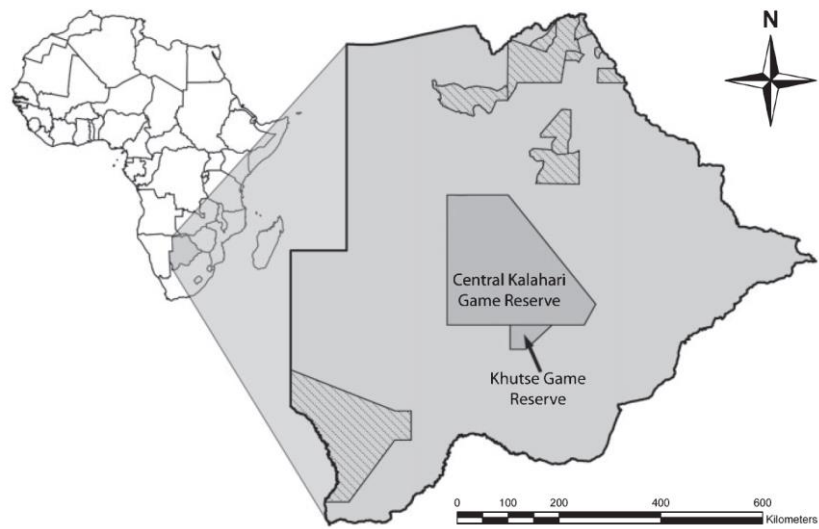
Figure 5. Map showing the frontiers of Botswana and the location of the study area (approximated by the area of the Khutse Game Reserve and Central Kalahari Game Reserve). The hatched areas represent further game reserves in Botswana. From Weilenmann et al. (2010: 703).
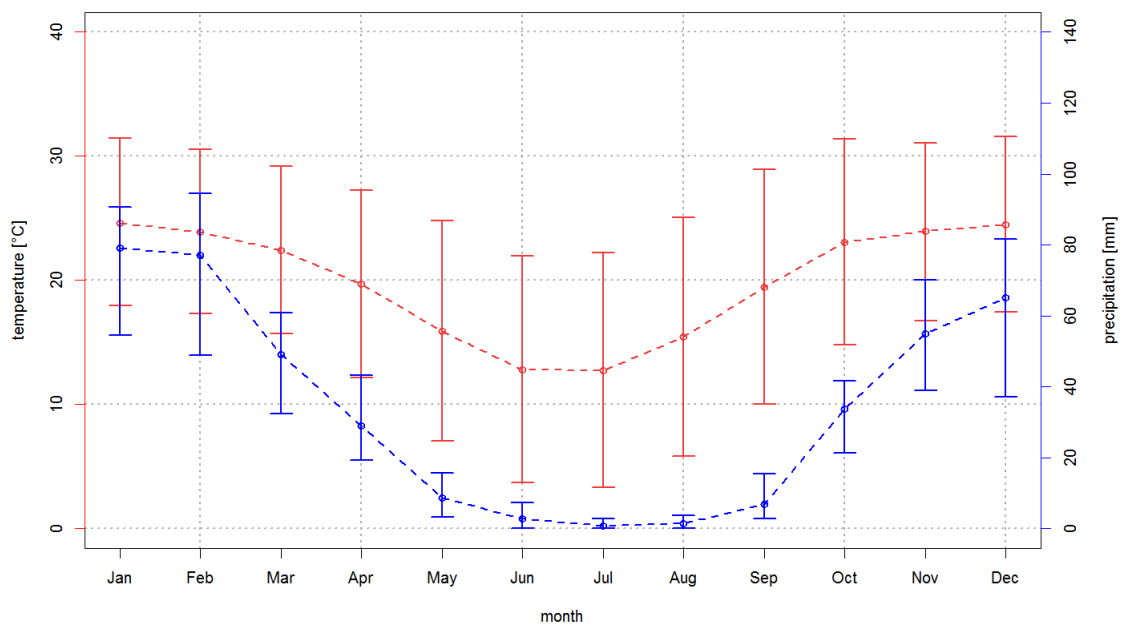

Figure 6. Mean monthly temperature (red) and mean monthly precipitation (blue) of the study area. In addition to the mean value (dashed line), the averaged daily minima and maxima are shown as vertical bars. The winter season is much drier and noticeably cooler than the summer. The diurnal temperature difference is often larger than the one over the year.

The data source used to compute the precipitation values is the *Climatology Version 2011*-Product of the Global Precipitation Climatology Centre (GPCC) in the 0.25° grid resolution version. Only those 0.25° x 0.25° tiles were considered that lie at least partially within the study area. The temperature measurements were provided by the web service *climate-data.org*. Only data from stations in or close to the study area were used for the analysis, including the monitoring stations in Ghanzi, Kang, Letlhakeng, Molepolole and Serowe.

Botswana's topography is pronounced only weakly and has an average elevation of 1'000 m above sea level (Food and Agriculture Organization of the United Nations (FAO)). Data from ASTER GDEM was used to obtain the elevations and slopes present in the study area. GDEM is a global digital elevation map product generated by the ASTER instrument of the Terra satellite with a spatial resolution of 30 m. It is made available by the Ministry of Economy, Trade, and Industry (METI) of Japan and the United States National Aeronautics and Space Administration (NASA). According to this data, more than 95 % of the study area has elevations of 950–1'300 m (above sea level). and slopes smaller or equal than 10°. Thus, areas inaccessible to animals are unlikely or at least very rare.

According to GlobCover (2009), a global land cover map produced by the European Space Agency (ESA), the prevailing part of the study area is classified roughly as grassland. A more detailed land cover analysis of the study area revealed that this grassland is in fact a mixture of open scrubland and open herbaceous vegetation (Mishra et al. 2015). Typically, representatives of the species *Acacia* can be found (Food and Agriculture Organization of the United Nations (FAO); Weilenmann et al. 2010). Some regions dominated by cropland are observable in the south-eastern edge of the study area, which are actually grazing areas used by the livestock of local farmers (Schiess-Meier et al. 2007).

III   Home range analysis

7   Theoretic background

7.1   The concept of home ranges

The home range is "[…] that area traversed by the individual in its normal activities of food gathering, mating, and caring for young. Occasional sallies outside the area, perhaps exploratory in nature, should not be considered as in part of the home range" (Burt 1943: 351). This definition from William H. Burt is, despite some criticism, still widespread and constitutes the basis of the home range concept. It rests on an observation made by Darwin (1861 in Börger et al. 2006) that animals usually restrict their movements to certain areas that they use repeatedly over time, rather than wander around the landscape randomly (Börger et al. 2008; Burt 1943; Fieberg & Börger 2012; Kie et al. 2010).

The afore-mentioned criticism mainly concerns three points of the definition: First, it contains vaguely defined terms such as "normal activities" or "occasional sallies" which are hard to substantiate in an ecologically meaningful way (Kie et al. 2010; Millspaugh & Marzluff 2001). Secondly, it leaves open how to delineate the actual boundary of the home range (Kie et al. 2010). And thirdly, it fails to incorporate the temporal dimension, although Burt himself stated that a home range may change over time (Burt 1943; Hansteen et al. 1997). Those deficiencies gave rise to an adjusted home range definition, which assigns individual probabilities of occurrence to certain parts of the home range (Katajisto & Moilanen 2006; Millspaugh & Marzluff 2001). This alternative perspective not only allows to exclude ecologically not meaningful parts of the home range, as proposed by Burt (1943), but also expands this idea by implying that even within the meaningful part of the home range some areas may be more important than others.

Assuming that an animal spends more time in areas of its home range that are more important to it (and thus will be sampled more often there) enables to measure their relevance by the density of the coordinate points (Benhamou & Cornélis 2010). This results in a density or utilization distribution (UD) (Gitzen et al. 2006) throughout the whole home range, which was defined by Van Winkle (1975: 118 in Seaman & Powell 1996) as "[…] the two-dimensional relative frequency distribution for the points of location of an animal over a period over time". Strictly speaking, the restriction to a two-dimensional frequency distribution is neither computationally nor ecologically necessary. Because both the time and elevation can contribute to a more comprehensive understanding of a movement pattern, the UD could also be enhanced to three or four dimensions for certain applications (Keating & Cherry 2009). Compared to Burt's definition, which implicitly assumes a homogeneous UD for the whole home range, the varying UD provides

useful additional information about the habitat usage of the subject of investigation (Benhamou 2011; Fieberg & Kochanny 2005).

It is not always sensible to use all measurement points for the home range estimation, since even GPS collars can occasionally provide imprecise or erroneous fixes (Hebblewhite & Haydon 2010; Frair et al. 2010). Furthermore, the home range is intended to represent areas that are important to the animal (Burt 1943; Getz et al. 2007). By designating the home range as the area in which the probability of occurrence of an animal is higher than or equals a certain percentage value, one can avoid unwanted outliers and thus returns Burt's definition of a homogeneous UD (Seaman & Powell 1996). Although ecologically hardly justifiable (Börger et al. 2006), the home range is delineated through the 95 % (Börger et al. 2006; Fieberg & Kochanny 2005; Getz et al. 2007) and 50 % isopleth (Downs & Horner 2008; Fieberg & Börger 2012; Lichti & Swihart 2011) by convention. The latter is also called core area (i.e. areas of more intense activity). For home range estimators that do not produce a UD, usually a percentage of points farthest away from the centroid of all points is excluded (Hayward et al. 2009; Laver & Kelly 2008; Marker & Dickman 2005; Weilenmann et al. 2010).

In this thesis, the term "core area" refers specifically to the 50 % home range isopleth (MCP: hull around the 50 % of points being closest to the centroid), whereas the term "home range" refers to the general concept of home ranges. When the 95 % isopleth (MCP: hull around the 95 % of points being closest to the centroid) is meant specifically, the term "home range" is always accompanied by the percentage value (e.g. "95 % home range").

7.2 Temporal autocorrelation: Problem or asset?

7.2.1 Definition

When dealing with movement data and home range estimation, it is widely assumed that the individual points are independent of one another (De Solla et al. 1999; Swihart & Slade 1985a). Independence in this context means that a specific point is not determined or influenced in any way by prior position points. Or, in other words: "[…] an animal's position … at time t + k is not a function of its position at time t" (Swihart & Slade 1985b: 1176). An animal whose sampled positions are completely independent would thus move in a random manner without any observable intention or primary direction. It is very unlikely that any animal, and lions or leopards in particular, would move in this manner (De Solla et al. 1999). Thus, movement data of real animals are temporally autocorrelated (Katajisto & Moilanen 2006). The degree of autocorrelation depends mainly on the sampling interval and the mobility of the animal under investigation. The sampling interval denotes the time that passed between two consecutive sampled positions. The shorter it is and the smaller the distance that an animal can at most move between two sampled positions (i.e. the lower its mobility), the higher the temporal autocorrelation (Hansteen et al. 1997; Huck et al. 2008; Swihart & Slade 1985a).

7.2.2   Effects

Simulations revealed that increasing values of positive autocorrelation generally lead to smaller home range size estimations (De Solla et al. 1999; Hansteen et al. 1997; Swihart & Slade 1985b). Negative temporal autocorrelation is very unlikely to be observed with animal movement data, especially when using short sampling intervals, and has therefore not been investigated (De Solla et al. 1999). In order to obtain the same dataset with different degrees of autocorrelation, the sampling interval must be artificially varied by means of subsampling (e.g. exclude every third entry of the list with all points ordered by date and time). This either reduces the sample size or requires comparing time series of varying duration. In both cases, other factors than only temporal autocorrelation are changed as well and will influence the resulting home range size (De Solla et al. 1999; Perotto-Baldivieso et al. 2012; Swihart & Slade 1985b). Since data of real animals are usually more complex than the simplified simulations and are also affected by the above-mentioned issues, there is no universally valid relation between autocorrelation and home range size (Hansteen et al. 1997). In addition, temporal autocorrelation does not affect all home range estimators to the same degree. Due to the assumption of temporally independent data, which is made by many statistical home range estimators (such as the conventional kernel density estimator), they are particularly affected by this issue (Katajisto & Moilanen 2006; Lyons et al. 2013; Swihart & Slade 1985b).

7.2.3   Ways to deal with it

Although the concrete effect of temporal autocorrelation on a specific dataset and methodology is often unknown, it became a widespread approach to deal with this issue by simply eliminating it (Perotto-Baldivieso et al. 2012; Katajisto & Moilanen 2006). This was accomplished by enlarging the temporal gap between two fixes through subsampling. For large sampling intervals, it is likely that an animal has changed its movement directions several times so that the fixes can be considered as independent (De Solla et al. 1999; Katajisto & Moilanen 2006). The downside of reducing the sample size is that it can lead to an underestimation of the area of the home range. This, however, is actually intended to be avoided through the elimination of the autocorrelation (Katajisto & Moilanen 2006; Kie et al. 2010). More importantly, (positive) autocorrelation is an inherent characteristic of animal movement data. Removing it reduces the biological expressiveness of the data severely (De Solla et al. 1999; Hansteen et al. 1997; Huck et al. 2008). Because of that, the perspective has changed recently from regarding autocorrelation as a problem to considering it an asset that must be retained and included in the analysis (Börger et al. 2006; Downs & Horner 2012; Dürr & Ward 2014; Horne et al. 2007).

7.3   Selected home range estimators

7.3.1   Minimum convex polygon (MCP)

The minimum convex polygon (MCP) was the first method used for home range estimation and is despite its age still popular among ecologists (Downs & Horner 2008; Getz & Wilmers 2004; Huck et al. 2008). According to Laver & Kelly (2008), who investigated 141 studies related to home range estimation within 2004 to 2006, 68 % (96 studies) of them used MCP. One reason for this is the simplicity of this method. Having a group of fixes for an animal, the minimum convex polygon (also known as convex hull in computational geometry) can be built by connecting adjacent exterior points of the group, so that the resulting polygon is as small as possible but includes all points. When connecting the exterior points, the angle created through three adjacent points must be smaller than 180 degrees at the inner face (Figure 7) (Burgman & Fox 2003).
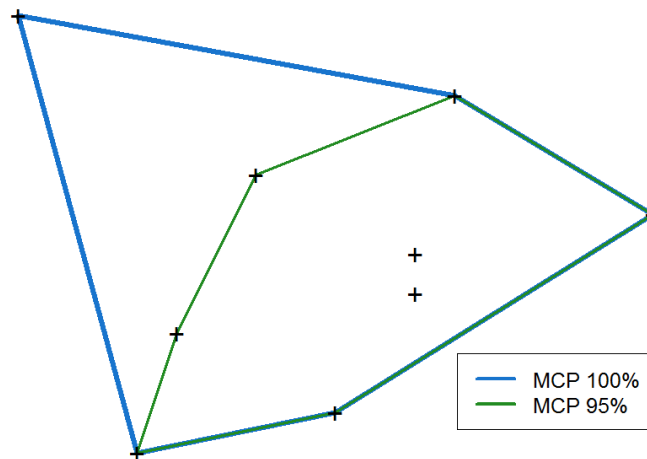

Figure 7. Construction of the minimal convex polygon from a group of spatial points. All of the points (blue polygon) are included by the hull and each angle between three consecutive points, when looking from the interior of the polygon, is smaller than 180 degrees (i.e. convex). For the green polygon, 5 % of the points farthest away from the centroid were excluded (in this case: one point).

Because no parameters have to be set for the construction of the home range, MCP is often thought to be particularly appropriate for the comparison of results across studies (Hansteen et al. 1997; Huck et al. 2008). Several more recent studies refuted this argument since the results of MCP depend highly on the sample size and presence of outliers (Börger et al. 2006; Downs & Horner 2008; Millspaugh & Marzluff 2001). Another disadvantage of MCP is the implicit assumption that an animal's home range has a convex shape. This not only cannot be justified ecologically, but also leads to a massive overestimation of the true area when the fixes are unevenly distributed in space (e.g. U-shaped) (Börger et al. 2006; Burgman & Fox 2003; Fieberg & Börger 2012; Huck et al. 2008). However, the influence of the sample size and degree of the overestimation may not be severe or present at all for certain data (Nilsen et al. 2008). Attempts to reduce the sensitivity

of minimum convex polygons to outliers are premised on the exclusion of extreme points, e.g. the exclusion of the 5 % of the points farthest from the centroid built by all data points, which is then labeled as "95 % MCP" (Figure 7) (Börger et al. 2006).

7.3.2   Kernel density estimation (KDE)

Unlike MCP, whose construction is based purely on geometry, a kernel density estimator (KDE) is a probabilistic method that was introduced to ecological applications by B. J. Worton in 1989 (Börger et al. 2006; Laver & Kelly 2008). The broad field of applications of KDE and its improvements compared to MCP, while still being relatively simple to compute, made it the most often used estimator in current home range studies (Lichti & Swihart 2011; Millspaugh & Marzluff 2001). Having a group of spatial points (representing an animal's measured positions), the basic idea of KDE is to calculate (most often two-dimensional) probability densities for several positions that are distributed at regular intervals over the area determined by the group of points. The sum of these individually calculated and partially overlapping probability densities at a position *x* results in the value of the utilization distribution at *x* (Figure 8) (Keating & Cherry 2009; Seaman & Powell 1996). In mathematical terms, the previous description is expressed as

$$\widehat{UD}_x = \frac{1}{nh} \sum_{i=1}^{n} K\left(\frac{x - X_i}{h}\right) \tag{1}$$

where $\widehat{UD}_x$ is the estimated utilization distribution at a defined position *x*, *n* is the number of fixes, *h* is the bandwidth, *K* is a kernel function, *x* is the position at which the probability density is estimated, and X_i represents the coordinates of the ith animal measurement point (Keating & Cherry 2009; Millspaugh & Marzluff 2001; Seaman & Powell 1996).

The estimated UD describes how intensively an animal uses its space at any position through a bivariate probability density function. The binary home range boundaries can be derived from this density function by delimiting the areas of the UD that contain a certain proportion of its volume, and drawing the maximum extent of these areas as borders projected on the ground (Seaman & Powell 1996). In order to delimit the respective areas of the UD, one has to start at the highest densities and then proceed downwards until the volume threshold (e.g. 95 %) is reached.
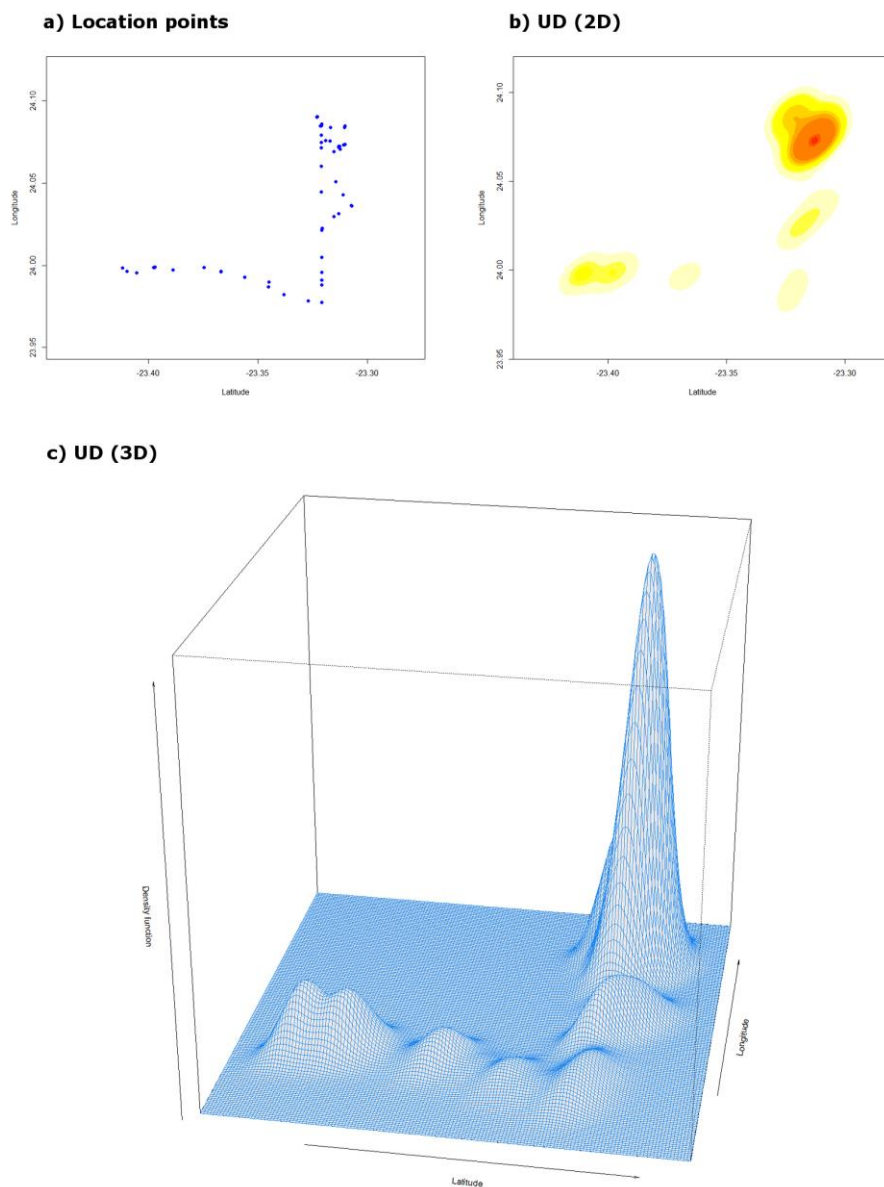
Figure 8. Illustration showing the functioning of KDE. a) Fixes of one or several animals serve as input data, for which multiple density distributions are being calculated and summed up to one overall utilization distribution (UD). b) 2-D view of the UD, where the color encodes the density (yellow: low, red: high). c) Illustration of the UD as a 3-D surface where the z-axis represents the density.

Bandwidth selection

The most influential parameter for the shape of the resulting UD is the bandwidth or smoothing parameter *h* (Downs & Horner 2008). The bandwidth determines whether and how strong fixes contribute to the density estimates depending on their distance to the current position of the kernel by varying its width (Kie et al. 2010; Millspaugh & Marzluff 2001). A small value of *h* leads to narrow kernels, whereby nearby fixes have a more pronounced influence on the density estimate,

while fixes further away are more likely to fall outside the kernel or have only a minimal impact (Seaman & Powell 1996). Although a small bandwidth helps exposing small-scale detail, it also causes the UD to break into its constituent kernels and thus creates artifacts of the sampling process and underestimations of the home range size. Larger bandwidths, on the other hand, reveal the general shape of the distribution but may result in oversmoothing (i.e. the loss of local peaks and valleys) and overestimation of the home range size (Gitzen et al. 2006; Jones et al. 1996; Keating & Cherry 2009; Millspaugh & Marzluff 2001; Seaman & Powell 1996).

A variety of methods exist to choose the smoothing parameter, whereby each of them is optimal only for a specific kind of data (Lichti & Swihart 2011; Kie et al. 2010). Therefore, the choice of the bandwidth should depend on an animal's space use properties, where known (Gitzen et al. 2006). The *reference bandwidth* (abbreviated as REF) is one of the earlier methods to estimate the smoothing parameter and can still be found sometimes in recent studies (Börger et al. 2006; Gitzen et al. 2006; Lichti & Swihart 2011). It derives h from the standard deviation of the input points, which are supposed to follow a unimodal normal distribution (Huck et al. 2008; Seaman & Powell 1996). Thus, the better the points follow this distribution, the better REF will perform. Since most real animals violate this assumption, REF often oversmooths the UD and thus overestimates the true home range size (Gitzen et al. 2006; Huck et al. 2008; Millspaugh & Marzluff 2001; Seaman & Powell 1996).

The currently most often used method for bandwidth selection is called *least-squares cross-validation* (LSCV) (Laver & Kelly 2008). Like the *biased cross validation* (BCV) or *smoothed cross-validation* (SCV) methods, it belongs to the category of cross-validation (CV) techniques (Duong & Hazelton 2005). The basic idea of the CV techniques is to set a value for h that minimizes the deviation between the estimated and true density distribution. To achieve this, the methods iteratively tests different bandwidths and seek to minimize the (asymptotic) mean integrated squared error (Duong & Hazelton 2005; Gitzen et al. 2006; Millspaugh & Marzluff 2001; Seaman & Powell 1996). LSCV is the most widespread CV technique and provides bandwidths that are usually unbiased and more accurate than those of REF, but at the expense of a high variability (Jones et al. 1996; Millspaugh & Marzluff 2001). It also computes UDs that tend to be smoothed insufficiently. Although LSCV is thought to be particularly suitable for space utilizations of multiple disjoint clusters, the method cannot determine a bandwidth when an excessive number of fixes are close to or at the same position, causing it to fail (Gitzen et al. 2006; Kie et al. 2010; Millspaugh & Marzluff 2001).

The *solve-the-equation plug-in* approach (PI) belongs to a second category of plug-in techniques (Duong & Hazelton 2005). It also attempts to analytically minimize the discrepancy between an estimated and a true density distribution (Millspaugh & Marzluff 2001). Unlike LSCV, PI accomplishes this by calculating an initial bandwidth h_0 on the basis of the covariance matrix of

the fixes, which is then inserted into a function that calculates h_1. The value of this h_1 is then again plugged in a lower-derivative function, resulting in h_2. This procedure can be repeated as often as desired although it is usually stopped after two stages (h_3 as the final bandwidth) (Gitzen et al. 2006). The performance of PI is comparable to the one of LSCV and can be somewhat better or worse depending on the input data (Gitzen et al. 2006; Lichti & Swihart 2011). PI tends to oversmooth the density distribution and its bandwidths may be slightly biased. On the other hand, its estimates are much less variable than those of LSCV (Gitzen et al. 2006; Jones et al. 1996; Lichti & Swihart 2011; Millspaugh & Marzluff 2001). Its main advantage against LSCV is probably the fact that it works regardless of the spatial configuration of the data.

Choice of the kernel

A second parameter of KDE that needs to be chosen is the kernel itself. When using a fixed kernel, the same bandwidth is applied to all data points. An adaptive kernel, however, adjusts the degree of smoothing in dependency of the spatial density of the data points. Regions with lower point densities (e.g. peripheral areas of the home range) are therefore smoothed more than those with a high density (Millspaugh & Marzluff 2001; Seaman & Powell 1996). In general, the fixed kernel is favored because it yields a lower bias in areas with low point densities (Gitzen et al. 2006; Millspaugh & Marzluff 2001). If one is interested primarily in the parts of the home range with a high UD, though, the adaptive kernel may be the better choice (Seaman et al. 1999).

In addition to the kind of interaction between the kernel and bandwidth, the function of the kernel can also be varied. Popular options are the bivariate normal, biweight or Epanechnikov kernel (Laver & Kelly 2008). For the ordinary 2-D kernel density estimation, however, the choice of the kernel function has little or no effect on the results and is therefore not even reported in numerous studies (Gitzen et al. 2006; Kie et al. 2010; Laver & Kelly 2008).

Problematic statistical assumptions

Due to its high sensitivity on the value of the smoothing parameter, which depends both on the data itself and the method used for its estimation, the performance of KDE can vary considerably (Benhamou & Cornélis 2010; Getz & Wilmers 2004; Seaman & Powell 1996). The main advantages of KDE are that it does not assume a certain spatial distribution of the data points and provides a continuous utilization distribution instead of only a binary home range border (Hansteen et al. 1997; Seaman et al. 1999). In addition, it allows home ranges with multiple centers of activity (i.e. disjoint or disconnected home range regions) (Börger et al. 2006). Nevertheless, KDE has some problems to reproduce sharply delimited unused areas such as gaps or outer boundaries in certain cases (Getz & Wilmers 2004; Gitzen et al. 2006; Lichti & Swihart 2011). Another conceptual problem of using KDE with movement data arises because it assumes independent points as input (Benhamou & Cornélis 2010; Downs & Horner 2012; Katajisto &

Moilanen 2006). As discussed in Chapter 7.2, particularly movement data sampled at short temporal intervals are highly temporally autocorrelated and therefore not independent.

7.3.3 Time local convex hull (t-LCH)

Local convex hull (LCH) can be seen as a mixture of the generalized MCP and the KDE approach developed by Getz & Wilmers (2004; Huck et al. 2008). Just as KDE, it places individual kernels over each point. However, these kernels are not parametric but get their shape directly from the spatial distribution of the points by constructing them as minimum convex polygons. (Getz et al. 2007). The creation of these convex polygons represents the first step of the LCH approach. Afterwards, these polygons are merged one by one in order to obtain the home range. Each of the single hulls uses only a fraction of all points as its neighborhood, which is selected according to a specific rule (Lyons et al. 2013). The steps of this procedure are illustrated in Figure 10.

Selecting a neighborhood: *k*-, *r*- and *a*-method

One rule for choosing the neighborhood of each single hull is based on the number of enclosed points *k* (applied in Figure 10b). Thus, each local hull is constructed around the selected point itself and its *k*-1 closest neighbors (Figure 9 A) (Getz & Wilmers 2004). According to this rule, higher point densities will lead to smaller polygons. We will term this version of the LCH method subsequently as the *k*-method. A second rule, called *r*-method, uses all neighbors within a distance *r* from the selected point for its local hull (Figure 9 B) (Getz et al. 2007). Although the search radius (kernel) has always the same size by definition, the area and shape of the hulls themselves will vary due to the convexity-requirement. The third rule, the *a*-method, includes all neighbors whose summed distances to the selected point are less or equal to a threshold value *a* (Figure 9 C) (Lyons et al. 2013). This method involves the prior calculation of the distances to all neighbors, which are then ordered and summed up one, by one beginning from the smallest distance (Getz et al. 2007).
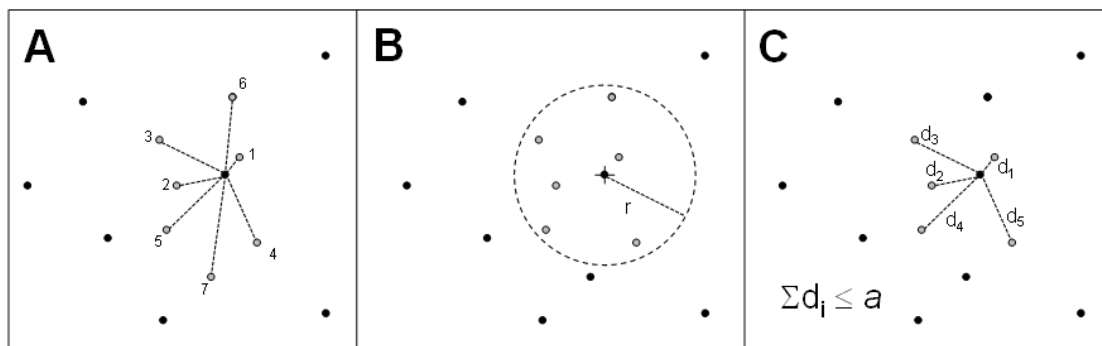

Figure 9. Illustration of the three methods to select a neighborhood: (A) *k*-method, (B) *r*-method and (C) *a*-method. From additional files of Lyons et al. 2013: 7.

After having constructed the individual hulls, they need to be merged in order to obtain the home range. This step varies according to the chosen neighborhood method. For the *k*-method, the hulls with the smallest areas indicate the most frequently used regions of the home range, which therefore should be preserved in each isopleth (Getz et al. 2007). This is why the hulls are sorted by their area before the approach starts with the smallest hull and continuously selects the next larger one, merging their areas (see Figure 10c)). This process of repeatedly building the union of the individual hulls stops as soon as a defined percentage of all points is covered by the united area. In order to build the 95 % home range, 95 % or all points need to be covered (Getz & Wilmers 2004). Because all hulls have a similar size when using the *r*-method, the hulls are ordered by the number of points contained. Hulls including the same number of points are sorted by their area. Starting from the hull with the most points (and the smallest area as a secondary criterion), the union is constructed in the same way as for the *k*-method (Getz et al. 2007). If the neighborhood was chosen by using the *a*-method, the hulls that include the most points are indicative of often used areas. Thus, as for the *r*-method, the hulls are sorted by the number of contained points (Getz et al. 2007; Lyons et al. 2013).

Rules to set the value of *k*, *r* and *a*

There are three ways to choose appropriate values for the neighborhood parameter. If the true topology is known, the minimum spurious hole covering (MSHC) rule can be applied. It requires selecting the smallest value of the parameter for which the home range isopleths match the true topology best (Getz & Wilmers 2004; Lyons et al. 2013). While the MSHC rule is suitable for simulated home ranges, the true topology is unknown when investigating real animals. In that case, the topography of the study area together with ecological knowledge about the animal under investigation can be utilized. If the animal is known to avoid certain large physical features such as lakes or hills, the parameter should be chosen so that the estimated home range leaves these features out (Getz & Wilmers 2004; Getz et al. 2007). If a study area lacks such large-scale obstacles or the ecology of the animal is not known well enough, a third method of parameter estimation is to plot the parameter value against the home range area. While the curve will be steep for small parameter values because spurious holes are filled, it will level-off at a certain point, before the gradient of the curve will increase again due to the erroneous inclusion of real holes (Getz et al. 2007). Such plateaus indicate proper estimates for the parameter value (Getz et al. 2007; Lichti & Swihart 2011). Instead of computing the local convex hulls for a vast number of parameter values, Getz (2004) suggests to use the following rules of thumb in order to get an idea of their magnitude.

- *k*: equals the square root of the number of data points
- *r*: having all nearest neighbor distances between 2 points calculated (i.e. the straight line that connects a point with its closest neighbor), *r* equals half the largest occurring distance
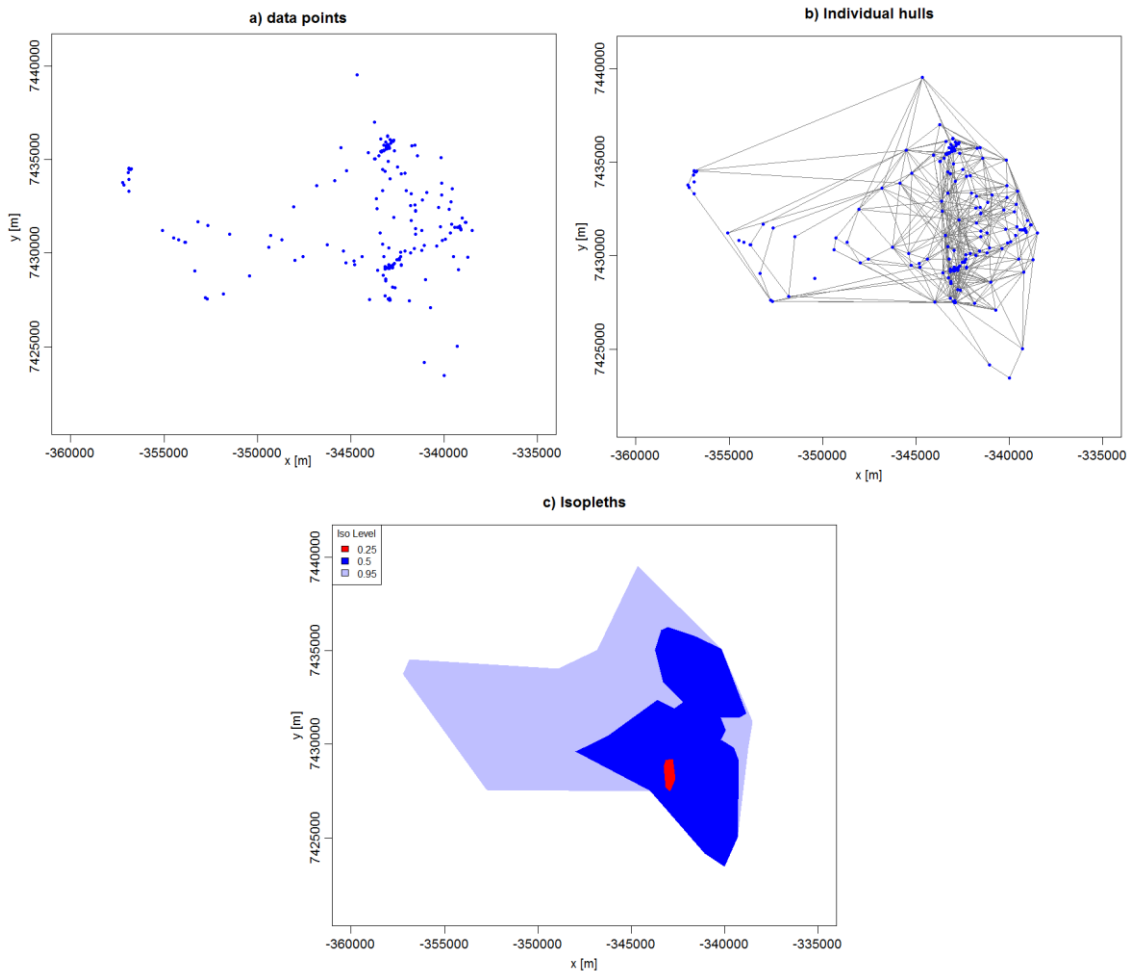- *a*: equals the distance of the two points furthest apart from each other

Figure 10. a) The data points of the sample dataset. b) Illustration of the first step of the LCH estimator, which consists of building hulls for each data point, whereby its neighborhood can be chosen according to three methods (Figure 9). Here, the *k*-method was applied. c) The isopleths can be constructed by drawing the boundary around the hulls with the smallest areas, which contain X % of all points.

Adding the temporal dimension: t-LCH

LCH ignores the timestamps of the point data by selecting the neighborhood exclusively on the basis of a 2-D Euclidean space. Lyons et al. (2013) developed an extension of the approach, called time local convex hull (t-LCH), which expands this 2-D space to a third dimension by including the time. The respective metric is called time-scaled distance (TSD) and defined as

$$TSD_{ij} = \sqrt{\Delta x_{ij}{}^2 + \Delta y_{ij}{}^2 + (sv_{max}\Delta t_{ij})^2} \tag{2}$$

where *i* and *j* denote the two points between which the TSD is calculated, *x* and *y* are the projected coordinates of the points, *s* is a dimensionless scaling factor, v_{max} the maximum theoretical velocity and *t* the timestamp of a point. *s* can be seen as parameter to adjust the influence of the

time on the TSD (Dürr & Ward 2014). When $s = 0$, the TSD is reduced to its two spatial dimensions and thus corresponds to the metric of the conventional LCH. v_{max} can be chosen on the basis of ecological expert knowledge or calculated from the data (Lyons et al. 2013).

The selection of the neighborhood and construction of the isopleths works in the same way as described for LCH, except that t-LCH deals with time-scaled distances. This often leads to the situation that, e.g. for the k-method with $k = 5$, not the five spatially closest points will be selected as a neighborhood because they were recorded much later and are therefore located temporarily far away. The TSD does not alter the subsequent step of sorting the hulls when using the same criteria as for LCH but offers additional sorting criteria (Lyons et al. 2013).

Advanced geometric estimator without a continuous UD

Both LCH and t-LCH make no assumptions about the spatial distribution of the data but rather form their kernel according to the data (Getz et al. 2007; Huck et al. 2008). This characteristic enables local convex hull based methods to take into account regions of the home range that are inaccessible for or not used by the animal anyway (Benhamou & Cornélis 2010; Getz & Wilmers 2004; Getz et al. 2007). However, since LCH and t-LCH are non-statistical estimators, they cannot model the spatial uncertainty (Lyons et al. 2013). Another drawback is that due to a lack of a probability density function a continuous UD cannot be obtained. In addition, only a limited number of isopleths can be generated (particularly with a low number of points n) and the smallest possible isopleth is limited to *3/n*100* % (Lichti & Swihart 2011). Similar to the bandwidth of KDE, the choice of the optimal neighborhood parameter is difficult and somewhat subjective. To mitigate this issue, the *a*-method is usually applied because it is very stable over broad value ranges (Getz & Wilmers 2004; Getz et al. 2007; Huck et al. 2008).

The main advantage of t-LCH is the inclusion of the temporal dimension. Simulations have shown that this leads, especially for complex patterns, to a better reproduction of movement paths (Lyons et al. 2013). t-LCH also allows the computation of additional metrics for deepened analyses such as the frequency or duration of visits at a certain position of the home range. Because these metrics are sensitive to gaps or bursts in the data, a regular sampling interval is essential to avoid biased results. A main disadvantage of the temporal extension of LCH is the additional parameter s. Its value is not only largely subjective, but also impedes the choice of the neighborhood parameter due to the abstractness of the TSD (Lyons et al. 2013).

7.3.4 Biased random bridges (BRB)

Based on Brownian motion

Instead of analyzing a set of points to estimate the home range, the Brownian Bridge (BB) approach models the movement trajectory to estimate the UD (Byrne et al. 2014; Kranstauber et al. 2012). Since only individual fixes are known, the trajectory must be estimated. Without any *a priori* knowledge of the true motion pattern, a reasonable approximation is to model it by using

Brownian motion (Horne et al. 2007; Kranstauber et al. 2012). For this kind of movement, the directions taken at previous time steps have no impact on the direction taken at a given time. Thus, a series of independently chosen directions finally lead to a random walk between two subsequent fixes (Codling et al. 2008; Horne et al. 2007). Mathematically, the space use density between two fixes follows a bivariate normal distribution and is expressed as[1]

$$\varphi(z;\ \mu, \sigma^2) = \frac{1}{2\pi\sigma^2} exp\left[\frac{-(z - \mu)^2}{2\sigma^2}\right] \tag{3}$$

with

$$\mu(t) = a + \frac{t}{T}(b - a) \qquad\qquad \sigma^2(t) = \frac{t(T - t)}{T}\sigma^2{}_m \tag{4}$$

where z denotes any position in a two-dimensional space, μ the mean value, σ^2 the variance, a the (two dimensional) starting position of a segment between two successive points, b the (two dimensional) ending position, T the duration of the segment and t the evaluation time (ranging between 0 and T). $\sigma^2{}_m$ represents the variance of the Brownian motion and is termed diffusion coefficient (Horne et al. 2007). Without going into detail, which is discussed extensively in Horne et al. (2007) and Bullard (1991), the density function of Brownian bridges *(df_BB)* at a position z is defined as

$$df_{BB}(z) = \frac{1}{T_{tot}}\sum_{i=0}^{n-1}\left\{\int_0^{T_i}\varphi(z; \mu_i(t), \sigma_i{}^2(t))dt\right\} \tag{5}$$

where T_{tot} is the total time span of all data points and n the number of points.

According to equation (5), the density function of Brownian bridges depends on the spatial position and time of the data points, the spatial uncertainty of the fixes and the diffusion coefficient (Horne et al. 2007). The latter parameter $(\sigma^2{}_m)$ is a key driver in the Brownian bridge model and quantifies how diffusive or irregular the path of an animal is (Byrne et al. 2014; Kranstauber et al. 2012). Since the diffusion coefficient can be directly estimated from the trajectory itself, it depends on the mobility of the animal under investigation (Bullard 1991; Horne et al. 2007). The variance term $\sigma_i{}^2(t)$ inserted into equation (5) is zero at positions z that coincide with the two measured points of a segment and is maximal mid-way between them (Bullard 1991; Kie et al. 2010). The probability density shows the opposite pattern: It is minimal between the two points of a segment and maximal at their position (Bullard 1991; Kie et al. 2010). In fact, its

---

[1] The original equation (3) in Horne et al. (2007) contains an erroneous square root around $(2\pi\sigma^2)$ which leads to maximum probabilities higher than 1. The error was found thanks to the help of Patrick Donà.

value is infinitely high because the coordinates of the points are known precisely. The solution to this problem is to treat the point positions *a* and *b* as not precisely known by applying a smoothing at the end by means of $\sigma_i^2(t)$ (included in equation (5)) (Bullard 1991; Horne et al. 2007). Figure 11 shows the general shape and distribution of probability densities of a Brownian bridge. In order to create a UD of a home range, the bridges between all segments are integrated and averaged over the total time span (Bullard 1991).
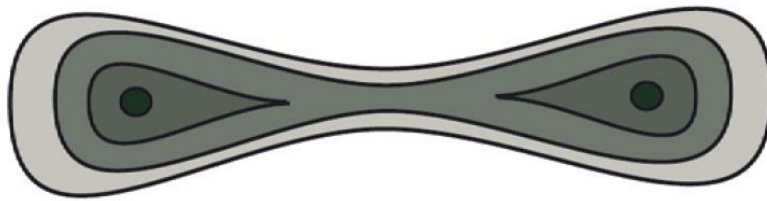
Figure 11. Schematic representation of a Brownian bridge between two fixes (black dots). The brightness of the gray tone corresponds to the value of the probability density. The highest values can be found close to the two points. From Downs & Horner (2012: 2).

Adding a directional bias

A fundamental problem of the BB estimator is its assumption of random movement. If an animal moved really totally random, studying home ranges would be pointless (Benhamou 2011; Bullard 1991). Thus, it is in fact necessary that the motion pattern deviates from this assumption. However, the coarser the sampling interval and the higher the mobility of an animal, the less realistic the assumption of the BB approach becomes (Byrne et al. 2014; Horne et al. 2007; Huck et al. 2008). In order to base the approach on a more realistic assumption, especially for coarser sampling intervals, Benhamou (2011) included a drift (i.e. a directional bias) into the Brownian motion and called the resulting home range estimator biased random bridges (BRB).

Because of this drift, the likelihood of moving in a specific direction is not uniformly distributed anymore (Börger et al. 2008; Codling et al. 2008). Instead, the drift ensures that an animal rather moves in a preferred direction that is independently determined for each segment between two points (Benhamou 2011; Dürr & Ward 2014). Because of this added advection component the orientation and shape of the bridges is altered compared to Brownian bridges (see Figure 11): The stronger the drift, the longer and lower the biased random bridge is on average (Benhamou 2011). Mathematically, the space use density of these bridges is defined as follows:

$$\varphi(z; \, \mu, \sigma^2) = \frac{1}{2\pi\sigma^2{}_{tot}} exp\left[\frac{-(z-\mu)^2}{2\sigma^2{}_{tot}}\right] \tag{6}$$

The mean value μ stayed the same as for the Brownian bridge (see equation (4)) while the variance $\sigma^2{}_{tot}$ changed to

$$\sigma^2{}_{tot}(t) = \sigma^2{}_{min} + \frac{4t\left(1-\frac{t}{T}\right)}{T_{max}} * \frac{D * T_{max}}{2} \tag{7}$$

$\sigma^2{}_{tot}$ is the total variance, $\sigma^2{}_{min}$ the relocation variance, D the diffusion coefficient and T_{max} an upper time threshold. The latter parameter ensures that segments of the trajectory, which are exceptionally large due to gaps, are not considered in the calculation (Benhamou 2011; Dürr & Ward 2014). Although both D and $\sigma^2{}_m$ term the diffusion coefficient, they are not equivalent as D equals $\sigma^2{}_m/2$. The density function of the biased random bridges approach is defined as

$$df_{BRB}(z) = \frac{1}{T_{tot}}\sum_{i=0}^{n-1}\left\{\int_0^{T_i}\varphi(z; \mu_i(t), \sigma^2{}_{tot_i}(t))dt\right\} \tag{8}$$

The detailed explanation of the BRB approach can be found in Benhamou (2011).

Selection of parameters

T_{max} needs to be chosen according to the sampling interval present in the data, as all segments whose time span exceeds this threshold will get a diffusion coefficient of zero and hence will be ignored for the computation of the UD (Benhamou 2011; Dürr & Ward 2014). Therefore, T_{max} should include all segments sampled at the regular intervals but exclude the ones that connect a large temporal gap. An upper limit of the parameter value is given by the serial autocorrelation, which is a basic requirement of the BRB approach (Benhamou 2011).

As mentioned for the Brownian bridges, smoothing must be applied to avoid infinite values at the measured points. The same is true for biased random bridges approach (Benhamou 2011; Bullard 1991). The smoothing parameter should take the uncertainty of a recorded position as well as the animal's behavior into account, so that all potential positions of the individual at that time are included (Benhamou & Cornélis 2010). For GPS measurements of animals with a high mobility, the latter component is usually larger than the uncertainty of the fix.

Advantages and drawbacks

A main advantage of Brownian and biased random bridges is that they explicitly makes use of the autocorrelation in the data by analyzing trajectories instead of a set of points (Dürr & Ward 2014; Horne et al. 2007; Huck et al. 2008). Because of that, the approaches can deal with varying sampling intervals, which are rather the normal case than the exception (Horne et al. 2007).

However, at coarse sampling intervals, the basic assumption of the Brownian bridges estimator becomes quite unrealistic. The BRB approach on the other hand may be still applicable to such data because of its advection component (Benhamou 2011; Horne et al. 2007). A main limitation for both approaches is their dependence on sufficiently autocorrelated data, whereby a clear definition of a 'suitable' value is lacking. Thus, there is no clear demarcation between a sampling interval that is high enough and one that is too coarse (Benhamou 2011; Huck et al. 2008; Kie et al. 2010).

7.4   Review of additional home range estimators

The selected home range estimators for this study represent only a small fraction of all available methods. Some of them are introduced in this paragraph to provide a more comprehensive overview. A simple geometrically-based alternative to MCP is the α-hulls method. It is based on a Delaunay triangulation in which all lines longer than the average line length are deleted (Burgman & Fox 2003). Because of that, the α-hulls method is not restricted to a convex shape and may even account for large holes. Many authors, however, focus on extending the widely used location-based kernel density estimator. One of these extensions comes from Katajisto & Moilanen (2006) and is called *time kernel*. It is based on the conventional KDE but weights the individual fixes according to their temporal and spatial density: The higher these densities are, the lower the weight of the affected fixes. This allows to reduce the bias due to autocorrelation but also reduces the effective sample size and induces a higher degree of subjectivity (Katajisto & Moilanen 2006). These disadvantages are avoided by the *product kernel* approach of Keating & Cherry (2009), which treats time as a covariate for the kernel function following a wrapped Cauchy distribution. Another method, KDE-DT, is presented in Downs & Horner (2012). Other than the before mentioned extensions, KDE-DT ignores time and looks at trajectories rather than location points. It performs a Delaunay triangulation over which a modified KDE is being run. This modified KDE is restricted to the triangulation network and its fixes (instead of a regular grid that is overlaid over the fixes) and computes the distances between the fixes according to the shortest-path network distances. Whereas other movement-based estimators such as Brownian Bridges provide unrealistic results for very coarse sampling intervals, KDE-DT is still applicable. The downsides of the method are its limited accuracy for fine sampling intervals and the ignorance of time (Downs & Horner 2012).

Instead of extending KDE, Downs et al. (2011) presents a method called time-geographic density estimation (TGDE) that is based on time-geographic techniques. In TGDE, a geoelliptical kernel is placed over two subsequent fixes and computes due to their spatial and temporal differences as well as the maximum velocity of the animal all places where the latter could have been theoretically. By shifting the kernel point by point and summing up the resulting density values, overall isopleths are obtained (Downs et al. 2011; Wall et al. 2014). A slightly modified version

of TDGE can be found in Wall et al. (2014) which estimates all parameters directly from the data. The main advantages of time-geographic techniques are their immunity against varying sampling intervals, the limitation of the kernel to regions that are reachable for the animal, and the ecologically derived smoothing. As a disadvantage, the results strongly depends on the value of the maximum velocity, which may be observed for a specific animal only infrequently (Downs et al. 2011).

With Brownian bridges and biased random bridges, two representatives of mechanistic methods have already been discussed. Dynamic Brownian bridges are another extension to Brownian bridges developed by Kranstauber et al. (2012). As the movement pattern of an animal often varies over time, keeping the variance of the Brownian motion (σ^2_m) constant during an entire trajectory may account for those variations inadequately. Therefore, by using an adjusted version of behavioral change point analysis (Gurarie et al. 2009), different values for the variance are calculated for different behavioral patterns (Kranstauber et al. 2012; Byrne et al. 2014). Instead of using only Brownian motion as a movement model, Börger et al. (2008) and Codling et al. (2008) provide an overview of more complex mechanistic models such as (biased) correlated random walks, Lévy walks, multiscaled random walks or reinforced random walks. Depending on the animal under investigation, these models may lead to more realistic results.

8   Methodology

The coordinates of all datasets were converted from *WGS84* (EPSG: 4326) to the projected spatial reference system *Cape / UTM zone 36S* (EPSG: 22236) for all analyses of this study.

8.1   Selection criteria for the home range estimators

According to simulations, the performance of a home range estimator (HRE) largely depends on the spatial distribution of the data points (Downs & Horner 2008; Getz & Wilmers 2004; Horne & Garton 2006; Lichti & Swihart 2011). This is why the findings of studies that investigated the performance of different HRE were usually contradictory. Examples can be found in Downs & Horner (2008), Getz & Wilmers (2004), Getz et al. (2007), Lichti & Swihart (2011), Seaman & Powell (1999) or Wall et al. (2014). In order to evaluate the performance of the HRE for the present kind of data, simulations would be necessary that mimic the real data as closely as possible (Horne & Garton 2006). This, however, would require knowing the true home ranges, which is not possible. This is why it was not the goal to analyze the assumptions of each HRE to pick the "best" for the analyses. Instead, a variety of different methods were chosen that should provide a sound idea of possible estimations for this kind of data.

An important criterion for the choice of the HRE was their relevance for ecological analyses. That means that the most often used methods should be included in this study which are the MCP and KDE approaches (Downs & Horner 2008; Laver & Kelly 2008; Lichti & Swihart 2011). In

addition, two conceptually different estimators were selected that incorporate the temporal dimension of the data. The time local convex hull (t-LCH) and biased random bridges (BRB) estimators, which are both relatively new, were chosen for this purpose. Although both the t-LCH and BRB approaches are at least methodologically more sophisticated, their complexity keeps within limits, which may be an important factor when being applied to routine ecological analyses.

8.2   Temporal autocorrelation

Whether the GPS data of the leopards and lions are temporally autocorrelated was tested by means of the Schoener's ratio (t^2/r^2). The term t^2 represents the mean squared distance between subsequent fixes, whereas r^2 is the mean squared distance between each single fix and the center of activity (Swihart & Slade 1985b). It has been shown through simulations that the expected value of t^2/r^2 for independent successive observations and a large sample size is close to 2. Values larger than 2 indicate negative autocorrelation, values smaller than 2 positive autocorrelation (De Solla et al. 1999; Swihart & Slade 1985b). More details can be found in Swihart & Slade (1985b) and De Solla et al. (1999).

The Schoener's ratio was calculated using the package *adehabitat* (Calenge 2006) in *R* (R Core Team 2015). Due to memory constraints, the datasets of the lions had to be reduced to 15'000 records. Since some of the datasets include several distinctively different sampling intervals, the ratio was calculated for each of them separately. The dataset of the leopard Mothamongwe for example includes fixes at a sampling interval of 5 h and 90 min. Therefore, one ratio has been calculated for the fixes having the coarse and a second one for the higher sampling interval.

8.3   Uncertainty of collar data

Theoretically, state-of-the-art GPS systems allow horizontal position errors of 3 to 30 m (Lewis et al. 2007; Tomkiewicz et al. 2010). Depending on factors such as canopy closure, topography and collar orientation, position fixes may not only fail but also be biased and thus result in larger errors (Frair et al. 2010; Swanepoel et al. 2010). To quantify the accuracy of the leopards and lions GPS data, their mean deviation from the centroid was calculated by means of the following formula:

$$error = \frac{1}{n}\sqrt{\sum_{i=1}^{n}[(x_i - \bar{x})^2 + (y_i - \bar{y})^2]} \qquad (9)$$

where n is the number of records, x_i and y_i the ith x- and y-coordinate, and $\bar{x}$ and $\bar{y}$ the mean x- and y-coordinates of the whole dataset. Eight datasets from different collars of the two types *GPS Plus Iridium* and *Vertex Survey Iridium* (Vectronic Aerospace GmbH, Berlin, Germany) were available for the error analysis (Table 4).

Table 4. Overview of the datasets to quantify the GPS error. "Vertex" designates the *Vertex Survey Iridium* collar and "GPS Plus" the *GPS Plus Iridium* collar.

Dataset	No. of days	Sampling interval [h]	No. of records
Vertex 1	10	3	38
Vertex 2	10	3	37
Vertex 3	12	3	48
GPS Plus 1	2	1	28
GPS Plus 2	2	1*	29
GPS Plus 3	2	1	25
GPS Plus 4	2	1*	28
GPS Plus 5	29	1	650
*a minority of the records had a shorter sampling interval			

As shown in Table 4, most of the datasets include between 25 and 50 records. For one GPS Plus collar, a longer time series of 650 records was collected over 29 subsequent days. The collar was positioned near the LEC camp in KGR and not moved during the recording of the fixes. Note that all Vertex datasets were collected at a sampling interval of 3 h, while the GPS Plus collars have intervals of mostly 1 h.

8.4   Two stages of home range analysis

8.4.1   Effect of parameters and home range estimators

Due to the high sensitivity of some of the home range estimators on their parameters and the resulting home range on the used estimator (Dürr & Ward 2014; Getz & Wilmers 2004; Seaman & Powell 1996; Wall et al. 2014), it is important to get an idea of the range of potential results. Therefore, the first step of the home range analysis involved the investigation of the effect of the parameters that have been varied and the influence on the HRE itself. A main goal was to quantify the influence of the choice of the parameter values and the home range estimator for this specific kind of data. A second purpose was to provide a basis of decision-making for the reduction of the data volume for the subsequent analyses.

8.4.2   Differences between the individuals

After having quantified the effect of parameters and methods, the results of the home range estimation were compared between the individual leopards and lions. The findings of the previous analysis (Section 8.4.1) were used to reduce the number of comparisons. For example, if the home ranges of t-LCH for a specific leopard fall into two categories whose members are highly similar, one representative per category was chosen for the comparison between the individuals. At least one and at most two results per home range estimator were picked for each individual. The intentions of this analysis step were to compare the home ranges with the literature of other

authors and to analyze their shape and temporal variability. Finally, the differences between the leopards and lions as well as their interactions were discussed.

The temporal partitioning of the dataset is based on ecological expert knowledge. The climate data shown in Chapter 6 indicates a warm and wet season during the hemispherical summer and a cold and dry season during winter. One of the determinants for carnivores is the abundance of prey, which in turn depends on the availability of consumable plants and drinking water (Leopard Ecology & Conservation 2014; Tumenta et al. 2013; Winterbach et al. 2014). As the latter two follow the seasonal climatic variation, it is a key driver for the leopards and lions as well. Thus, in consultation with Stephen Henley[2], two ecologically relevant seasons have been defined: June to September and November to April. The months May and October constitute the transition between these two seasons and are highly variable. They are therefore excluded. For each HRE and individual several home ranges were calculated on the basis of their yearly seasons. The kernel density estimator using the reference bandwidth was chosen to compute the seasonal home ranges due to its tendency to oversmooth (see Sections 10.1.1 and 10.2.1). This characteristic ensures that the temporal variation is affected as little as possible by an inconsistent behavior of the HRE whose variations are mainly due to its functioning instead of real changes. The seasonal home ranges of all years of observation were compared to detect seasonal and other temporal changes.

8.5   Selection of the parameters

8.5.1   MCP

The percentage of points used for the computation of the convex polygon had to be set. For the computation of the home range, the commonly used values of 95 and 50 were chosen.

8.5.2   KDE

Smoothing parameter

Four different methods were selected to derive the bandwidth h from the data: Reference bandwidth (REF), Solve-the-equation plug-in (PI), Biased cross-validation (BCV), and Smoothed cross-validation (SCV). It was initially planned to include the least square cross-validation bandwidth estimator as well. A preliminary analysis, however, revealed that the deficiency of LSCV to compute a result for points that are close together (see Section 7.3.2) inhibited its utilization.

While the whole dataset was used for the bandwidth estimation for the leopard data, it had to be reduced by half for the lions (with points selected randomly). Otherwise the algorithms

---

[2] Personal communication on April 28, 2015. Dr. Stephen Henley works as field coordinator and researcher for LEC in Botswana.

implemented in the *R* package *ks* were not able to determine a value. The only exception is the reference bandwidth, which is simple to compute and therefore managed to use the whole dataset for the lions, too. A brief analysis was carried out (see Appendix A.1) to estimate the effect of the reduced sample size on the resulting bandwidth computed by PI, BCV and SCV. In this analysis, for each of the leopards, the resulting smoothing parameters (PI, BCV and SCV) were calculated when using the full and the half dataset. The bandwidths for the reduced datasets were calculated 10 times for each leopard in order to take possible fluctuations into account that may occur due to the random point selection of the subset. From the range of the resulting ratios between the bandwidth for the complete and the reduced dataset, the most conservative ones were used as correction factors. Thus, the estimated smoothing parameters for the lions were multiplied by the following correction factors: PI: 0.817, BCV: 0.902, SCV: 0.796. The resulting bandwidths for the KDE approach are listed in Table 5 for the leopards and in Table 6 for the lions.

Table 5. Smoothing parameters for the kernel density estimator (KDE) for the leopards.

Leopard	h_{REF}	h_{PI}	h_{BCV}	h_{SCV}
Ronja	2126.9	922.8	2022.5	881.3
Mothamongwe	1614.8	820.8	1488.1	843.9
Bogarigka	3093.5	1183.8	2861.6	1187.3
Gham	2015.7	966.7	1945.8	961.4

Table 6. Smoothing parameters for the kernel density estimator (KDE) for the lions.

Lion	h_{REF}	h_{PI}	h_{BCV}	h_{SCV}
Verity	2873.9	1229.7	2793.5	1171.6
Ella	2132.4	919.7	2102.0	869.6
Jane	2759.8	985.3	2676.7	1023.0
Hitchcock	3270.8	1356.4	3195.2	1308.8
Mexico	1665.0	450.5	1628.1	422.3
Madge	3080.0	680.7	2694.8	723.4
Orange	1694.3	697.6	1665.2	663.5
Getika	2173.3	842.6	2104.5	774.5

Kernel

The *kernelUD*-function of the *R* package *adehabitatHR*, which was selected to compute the KDE, allows to choose between the Gaussian and the Epanechnikov kernel function. According to the literature, the effect of the kernel function is negligible (Gitzen et al. 2006; Kie et al. 2010; Laver & Kelly 2008). This was also confirmed by an own brief analysis (see Appendix A.2), for which the volume of intersection (VI) between the UD provided by the two kernel functions (using h_{REF})

was calculated (for further information about the volume of intersection see Section 8.6.2). Index values between 0.92 and 0.95 indicate a negligible influence of the kernel function. Thus, a comparison of different functions was not carried out and all KDE calculations were performed using the Gaussian kernel.

Although the kernel type (fixed or adaptive) does have a significant effect on the result, a fixed kernel was used for all KDE results. One reason for this decision is that the literature generally recommends to use this kernel type (Gitzen et al. 2006; Millspaugh & Marzluff 2001; Millspaugh et al. 2004; Seaman et al. 1999). A second reason is that the *adehabitatHR* package (and all the others that have been reviewed) supports only the fixed kernel.

Grid and extent

The extent parameter allows to determine how much larger the area is compared to the minimum bounding rectangle around all the points that is considered by the UD. The grid parameter controls the number of cells in each dimension for which individual UD values are calculated. The higher the value of these two parameters, the higher the computational effort. An extent-factor of 0.3 and a grid of 700 cells were set for all individuals.

8.5.3   t-LCH

Due to computational issues, only every second point of the lion datasets was used for the t-LCH approach. The algorithms of the *R* package *tlocoh* (used for the computation of t-LCH) could not deal with more than approximately 15'000 data points. In order to process a reasonably broad range of k- and a-values, 10'000 data points appeared to be the threshold. With more points, the memory of the computer was overloaded and *R* crashed.

Thin out bursts

t-LCH is one of the home range estimators whose results may be biased by strongly varying sampling intervals within a dataset. In order to reduce potential bias, the *tlocoh* package provides a tool to remove the most extreme bursts based on a threshold (subsequently called *burst value)*. Its value was chosen so that at most 10 % of the data were discarded.

Neighborhood selection: *a*- and *k*-value

Of the three rules to select the neighborhood for the local convex polygons, the a- and k-rule are usually preferred over the r-rule due to their lower errors (according to simulations) and dependency on the exact neighborhood value (Dürr & Ward 2014; Getz et al. 2007; Lichti & Swihart 2011). For these reasons, the a- and k-method were selected to compute the t-LCH home ranges.

In order to choose an appropriate *a*- or *k*-value, a broad range of values needs to be calculated that can be analyzed subsequently. In a first step, the isopleth plots of the results were analyzed visually to narrow down the range of reasonable results. This means that neighborhood values that lead to very fragmented home ranges with a huge number of holes even in the 50 % core area, as well as values that result in massively "oversmoothed" home ranges lacking any level of detail got excluded. After that, the area of different isopleths (e.g. 95 %, 75 % and 50 %) was plotted against the neighborhood value. Sharp jumps in area indicate outliers and abrupt changes between relatively stable states. Whereas outliers were excluded from the list of appropriate neighborhood values, abrupt changes were used to partition the values into relatively homogeneous groups. As a third tool, the ratio of the total perimeter to the area was plotted against the *a*-/*k*-value. This plot shows how fragmented and patchy the isopleths are. Sharp jumps in this plot indicate neighborhood values at which spurious or legitimate holes are filled. Again, neighborhood values that indicate a transition between two stable states were excluded. Of the remaining range of values, two neighborhood values for both the *a*- and *k*-method were selected (using the isopleth plots) that represent a lower and upper bound. While the former provides a slightly fragmented but detailed view of the home range, the latter is rather oversmoothed and reduced to the most important features.

Influence of time

The parameter *s* is a scaling factor that controls the impact of the temporal difference between two fixes (Dürr & Ward 2014; Lyons et al. 2013). Since there is no optimal or right value for this scaling factor, the developers of the t-LCH approach recommend to start with an *s*-value that time-selects 60 % of the hulls and then try different values as well (Lyons et al. 2013). In this study, *s*-values were used that time-select 40, 60 and 80 percent of the hulls. In addition, an *s*-value of 0 was used, what actually eliminates the impact of time and results in the classical local convex hull (LCH) approach.

Parameter overview

Table 7 and Table 8 present the parameter values used for the t-LCH estimator for the leopards and lions, respectively. Two *a*- and two *k*-values were selected for each of the four *s*-values per individual. Thus, 16 home ranges were calculated in total for each leopard and lion using t-LCH.

Table 7. Parameter overview of the t-LCH approach for the leopards. The parameter values that were selected for the ecological analysis of the individuals are highlighted.

Leopard	burst value	s	a_1, a_2	k_1, k_2
Ronja	0.60	0	130'000, 220'000	95, 165
		0.023	160'000, 250'000	100, 150
		0.040	150'000, 220'000	*95, 165*
		0.096	160'000, 240'000	105, 135
Mothamongwe	0.280	0	100'000, 160'000	105, 135
		0.005	110'000, 300'000	70, 95
		0.010	150'000, 290'000	*90, 140*
		0.025	180'000, 260'000	95, 140
Bogarigka	0.960	0	240'000, 400'000	125, 210
		0.004	190'000, 300'000	125, 185
		0.009	200'000, 310'000	*145, 205*
		0.023	230'000, 350'000	155, 195
Gham	0.985	0	130'000, 240'000	90, 160
		0.0005	160'000, 270'000	115, 155
		0.0012	120'000, 220'000	*135, 170*
		0.0031	90'000, 170'000	115, 165

Table 8. Parameter overview of the t-LCH approach for the lions. The parameter values that were selected for the ecological analysis of the individuals are highlighted.

Lion	*burst value*	*s*	*a₁, a₂*	*k₁, k₂*
		0	310'000, 490'000	160, 250
		0.002	190'000, 340'000	160, 230
Verity	0.990	*0.008*	240'000, 340'000	*170, 270*
		0.022	290'000, 450'000	170, 250
		0	300'000, 480'000	180, 290
		0.001	140'000, 210'000	190, 300
Ella	0.980	*0.005*	160'000, 280'000	*180, 280*
		0.020	240'000, 320'000	170, 270
		0	280'000, 500'000	150, 250
		0.003	160'000, 290'000	180, 310
Jane	0.980	*0.007*	170'000, 290'000	*170, 250*
		0.022	190'000, 270'000	170, 260
		0	320'000, 440'000	150, 250
		0.002	140'000, 340'000	170, 250
Hitchcock	0.990	*0.006*	220'000, 310'000	*180, 270*
		0.025	240'000, 340'000	150, 270
		0	170'000, 370'000	110, 210
		0.002	160'000, 310'000	160, 250
Mexico	0.987	*0.007*	150'000, 270'000	*150, 260*
		0.028	190'000, 290'000	160, 270
		0	200'000, 400'000	150, 280
		0.002	260'000, 380'000	160, 270
Madge	0.980	*0.005*	240'000, 380'000	*180, 250*
		0.023	230'000, 400'000	180, 270
		0	200'000, 420'000	140, 260
		0.004	160'000, 290'000	110, 220
Orange	0.495	*0.010*	130'000, 290'000	*90, 230*
		0.038	180'000, 330'000	120, 230
		0	210'000, 310'000	190, 340
		0.004	160'000, 320'000	160, 250
Getika	0.985	*0.018*	230'000, 340'000	*160, 300*
		0.045	210'000, 310'000	190, 310

8.5.4   BRB

Section 7.3.4 describes the principles of the biased random bridges approach in theory. In practice, BRB is usually approximated by a movement-based KDE. The reasons for that are mathematical difficulties in solving some of the differential equations (particularly due to the anisotropy of the diffusion coefficient) (Benhamou 2011; Börger et al. 2008). So far, the exact version of BRB has not been implemented in any known R package. Since the mathematical differences are quite small and the lack of the diffusion anisotropy negligible, the usage of the movement-based KDE is a valid approximation of BRB (Benhamou 2011).

Smoothing parameter h_{min}

Since BRB is a mechanistic rather than a statistic approach as (location-based) KDE is, its smoothing parameter h_{min} should be based on ecological grounds (Börger et al. 2008; Kie et al. 2010; Wall et al. 2014). One component of h_{min} is the uncertainty of the position measurement. As presented in Section 9.2, the observed errors are between 2 and 15 m. Because the GPS error may be larger when the orientation of the collar is not ideal or the field of view between the satellites and the collar is restricted (e.g. animal lying under a tree), twice the maximum observed error (30 m) was selected for the uncertainty component.

In order to quantify the second component of h_{min} (all potential locations at a specific time, see Section 7.3.4), the recommendation of Benhamou & Cornélis (2010) and Jay et al. (2012) was applied. It intends that half the distance that can be covered by an animal over a longer time period using its maximum transit velocity is added to the uncertainty component. "A longer time period" was defined as 30 to 120 minutes, depending on the sampling intervals present in a dataset, whereas the maximum travel velocity was defined as the 99th percentile of speeds found in a dataset. Thus, the value of the 99th percentile velocity found in the part of the dataset that was sampled at the most abundant sampling interval between 30 and 120 min was multiplied with the respective sampling interval. Then, half this distance was added to the 30 m of the uncertainty component to obtain the value of h_{min}.

Due to the varying sampling intervals within a dataset the definition of h_{min} is somewhat ambiguous. For example, the lioness named Jane has two main sampling intervals of 30 min and 60 min. While the maximum travel velocity does not depend much on the choice of taking 30 min or 60 min as the sampling interval (3.32 km/h vs. 2.87 km/h), the smoothing parameter almost doubles (860.7 m vs. 1463.5 m). Except for the choice of the sampling interval used to compute h_{min}, the formula of Benhamou & Cornélis (2010) and Jay et al. (2012) is only a general recommendation and may not be equally adequate in all cases. To take these issues into account, a range of values for the smoothing parameter was calculated. The value of h_{min} obtained by the above-mentioned formula served as a reference value that was reduced and increased in steps of 20 %. Thus, h_{min} was scaled by a list of factors (e.g. [0.6, 0.8, 1.0, 1.2, 1.4]). The range of this list

was restricted manually so that only reasonable UD resulted that were not overly fragmented or oversmoothed. However, the BRB result using the unscaled smoothing parameter h_{min} was calculated for all individuals for comparison, even if it produced highly fragmented or oversmoothed results.

Maximum time difference t_{max}

T_{max} determines the maximally allowed time difference between two consecutive fixes so that they are considered for the computation of BRB. It should be large enough to incorporate the regular sampling intervals of a dataset but small enough to exclude time differences that are too large to guarantee serial autocorrelation (Benhamou 2011). The results of Section 9.1 clearly showed that all regular sampling intervals fulfill the condition of autocorrelation. Therefore, the value of t_{max} was set to be large enough to incorporate the regular sampling intervals of the respective datasets.

Minimum movement threshold l_{min}

In the absence of binary activity data indicating resting times, a value needs to be selected for l_{min}. This parameter defines the minimum distance between two consecutive points so that the bridge built by them is considered as movement. The selection of l_{min} followed the suggestion of Dürr & Ward (2014), which used twice the value of the measurement uncertainty. For this study, a value of 30 m was set for l_{min} for all individuals.

Number of segments for a bridge *tau*

The approximation of BRB through movement-based KDE requires subdividing a single bridge into several steps of duration *tau*. For each of these steps a kernel density estimation is performed. As rules or guidelines for selecting a value for *tau* are lacking, a brief analysis was conducted to quantify the effect of its value. Thus, a variety of values for *tau* (1, 3, 6, 12 and 15 min) was used to calculate the area of the 50 % and 95 % home range isopleth for the four leopards. In a second step, the obtained areas for each individual were divided by the maximum value (separately for the 50 % and 95 % result). The resulting values show the difference between the largest and the smallest area (see Appendix A.3). The biggest observed difference was 1.5 % for the 50 % isopleth area of Bogarigka. All the other differences of the 50 % and 95 % isopleths were between 0.1 % and 1.0 %. Therefore, the influence of *tau* was considered as negligible and a single constant value was used for each individual. A duration of 10 % of the smallest regular sampling interval was selected for the parameter *tau*.

Grid and extent

An explanation of the extent and grid parameters can be found in Section 8.5.2. The same values were used here as for KDE (extent = 0.3, grid = 700).

Parameter overview

Table 9 and Table 10 give an overview of the selected parameters for the BRB approach for the leopards and lions, respectively. Different results per individual were calculated by varying the h_{min} factors in steps of 20 % of the reference smoothing value.

Table 9. Selected parameters for the BRB approach for the leopards. The h_{min} factors are increased in steps of 0.2. The result using the reference value of h_{min} (1.0) was computed for every individual.

Leopard	h_{min} [m]	h_{min} factors	t_{max} [min]	l_{min} [m]	tau [min]
Ronja	1246.4	0.6–1.6	310	30	12
Mothamongwe	1924.2	0.4–1.4	310	30	9
Bogarigka	1396.1	1.6–2.4	190	30	6
Gham	1331.6	0.8–1.6	190	30	6

Table 10. Selected parameters for the BRB approach for the lions. The h_{min} factors are increased in steps of 0.2. The result using the reference value of h_{min} (1.0) was computed for every individual.

Lion	h_{min} [m]	h_{min} factors	t_{max} [min]	l_{min} [m]	tau [min]
Verity	893.9	1.8–2.2	40	30	3
Ella	925.4	1.4–2.2	70	30	3
Jane	1463.5	1.2–2.0	70	30	3
Hitchcock	1422.1	1.6–2.2	70	30	3
Mexico	1123.9	1.6–2.4	70	30	3
Madge	1479.2	1.6–2.4	70	30	3
Orange	1768.7	0.8–1.6	70	30	3
Getika	917.6	1.4–2.2	40	30	3

8.6 Criteria of home range comparison

For each of the home range estimators, the 95 % and 50 % isopleths were computed. For KDE and BRB, which result in a utilization distribution (UD), the UD was computed as well. A series of measures was determined to describe the resulting home ranges and allow comparisons between them.

8.6.1 Home range descriptors

The following measures were determined to describe the features of a 95 % or 50 % home range isopleth:

- Area
- Number of holes
- Number of disjoint areas
- Relative size of the 50 % core area to the 95 % home range
- Compactness

The size of the area includes all polygons of a home range (in case several disjoint polygons are present) but does not count the area of holes, if present. A hole needs to have an area of at least 0.25 km^2 to be counted. This threshold was set to exclude spurious holes that are probably only an artefact of the HRE. A lower limit was also applied for the number of disjoint areas. They need to have an area of at least 1 km^2, otherwise they were ignored. The relative size of the core area designates the size of the core area (50 % isopleth) in relation to the entire home range area (95 % isopleth). As a last measure, the compactness was computed. The compactness measure *S* used in this study is defined as

$$S = \frac{4A}{\pi D^2} \tag{10}$$

with *A* being the area of the isopleth (areas of holes are included) and *D* the diameter of the smallest circumscribing circle around all (possibly spatially disjoint) parts of the isopleth (Ebdon 1985). The compactness thus describes the ratio of the areas of the home range isopleth and the smallest circle that encircles the whole isopleth. It is an indicator of the ecological efficiency since a circle has the lowest perimeter at a given area (Ebdon 1985). Thus, such a home range allows an animal to reach every point of the area quickly and reduces the length of the perimeter that needs to be defended against intruders.

8.6.2 Overlap measures

Two measures of spatial overlap were calculated to quantify how well two home range results equal each other. The first of them is a spatial intersection of two isopleths stemming from different results. The overlapping area is divided by the areas of the respective isopleths to obtain the relative value of intersection.

For those HRE that produce a utilization distribution (KDE and BRB), the intersection of their UD was computed as well. Other than the home range isopleths, which only inform about where an animal has been, the UD also informs about how frequently a specific region has been used by the animal (Fieberg & Kochanny 2005; Gitzen et al. 2006). Thus, an intersection of two utilization distributions also takes into account how frequently the overlapping regions have been used (Fieberg & Kochanny 2005; Millspaugh et al. 2004). Seidel (1992 in Fieberg & Kochanny 2005) developed an index called volume of intersection (VI) index that applies the idea of an intersection of UD. The values of this index range between 0 (no overlap) and 1 (complete overlap). Further details about the VI index can be found in Fieberg & Kochanny (2005) and Millspaugh et al. (2004). The VI index was applied as a second measure to quantify the overlap for KDE and BRB. A threshold of 95 % was used for the computation, which means that the 5 % of the UD with the lowest space use density were excluded from the intersection.

8.6.3   Coefficient of variation

The coefficient of variation (CV) was used to summarize the results of the individual leopards and lions to exclude their impact on the performance of the HRE and their parameters. It divides the standard deviation by the average to normalize its value. This normalization allows to quantify the variation irrespectively of the absolute values. The CV was calculated for the area and compactness of the 50 % and 95 % isopleths of each HRE for each individual separately.

8.7   Hardware and Software

All analyses were done in *R* (version 3.2.0) (R Core Team 2015) using *RStudio* (version 0.99.442) as an integrated development environment (IDE). The programming software ran on a Windows 8.1 (64 Bit) machine with 16 gigabytes of memory. Except for the basic functionalities provided by *R*, different additional packages were used for the different analyses. Table 11 gives an overview of the most important packages.

Table 11. Summary of the most important *R* packages used for the analyses.

R package	Usage in this study
adehabitat	Computation of Schoener's ratio
adehabitatHR	Computation of MCP, KDE and VI index
adehabitatLT	Provides the data structure for BRB
hab	Calculation of the Euclidean distances between two individuals
ks	Estimation of bandwidths for KDE
maptools	Provides tools to manipulate spatial objects
move	Get basic movement measures
rgdal	Reprojection of the spatial reference system
rgeos	Computation of home range overlap
sp	Provides spatial data structures
T-LoCoH	Computation of t-LCH
tripack	Computation of shape measures

9   Results

9.1   Temporal autocorrelation

The Schoener's ratios t^2/r^2 shown in Table 12 (lions) and Table 13 (leopards) are clearly below the critical region around the value of 2. The highest value of the observed lions is 0.00998 for the part of the data of Orange that has been sampled at 60 min intervals. Since this value is much smaller than 2, the lion data can be regarded as positively autocorrelated. The Schoener's ratios of the leopards are considerably higher than those of the lions, with a maximum value of 0.09582 (Mothamongwe, 300 min.). This difference is caused by the coarser sampling interval: The lower

it is, the lower is the temporal autocorrelation and accordingly the higher is the Schoener's ratio (De Solla et al. 1999; Swihart & Slade 1985b). Nevertheless, even the 5 h sampling intervals of the leopards lead to values well below the threshold of 2. Therefore, also the leopard data is positively autocorrelated.

Table 12. Schoener's ratios for the different sampling intervals of the lions

Individual	Sampling interval [min]	t^2/r^2
Verity	30	0.00062
Ella	30	0.00098
	60	0.00320
Jane	30	0.00070
	60	0.00219
Hitchcock	30	0.00073
	60	0.00246
Mexico	30	0.00247
Madge	30	0.00118
	60	0.00384
Orange	30	0.00349
	60	0.00998
Getika	30	0.00149

Table 13. Schoener's ratios for the different sampling intervals of the leopards.

Individual	Sampling interval [min]	t^2/r^2
Ronja	120	0.00217
	180	0.02083
	300	0.02186
Mothamongwe	90	0.01807
	300	0.09582
Bogarigka	60	0.00240
	180	0.01389
Gham	60	0.00908
	180	0.04646

9.2   Uncertainty of collar data

The eight control datasets shown in Table 4 resulted in horizontal errors of 2.1 m to 15.0 m. The individual results are listed in Table 14. The dataset containing 650 records (GPS Plus 5) corresponds fairly well to the other, much smaller GPS Plus datasets. The Vertex datasets seem to have higher errors (4.9–15.0 m) than the GPS Plus datasets (2.1–7.6 m). Since the former

belong not only to a different collar type but were also sampled at a coarser sampling interval (3 h instead of 1 h), the cause for the discrepancy could not be determined. In addition, the low number of records of the datasets (except for GPS Plus 5) does not allow inferences about the statistical significance of the discrepancy. However, for the purpose of home range estimation, the magnitude of the errors is unobjectionable.

Table 14. Horizontal errors of the eight control datasets.

Dataset	Horizontal error
Vertex 1	15.0 m
Vertex 2	4.9 m
Vertex 3	11.4 m
GPS Plus 1	2.2 m
GPS Plus 2	2.2 m
GPS Plus 3	7.6 m
GPS Plus 4	2.1 m
GPS Plus 5	2.3 m

9.3   Effect of parameters

9.3.1   KDE

Table 15 shows the coefficients of variation of the KDE approach. The relative variations of the area are comparable for the 50 % and 95 % home range isopleths, with mean CV values of 13 % and 17 %, respectively. The difference of the compactness values is much more pronounced, with values of 13–85 % for the core area and 7–45 % for the 95 % isopleth. While the mean and median CV values are moderate for the compactness of the 95 % home range boundary, they are considerably larger for the core area. A Kruskal-Wallis test with the normalized areas and compactness indices (of both the 50 % and 95 % isopleths) was conducted to test whether the KDE home range estimates produced by the four different bandwidth estimators differ significantly. P-values smaller than 1.13×10^{-08} (χ^2 between 39.89 and 158.29, df = 3) required to reject the null hypothesis ($\alpha = 0.05$). Thus, there is a difference between the results of KDE.

Table 15. Coefficient of variation values of KDE. A summary of the coefficients of all individuals is shown.

	50 %		95 %	
CV measure	Area [%]	Compactness [%]	Area [%]	Compactness [%]
Minimum	9	13	6	7
Maximum	29	85	25	45
Median	17	53	11	16
Mean	17	53	13	17

A closer look at the differences between the parameter sets of KDE revealed that the results of each individual can be assigned to one of two groups (see Figure 12). One of them comprises the results of REF and BCV. Their area sizes and compactness values of both the 50 % and the 95 % isopleth differ on average less than 3 %. In addition, their VI indices are above 0.96, which means nearly identical utilization distributions. The home range estimates of the second group, which comprises the results of PI and SCV, show the same degree of conformity. The high similarity of the KDE results estimated using PI and SCV was confirmed through a Kruskal-Wallis test statistic: The areas and compactness indices of the 50 % and 95 % isopleth do not differ significantly when using a threshold of 5 % (χ^2 :0.024–0.068, df: 1, p: 0.59-0.88). The contrary is true for REF and BCV which produce significantly different results according to the test (χ^2: 30.75–53.39, df: 1, p smaller than $2.74*10^{-5}$). However, this seems to be an issue with the functioning of the test (see discussion in Section 10.1.1).

The differences between PI/SCV and REF/BCV are quite pronounced. The areas of the 50 % and 95 % home range boundaries produced by PI and SCV are on average roughly 30 % resp. 20 % smaller than those of the other group. The compactness of the 50 % isopleth is on average approx. 65 % smaller (95 % isopleth: 30 % smaller). Considering also the number of disjoint areas and the number of holes (see Appendix A.5, which are usually much higher for PI and SCV, the home range estimates produced by PI and SCV tend to be undersmoothed and fragmented (compare Figure 12). The datasets of the lions are affected more severely by the undersmoothing of PI and SCV than those of the leopards. For all of them, the number of regions for both the 50 % and 95 % isopleth is considerably increased. Whereas the number of holes of the 95 % isopleth is increased as well for most of the lions (when using PI or SCV), no such trend can be observed for the number of holes of the core area.
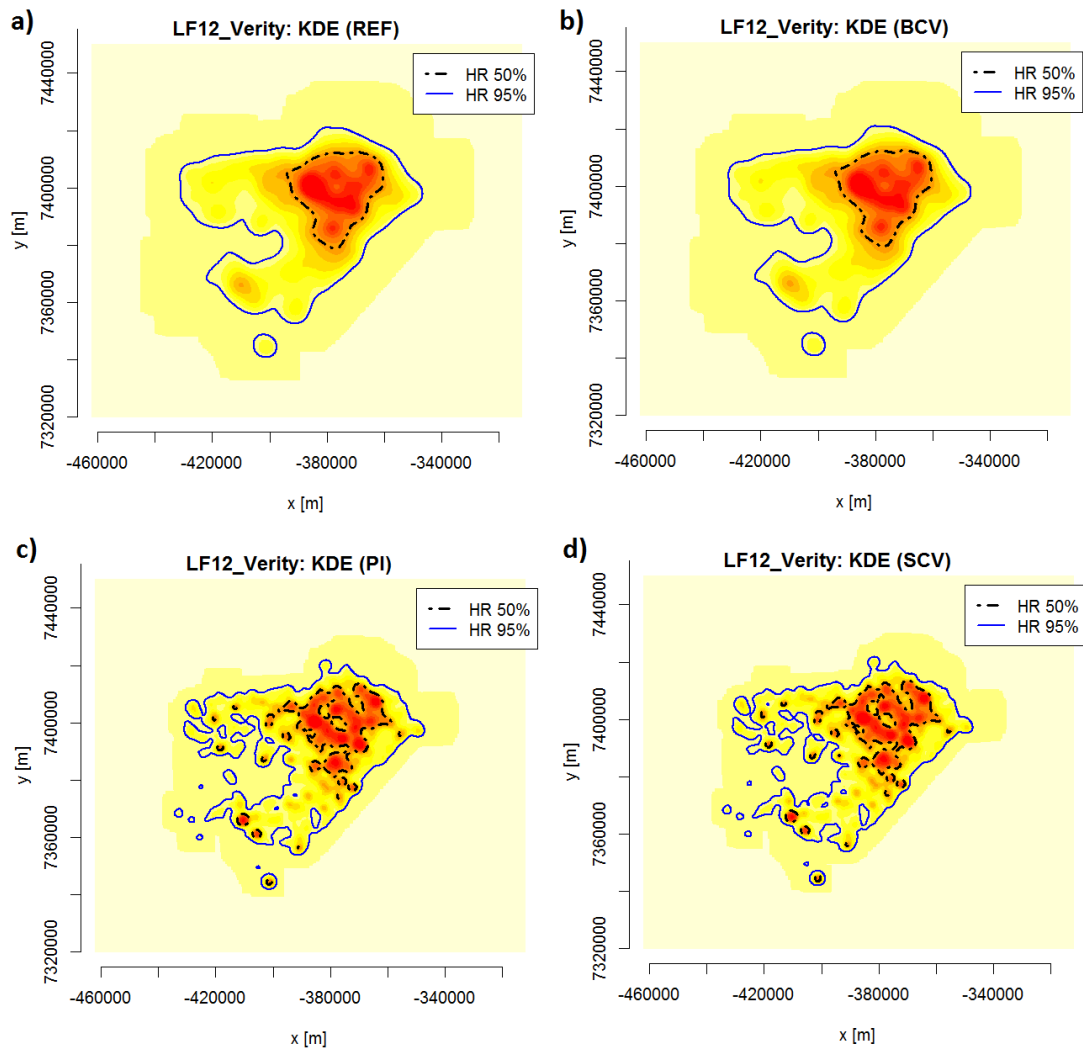
Figure 12. Example of the high similarities between REF (a) and BCV (b), as well as PI (c) and SCV (d). The home ranges of PI and SCV tend to be fragmented and undersmoothed, whereas REF and BCV seem to oversmooth slightly.

9.3.2 t-LCH

The summarized CV values for the time local convex polygon estimator are presented in Table 16. Both the relative standard deviations of the area and the compactness are clearly smaller for the 95 % home range isopleth than for the core area. Particularly the compactness of the latter shows a wide range (19–71 %) and has a high mean CV of 34 %. The scattering of the 50 % area is also quite pronounced, with a maximum value of 33 % and a mean value of 21 %. The area and compactness of the 95 % isopleth can be termed as stable, with mean and median values of 7 % resp. 10 %. Overall, there is a significant difference between the area values and compactness indices for both isopleths of all computed t-LCH home ranges. Due to the large number of

statistical tests conducted for t-LCH, their results are listed in Table 17 instead of being mentioned in the running text.

Table 16. CV-values of t-LCH. A summary of the coefficients of all individuals is shown.

	50 %		95 %	
CV measure	**Area [%]**	**Compactness [%]**	**Area [%]**	**Compactness [%]**
Minimum	9	19	4	5
Maximum	33	71	10	16
Median	22	31	7	10
Mean	21	34	7	10

In addition to the overall similarity it was investigated whether there are trends observable for the individual parameters. Neither for the results produced by the *a*-rule nor by the *k*-rule the null hypothesis could be met for any of the four measures (see Table 17, columns "a-rule" and "k-rule"). However, the p-values for the *k*-rule are several magnitudes larger than those of the *a*-rule. There are also significant differences between the results produced by using the *s*-value that time-selects 0 %, 40 %, 60 % or 80 % of the hulls (columns "s0", "s40", "s60" and "s80"). The only exception to this is the area of the 50 % isopleth when testing all results with an *s*-value of 0. When looking at the combinations of the neighborhood rule parameter and the time parameter separately, high similarities can be observed between the *s*-values that time-select 40 %, 60 % and 80 % of the hulls. In fact, there is no significant difference for nearly all of the measures between the 60 % and 80 % *s*-values when looking at the *a*- and *k*-rule results separately (columns "a-rule: s60-s80" and "k-rule: s60-s80"). The same is true for the 40 % and 60 % *s*-values (columns "a-rule: s40-s60" and "k-rule: s40-s60").

The findings of the tests are in agreement with the optical analysis of the results (compare Figure 13): The *a*-rule results in distinctively different isopleths than the *k*-rule as soon as the time is incorporated. The 50 % isopleth of the latter show much more spatial detail, are more fragmented and usually consist of more disjoint polygons. The core areas of the *a*-rule, on the other hand, are very compact (mean compactness of 0.53 compared to 0.35 for *k*) and resemble a circle in shape. Because of that, they show much less spatial detail. The mentioned tendencies are also true for the 95 % isopleth, but are much less pronounced there. Another substantial differences is observable between the exclusion and inclusion of time. When no hulls are time-selected, the above-mentioned differences between the *a*- and *k*-rule are mostly absent. In that case, both the 50 % and 95 % isopleth are quite fragmented and the core area consists of a collection of circular polygons which can be connected to each other or disjoint. As soon as time is included, the isopleths (particularly the 50 % isopleth) are strongly directed and interconnected when using the *k*-rule. For the a-rule, the isopleths become also slightly directed but tend heavily towards a

compact shape. The degree to which the time is included does hardly alter the mentioned patterns, although they seem to become marginally stronger from 40 % to 80 % of time-selected hulls.
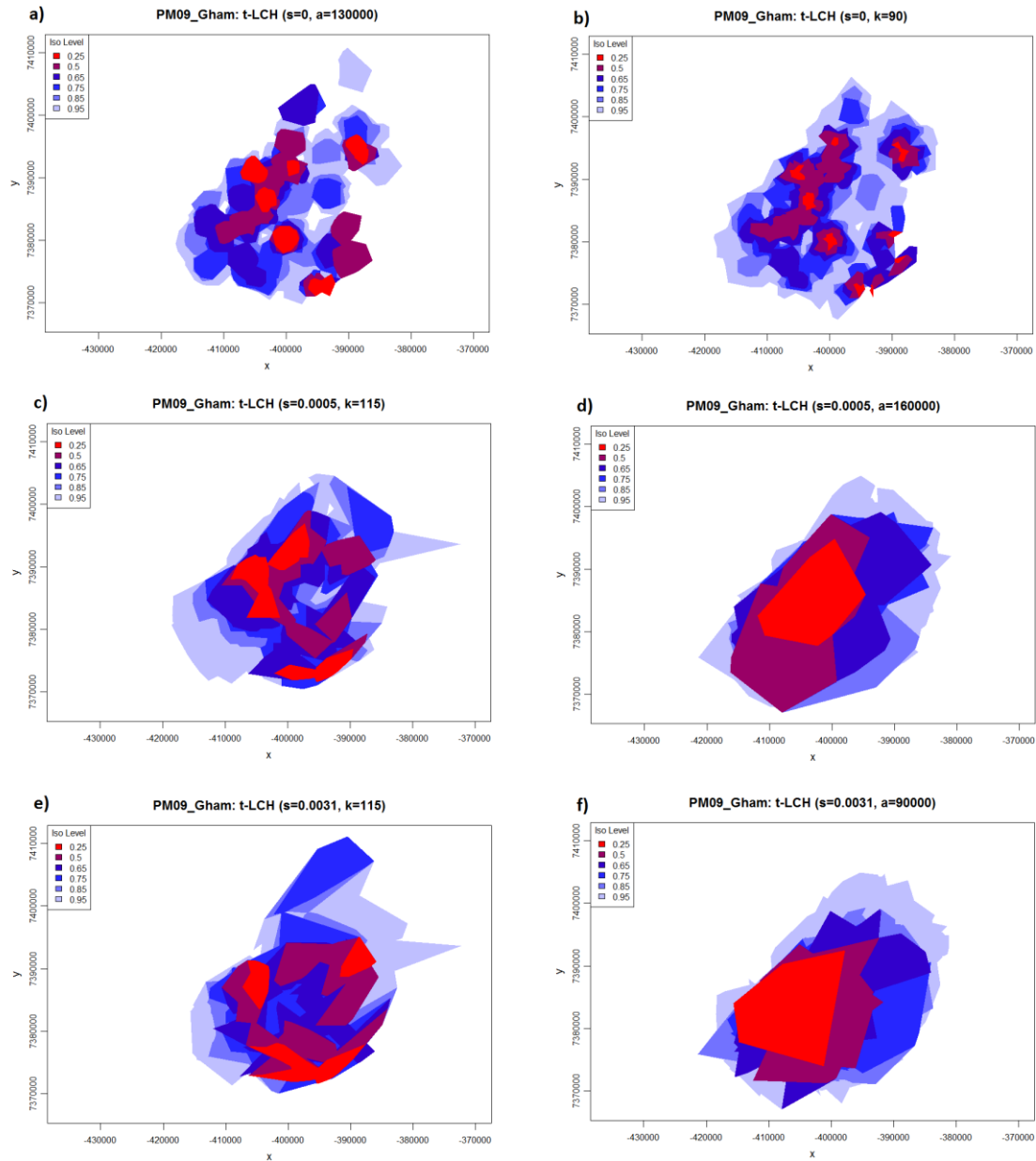
Figure 13. Influence of the parameters of t-LCH. The results of the *k*-rule (a), c), e)) have more detailed and fragmented isopleths, whereas those of the *a*-rule (b), d), e)) are very compact when time is included (illustrations c)–f)). The exclusion of time (a) and b) leads to a dot-like pattern. The differences between 40 % (c) and d)) and 80 % (e) and f)) of the hulls being time-selected are small and inconsistent.

Table 17. Statistical test results of the effect of parameters for t-LCH. The column "data basis" refers to the selection of home range results used as input for the test statistic. Significant p-values (p ≥ 0.05) are highlighted in bold characters. p-values that are close to significance (p ≥ 0.03) are underlined with a dotted line.

Data basis	Area 50% isopleth			Compactness 50% isopleth			Area 95 % isopleth			Compactness 95% isopleth		
	χ^2	df	p	χ^2	df	p	χ^2	df	p	χ^2	df	p
overall	101.930	15	$5.61*10^{-15}$	116.36	15	$< 2.2*10^{-16}$	88.698	15	$1.73*10^{-12}$	50.972	15	$8.34*10^{-6}$
a-rule	50.848	7	$9.84*10^{-9}$	56.133	7	$8.89*10^{-10}$	57.120	7	$5.66*10^{-10}$	20.595	7	0.0044
k-rule	32.997	7	$2.65*10^{-5}$	25.29	7	0.0007	21.158	7	0.0035	21.959	7	0.0026
s0	6.227	3	**0.1011**	11.225	3	0.0106	16.825	3	0.0008	12.200	3	0.0067
s40	12.394	3	0.0061	29.145	3	$2.09*10^{-6}$	7.941	3	0.0472	14.252	3	0.0026
s60	14.272	3	0.0026	23.892	3	$2.63*10^{-5}$	11.643	3	0.0087	15.055	3	0.0018
s80	14.376	3	0.0024	18.824	3	0.0003	12.502	3	0.0058	8.058	3	0.0448
a-rule: s40-s80	8.379	5	**0.1366**	14.496	5	0.0128	15.670	5	0.0079	2.597	5	**0.7618**
k-rule: s40-s80	4.798	5	**0.4411**	13.582	5	0.0185	9.138	5	**0.1037**	12.276	5	0.0312
a-rule: s40-s60	3.484	3	**0.3228**	5.5465	3	**0.1359**	6.292	3	**0.0983**	0.578	3	**0.9014**
a-rule: s60-s80	7.910	3	0.0479	4.6827	3	**0.1966**	7.150	3	**0.0673**	1.973	3	**0.5780**
k-rule: s40-s60	2.004	3	**0.5715**	8.1516	3	0.0430	6.904	3	**0.0750**	10.907	3	0.0122
k-rule: s60-s80	4.008	3	**0.2606**	7.7451	3	**0.0516**	5.969	3	**0.1131**	6.381	3	**0.0944**

9.3.3 BRB

Note that the results of BRB were not derived from independently determined values for one or several parameters but were rather scaled versions of a single reference value (h_{min}) and thus interrelated.

As shown in Table 18 the relative standard deviations are quite small for the areas of both isopleths (mean of 6 % resp. 5 %). In addition, the areas can be regarded as stable, with ranges of 6 % and 4 %. Although the area correlates with the (scaled) value of h_{min} (compare Figure 14), its coefficient is smaller than 1. The CV of the compactness for the 95 % isopleth has a moderate mean and median, but reached a maximum value of 17 %. The compactness of the core area is markedly less stable, with a maximum of 35 % for the CV and a quite pronounced mean value of 18 %. The compactness index increases together with h_{min} but the relation is not linear and has a slope smaller than 1. According to the Kruskal-Wallis test, the results (Table 18) are significantly different regarding both their area (χ^2: 34.349, df: 3, p: $1.67*10^{-7}$) and compactness (χ^2: 27.271, df: 3, p: $1.36*10^{-5}$) of the 50 % isopleth. For the 95 % isopleth, the area (χ^2:35.822, df: 3, p: $8.164*10^{-8}$) and the compactness (χ^2: 16.645, df: 3, p: 0.0008) are significantly different, too.

Table 18. CV-values of BRB. A summary of the coefficients of all individuals is shown.

CV measure	50 %		95 %	
	Area [%]	Compactness [%]	Area [%]	Compactness [%]
Minimum	3	5	4	3
Maximum	9	35	8	17
Median	6	20	5	6
Mean	6	18	5	8
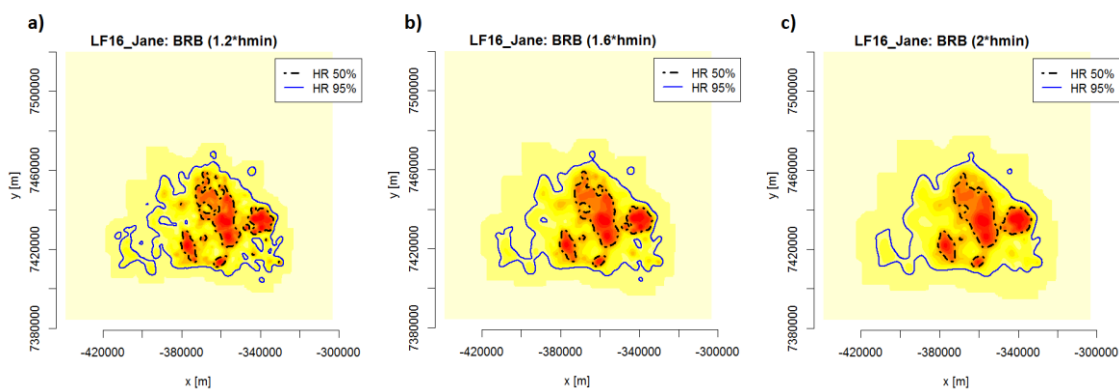
Figure 14. Effect of the parameter h_{min} of BRB. The areas and the compactness indices of both isopleths are positively correlated to the value of h_{min} (scaling factor increases from image a) to c)).

9.4   Evaluation of the home range estimators

The following results were obtained by taking the average over all parameter versions per home range estimator (see Section 8.5). These mean values were normalized by the largest value found for each HRE so that values between 0 and 1 were obtained.

The MCP approach resulted in the largest 50 % and 95 % home range areas in 10 of 12 cases each. In the other two (respectively four) cases, it produced isopleths that are between 87 % and 98 % of the largest area. This trend was also confirmed by the results listed in Table 19, which presents averaged values over all 12 individuals. At the other end of the range, KDE yielded the smallest estimates for both isopleths in the most cases (on average 70 % and 82 % of MCP for the 50 % and 95 % isopleths). The core areas of the t-LCH approach are usually the second largest (in 10 of 12 cases). The minimum area per individual is, except for one case, between 65 % and 75 % of the maximum area. The typical range for the 50 % isopleth area is accordingly smaller than the one for the 95 % isopleth (70–85 % of the maximum). However, when MCP is ignored, the 95 % isopleths are more similar to each other than the core areas with differences of less than 10 % (on average less than 5 %, compare Table 19) for most individuals. The Kruskal-Wallis test statistics confirms the higher similarity of the 95 % isopleth: Whereas there is a significant difference between the areas of KDE, t-LCH and BRB for the core area (χ^2: 9.480, df: 2, p: 0.0073), they can be considered as being the same for the 95 % isopleth (χ^2: 1.526, df: 2, p: 0.4664). For this and the subsequent tests of Section 9.4 MCP was excluded as it has nearly always a value of 1 for the area and compactness and thus interferes with the test (for the detailed reasons see the discussion in Section 10.1.1). When looking only at individual pairs for the 50 % isopleth, no differences exist between BRB and KDE (χ^2: 3.323, df: 1, p: 0.0683) and BRB and t-LCH (χ^2: 1.847, df: 1, p: 0.1741).

Table 19. Mean normalized descriptive measures of the four HRE. The mean value of all versions of a single HRE was normalized by dividing it by the maximum value of the four HRE (per individual). Here, the average of these values of all individuals are presented. *Comp.* stands for compactness.

Method	50 %				95 %			
	Area	Holes	Regions	Comp.	Area	Holes	Regions	Comp.
MCP	0.99	0.00	0.16	1.00	0.99	0.00	0.18	1.00
KDE	0.70	0.49	1.00	0.30	0.82	0.89	0.92	0.52
t-LCH	0.83	0.36	0.33	0.42	0.85	0.25	0.20	0.64
BRB	0.79	0.70	0.57	0.30	0.87	0.57	0.68	0.57

In the matter of compactness, MCP consistently produced the most compact home range isopleths (normalized values of 1.00 in Table 19). Particularly the core area exhibits particularly high absolute values of at least 0.94, which is very close to a circle (compare Figure 15 a)). The compactness indices of the other methods are only 25–50 % of the one of MCP for the core area

(on average 30–42 %, see Table 19). KDE typically resulted in the lowest compactness, although BRB yielded comparably low values for the core area. t-LCH produced especially for the 50 % isopleth more compact estimates than KDE and BRB. The range of compactness indices is smaller for the 95 % than for the 50 % isopleth in most cases, with relative differences of less than 15 %. Because of two "outliers", the ranges are on average are similar to those of the core area. Statistically, the compactness indices of KDE, t-LCH and BRB are significantly different for the 50 % (χ^2: 13.358, df: 2, p: 0.0013) and 95 % (χ^2: 10.293, df: 2, p: 0.0058) isopleths. However, KDE and BRB (compare Figure 15 c) and d)) result in values that can be considered as being the same (χ^2: 0.054, df: 1, p: 0.8170 for the 50 % boundary and χ^2: 1.548, df: 1, p: 0.2134 for the 95 % boundary). The same is true for the 95 % isopleths of BRB and t-LCH (χ^2: 3.764, df: 1, p: 0.0524), whereas the compactness indices of the 50 % isopleths are too diverse (χ^2: 6.316, df: 1, p: 0.0120).
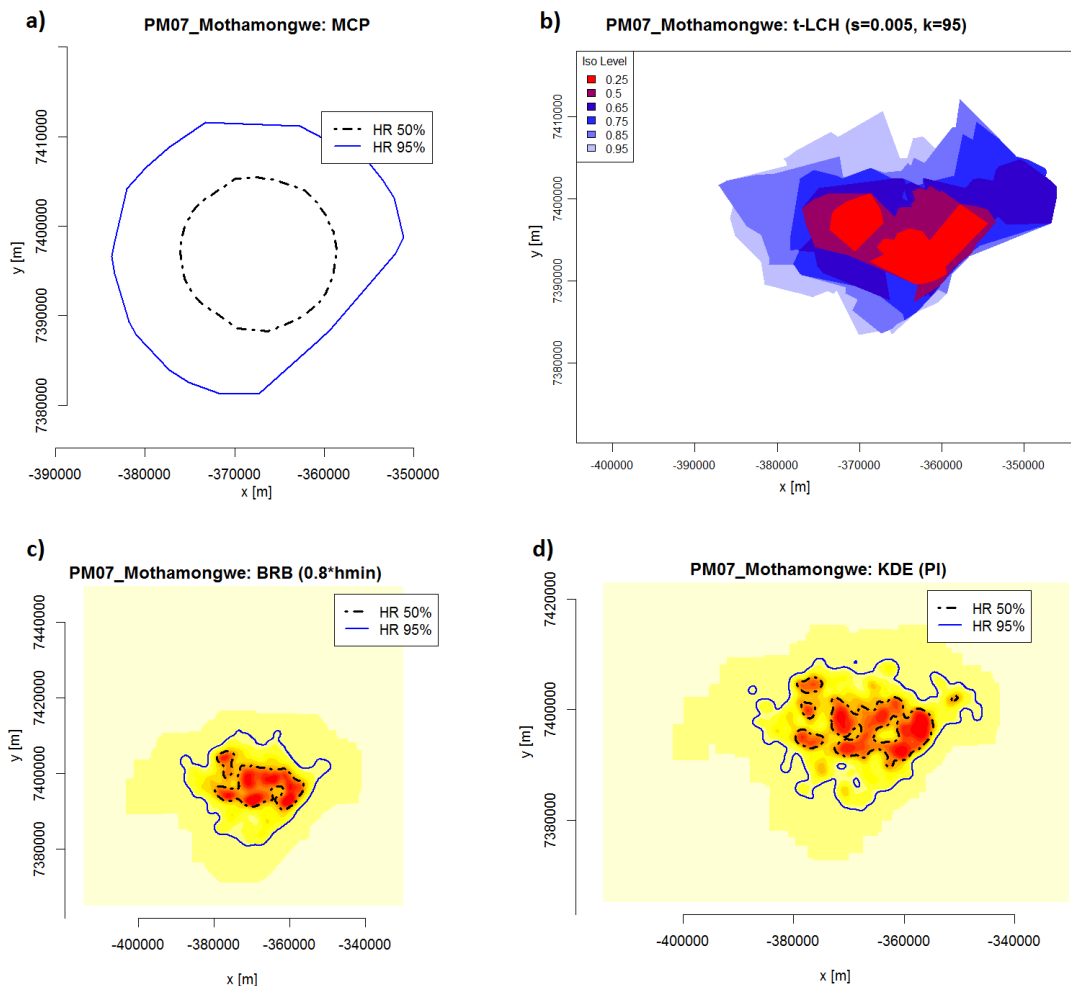
Figure 15. Major trends of the home range estimators in the example of Mothamongwe: MCP (a) with a nearly circular core area, t-LCH (b) with a low number of regions and holes, BRB (c) with a similar size and shape as KDE (d), which tends to have the highest number disjoint regions.

In general KDE resulted in the most fragmented home ranges with the largest number of regions for both isopleths and holes for the core area (compare Figure 15). Only BRB produced similarly high or even higher values (compare the number of holes for the 50 % isopleth in Table 19). t-LCH is quite stable concerning the absolute number of holes and areas and is only undercut by MCP, which has zero holes and one region per definition. While the averaged maximum absolute values for the number of holes of KDE and BRB are small for the core area and moderate for the 95 % isopleth, extreme values were obtained for the number of regions, particularly for KDE.

9.5 Home ranges of individuals and their interactions

9.5.1 Reducing the set of results

Based on the findings from the investigation of the effect of the HRE and their parameters (Sections 9.3, 9.4, 10.1 and 10.2), only a subset of the results per individual is used for the comparison between them. For KDE, the result obtained by using REF as a bandwidth estimator was selected. Other than SCV and PI, which resulted in massively undersmoothed estimates for most of the individuals, REF (and BCV) produced more appropriate home ranges. Because the results of REF are nearly identical to those of BCV but much faster to compute, the former was selected. For t-LCH, the lower and upper boundary value of the k-rule (k_1 and k_2) determined at the s-value that time-selects 60 % of the hulls were considered (compare Table 7 and Table 8). Other than the a-rule, the results of the k-rule show a reasonable level of spatial detail. As the inclusion of time leads to less disjoint regions for both the 50 % and 95 % isopleth and the differences between time-selecting 40 %, 60 % or 80 % of the hulls are minor, the 60 % time inclusion was selected. For BRB, one of the results in the mid-range of the computed values (see Table 9 and Table 10) was selected. Since the different results are equally scaled versions of a reference value, the average of e.g. two more extremes values would lead to an almost identical outcome as taking a result from the middle area. Table 20 gives an overview of the result used for the comparison for each individual.

Table 20. Selected h_{min} factors for BRB for the comparison between the individuals

Individual	Species	h_{min} factor
Ronja	Leopard	1.2
Mothamongwe	Leopard	0.8
Bogarigka	Leopard	2.0
Gham	Leopard	1.4
Verity	Lion	2.0
Ella	Lion	1.8
Jane	Lion	1.6
Hitchcock	Lion	2.0
Mexico	Lion	2.2
Madge	Lion	1.8
Orange	Lion	1.4
Getika	Lion	1.8

9.5.2   Leopards

The average home range sizes of the leopards range between 695 and 2357 km^2 for the 95 % isopleth and between 202 and 487 km^2 for the 50 % isopleth (compare Table 21 and Appendix A.4 for the detailed results). Both the biggest and smallest (50 % and 95 %) home ranges were obtained for males (Bogarigka and Mothamongwe). The only female leopard, Ronja, occupies the second largest 95 % home range while her core area is similarly small as that of Mothamongwe. Consequently, her core area is only 16 % of her whole home range instead of 21– 34 % as for the other leopards (Table 21). The home range of Ronja is the only one of all leopards in this study that lies considerably (on average 28.3 % ± 6.7 % for the 95 % isopleth, 1.4 % ± 1.7 % for the 50 % boundary) outside the protected area of KGR and CKGR (compare Figure 16 and Figure 17). However, the 95 % boundaries of Mothamongwe and Bogarigka also transgress the protected area marginally (3.6 % ± 0.8 % resp. 0.6 % ± 0.8 %). The mean compactness values of the core area are identical for all male leopards, with a value of 0.40 (± 0.12). Only the home range of Ronja is less compact, with an index value of 0.32 (Table 21). Note that only KDE, t-LCH and BRB were considered to compute the average compactness of both isopleths as the value of MCP is mostly predetermined by its functioning. For the 95 % isopleth, the two individuals whose area is markedly larger (Bogarigka and Ronja) also have lower compactness values (0.37 ± 0.02 and 0.29 ± 0.02). As for the core area, the males Gham and Mothamongwe have identical compactness values of 0.53 (± 0.04). According to a Spearman correlation test there is neither for the 50 % (ρ: 0.258, df: 2, p: 0.7418) nor the 95 % isopleth (ρ: -0.738, df: 2, p: 0.2621) a significant relationship between the size of a home range and its compactness. The influence of sex on the area and the compactness could not be tested due to an insufficient number of individuals.
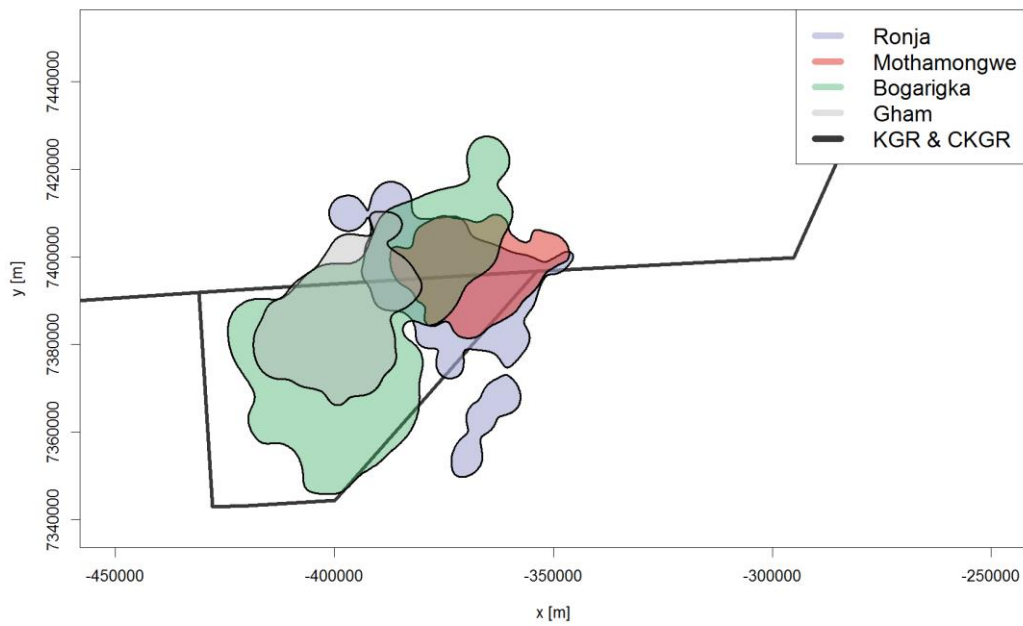
Figure 16. Positions and overlaps of the 95 % home range isopleths of the leopards. The home ranges obtained by using KDE and the reference bandwidth are presented. See Figure 3 for the time spans over which data was recorded for each individual.
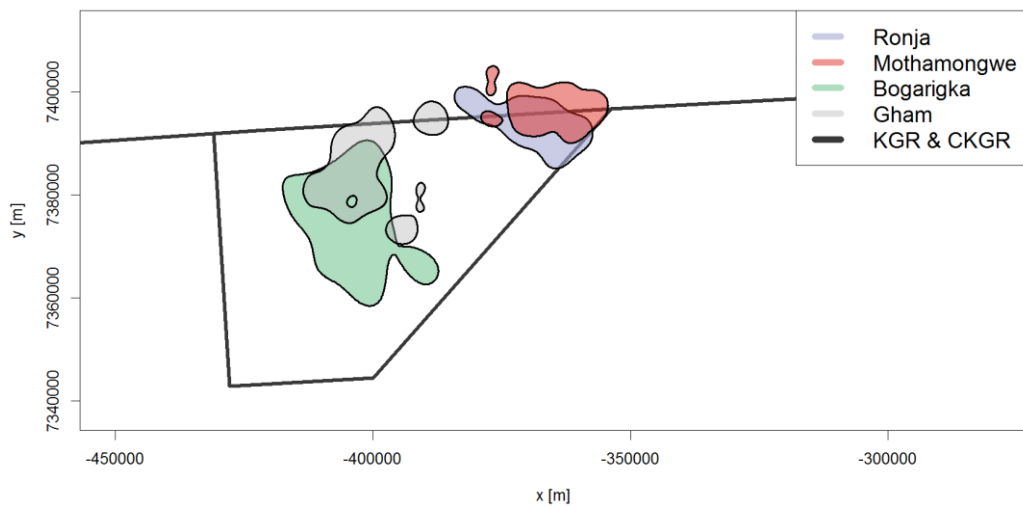
Figure 17. Positions and overlaps of the 50 % home range isopleths of the leopards. The home ranges obtained by using KDE and the reference bandwidth are presented. See Figure 3 for the time spans over which data was recorded for each individual.

The temporal variations of the home range size are shown in Figure 18, those of the compactness in Figure 19. As the trends do not change markedly between the 50 % and the 95 % isopleth, only the graphs of the latter one are presented. While there is only a subtle change for Mothamongwe, the three seasons analyzed for Bogarigka shows a strong increase of the home range area (compare Figure 20). The time series of Ronja exhibits distinctive alternating trends but they do not coincide

with seasons or single years. Figure 21 reveals that the sharp increase of her area during the summer of 2013 is caused by a second center of activity in the south. About equally heterogeneous trends are observable for the compactness index (Figure 19). Ronja has quite pronounced increases of compactness during the winter while Bogarigka shows just the opposite pattern. As for the plot of the home range area, the curve of Mothamongwe neither varies strongly nor follows a clear pattern.
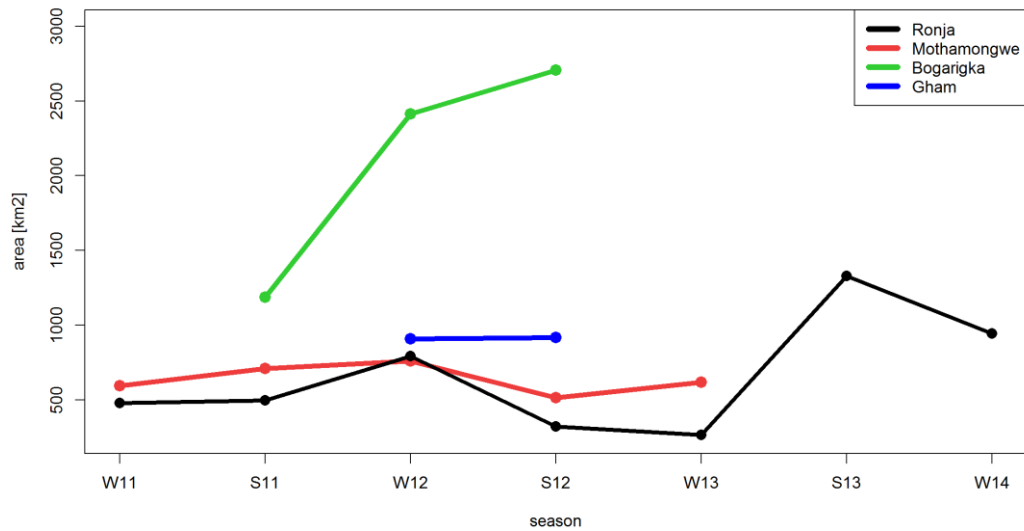
Figure 18. Temporal variability of the 95 % home range size of the leopards. W stands for winter season (June–September), S for summer season (November–April). The subsequent number designates the year (2011–2014).
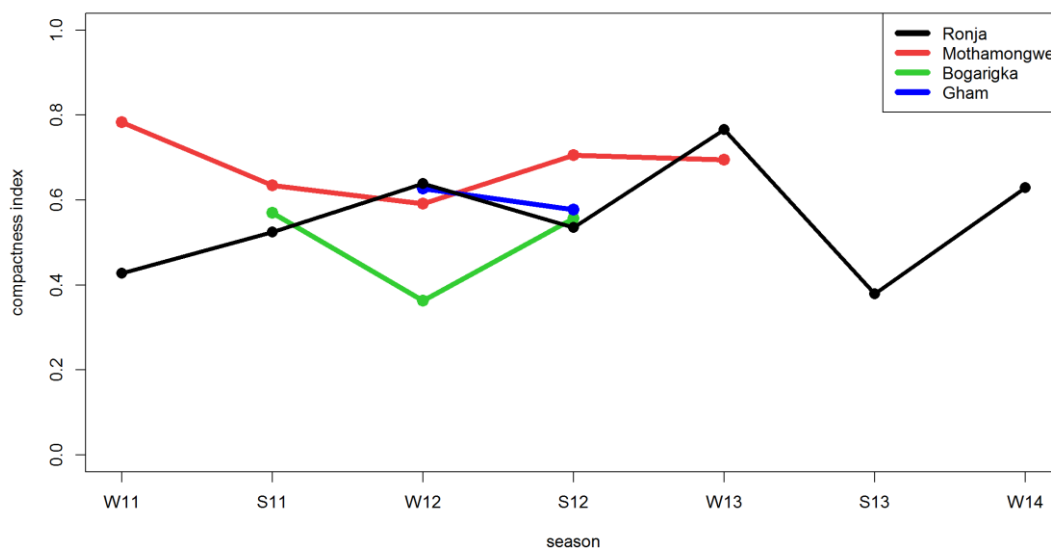
Figure 19. Temporal variability of the 95 % home range compactness of the leopards. W stands for winter season (June–September), S for summer season (November–April). The subsequent number designates the year (2011–2014).
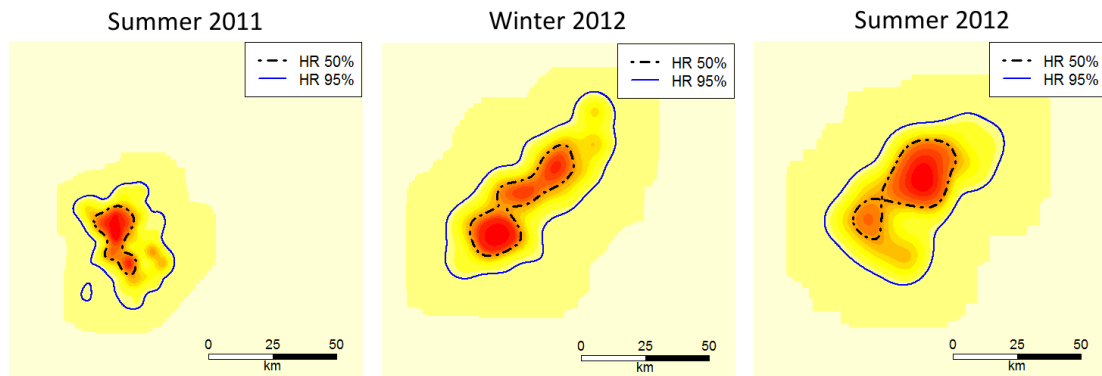
Figure 20. Spatiotemporal variation of Bogarigka's home range. After summer 2011, the home range was extended towards the northeastern direction. The same spatial reference frame was used for all of the individual images.
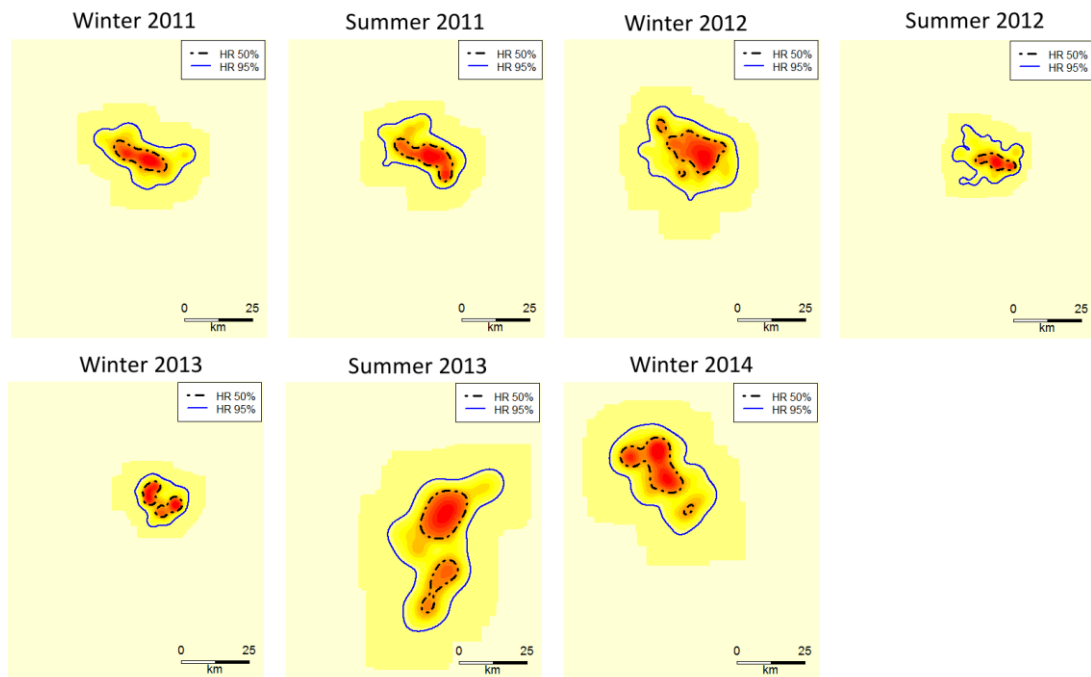
Figure 21. Spatiotemporal variation of Ronja's home range. There is an additional core area in the south that is only present during summer 2013. The same spatial reference frame was used for all of the individual images.

There is a striking overlap of the (static) home range of Ronja with the one of Mothamongwe of 81 % resp. 44 % for the 95 % isopleth (Table 22). Even for the core area about half of the two home ranges overlap each other (Table 23). When looking at the utilization distribution instead of individual probability isopleths, a value of 63 % indicates a fairly high similarity (Table 24). The computation of the Euclidean distances between the GPS points that were recorded approximately at the same time (maximum time shift of 90 min.) resulted in a minimum distance

of 0 m (3.5 km for the 10 %, 6.6 km for the 25 % and 10.2 km for the 50 % quantile). Figure 23 a) shows the histogram of the Euclidean distances that meet the criteria for the maximum allowed time difference between Ronja and Mothamongwe. The smoothed curve of the distances are visualized in Figure 22 a). There is also an overlap between Ronja and Bogarigka (42 % resp. 23 %) at the 95 % isopleth. However, the importance of this interaction shrinks when looking at the VI index (15 %) and the core areas (0 % resp. 1 %). Another remarkable overlap occurred between the home ranges of the male leopards Bogarigka and Gham. At the 95 % isopleth, Bogarigka covers almost the entire home range of Gham (94 %) whereas still 53 % resp. 34 % of their areas overlap at the 50 % isopleth (the VI value is 52 %). Despite the largely overlapping home ranges, the two leopards rarely meet each other directly (Figure 22 b) and Figure 23 b)). The minimum Euclidean distance for them is 639 m, with a mean distance of 21.9 km (8.7 km and 14.2 km for the 10 % and 25 % quantiles).
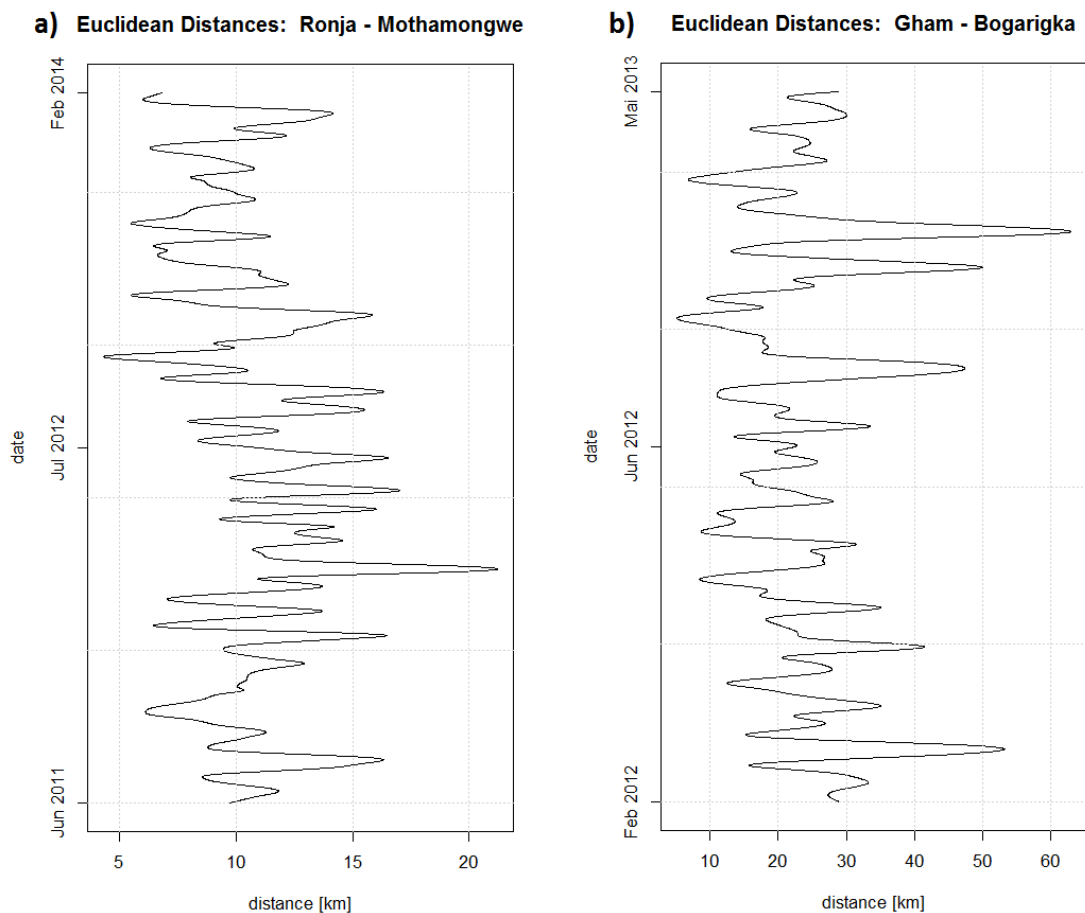
Figure 22. Visualization of the distances between the GPS points recorded at similar times between a) Ronja and Mothamongwe and b) Gham and Bogarigka. Note that the curve of the visualized distances has been smoothed and therefore lacks the actual minima/maxima.
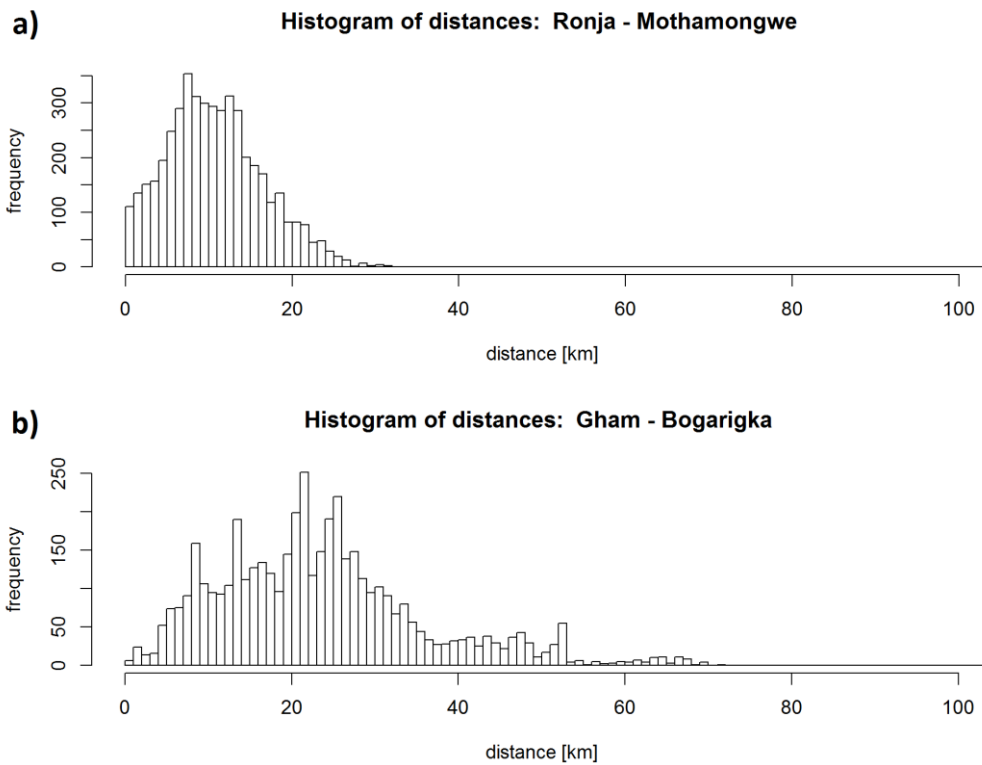
Figure 23. Histograms showing the frequencies of the distances between a) Ronja and Mothamongwe, and b) Gham and Bogarigka. The interval length is 1 km. The cut-off value for the histogram is 100 km.

Table 21. Mean area, compactness and core area ratio values (with standard deviation) for the 4 leopards and 8 lions (separated by a heavy gray line). The averages of all HRE are presented. The highest value is printed bold and the lowest is indicated in italics for the leopards and lions, respectively. Females are underlined. Note that MCP was ignored for the average compactness.

	50 % isopleth		95 % isopleth		
Individual	**Area [km2]**	**Compactness**	**Area [km2]**	**Compactness**	**core area ratio**
<u>Ronja</u>	211.6 ± 30.6	*0.32* ± 0.01	1315.0 ± 191.3	*0.29* ± 0.02	*0.16* ± 0.01
Mothamongwe	*202.4* ± 18.3	**0.40** ± 0.03	*694.7* ± 22.3	**0.53** ± 0.02	0.29 ± 0.02
Bogarigka	**486.8** ± 65.2	**0.40** ± 0.12	**2357.4** ± 112.6	0.37 ± 0.02	0.21 ± 0.02
Gham	303.5 ± 14.6	**0.40** ± 0.08	908.5 ± 48.9	**0.53** ± 0.04	**0.34** ± 0.03
<u>Verity</u>	746.6 ± 73.3	0.37 ± 0.20	3277.8 ± 219.8	0.50 ± 0.01	0.23 ± 0.02
<u>Ella</u>	473.4 ± 57.6	0.37 ± 0.12	2411.8 ± 125.9	0.57 ± 0.03	0.20 ± 0.01
<u>Jane</u>	788.7 ± 122.0	0.33 ± 0.03	3093.8 ± 193.0	0.52 ± 0.02	0.26 ± 0.03
Hitchcock	**1061.4** ± 83.7	0.31 ± 0.06	**4317.4** ± 361.6	0.52 ± 0.01	0.25 ± 0.00
Mexico	*187.2* ± 19.1	**0.56** ± 0.07	1707.0 ± 132.1	0.53 ± 0.07	*0.11* ± 0.01
<u>Madge</u>	482.3 ± 153.1	*0.26* ± 0.17	3430.6 ± 619.0	0.50 ± 0.03	0.14 ± 0.02
Orange	344.1 ± 26.6	0.45 ± 0.02	*1131.1* ± 50.2	**0.63** ± 0.02	**0.31** ± 0.04
<u>Getika</u>	427.1 ± 29.8	0.40 ± 0.06	2090.2 ± 95.2	*0.39* ± 0.10	0.21 ± 0.00

Table 22. Mean overlap [%] of the 95 % isopleths of the lions and leopards. The average of the overlaps of all HRE per individual are shown. The table has to be read as: "The HR of the individual at row *A* overlaps the HR of the individual at column *B* to *X* %". Females are underlined and leopards are separated from the lions by heavy gray lines. Values equal to or higher than 50 are highlighted bold. The following abbreviations were used: Motha: Mothamongwe, Boga: Bogarigka, Hitch: Hitchcock.

	<u>Ronja</u>	Motha	Boga	Gham	<u>Verity</u>	<u>Ella</u>	<u>Jane</u>	Hitch	Mexico	<u>Madge</u>	Orange	<u>Getika</u>
<u>Ronja</u>	100	**81**	23	17	29	20	1	1	6	0	**60**	13
Motha	44	100	15	3	21	9	0	0	1	0	**53**	2
Boga	42	**51**	100	**94**	**57**	**60**	4	1	**60**	0	**52**	48
Gham	12	4	36	100	23	36	0	0	47	0	9	37
<u>Verity</u>	**73**	**97**	**79**	**82**	100	**80**	10	6	**72**	0	**92**	**68**
<u>Ella</u>	36	30	**62**	**96**	**59**	100	4	5	**86**	0	30	**80**
<u>Jane</u>	3	2	5	0	9	5	100	42	1	24	27	7
Hitch	5	0	1	1	7	9	**59**	100	3	3	16	20
Mexico	8	1	43	**88**	38	**61**	0	1	100	0	4	**61**
<u>Madge</u>	0	0	0	0	0	0	25	3	0	100	0	0
Orange	52	**86**	25	11	32	14	10	4	2	0	100	11
<u>Getika</u>	21	7	43	**85**	43	**69**	5	10	**75**	0	19	100

Table 23. Mean overlap [%] of the 50 % isopleths of the lions and leopards. The average of the overlaps of all HRE per individual are shown. The table has to be read as: "The HR of the individual at row A overlaps the HR of the individual at column B to X %". Females are underlined and leopards are separated from the lions by heavy gray lines. Values equal to or higher than 50 are highlighted bold. The following abbreviations were used: Motha: Mothamongwe, Boga: Bogarigka, Hitch: Hitchcock.

	Ronja	Motha	Boga	Gham	Verity	Ella	Jane	Hitch	Mexico	Madge	Orange	Getika
Ronja	100	53	0	0	15	0	0	0	0	0	29	0
Motha	51	100	0	0	12	0	0	0	0	0	31	0
Boga	1	0	100	53	4	7	0	0	67	0	0	12
Gham	0	0	34	100	6	17	0	0	77	0	0	25
Verity	53	43	6	17	100	13	0	0	11	0	66	14
Ella	0	0	7	27	8	100	0	0	33	0	0	61
Jane	0	0	0	0	0	0	100	1	0	30	3	0
Hitch	0	0	0	0	0	0	1	100	0	0	0	4
Mexico	0	0	26	46	3	13	0	0	100	0	0	20
Madge	0	0	0	0	0	0	16	0	0	100	0	0
Orange	48	54	0	0	31	0	2	0	0	0	100	0
Getika	0	0	10	34	7	56	0	2	45	0	0	100

66

Table 24. Mean volume of intersection [%] of the UD of the lions and leopards. The average of the index values of KDE and BRB per individual are shown. The table has to be read as: "The HR of the individual at row A overlaps the HR of the individual at column B to X %". Females are underlined and leopards are separated from the lions by heavy gray lines. Values equal to or higher than 50 are highlighted bold. The following abbreviations were used: Motha: Mothamongwe, Boga: Bogarigka, Hitch: Hitchcock.

	<u>Ronja</u>	Motha	Boga	Gham	<u>Verity</u>	<u>Ella</u>	<u>Jane</u>	Hitch	Mexico	<u>Madge</u>	Orange	<u>Getika</u>
<u>Ronja</u>	100	63	15	8	42	14	2	2	3	0	49	6
Motha	**63**	100	13	4	41	8	1	0	2	0	**56**	2
Boga	15	13	100	**52**	36	31	4	2	39	0	18	28
Gham	8	4	**52**	100	21	34	0	0	**61**	0	7	42
<u>Verity</u>	42	41	36	21	100	41	6	4	21	0	**54**	28
<u>Ella</u>	14	8	31	34	41	100	2	3	42	0	11	**62**
<u>Jane</u>	2	1	4	0	6	2	100	29	1	26	12	4
Hitch	2	0	2	0	4	3	29	100	1	2	4	9
Mexico	3	2	39	**61**	21	42	1	1	100	0	3	47
<u>Madge</u>	0	0	0	0	0	0	26	2	0	100	0	0
Orange	49	**56**	18	7	**54**	11	12	4	3	0	100	5
<u>Getika</u>	6	2	28	42	28	**62**	4	9	47	0	5	100

9.5.3 Lions

The average home range size (95 %) of all 4 HRE for the lions range between 1131 and 4317 km^2, whereas that of the core area ranges between 187 and 1061 km^2 (compare Table 21 and Appendix A.4 for the detailed results). Both the smallest and largest area for the 50 % and 95 % isopleth were obtained by male individuals. For example, the core area size of the male with the largest values, Hitchcock, is about the same as the 95 % area of the male Orange (1061.4 ± 83.7 km^2 vs. 1131.1 ± 50.2 km^2). An influence of the sample size or the time span over which fixes have been recorded does not seem to play a major role since the individuals with the largest and smallest values all have almost identical datasets in these regards. The core areas are 20–31 % of the size of the 95 % boundaries for most lions. The female Madge and the male Mexico are exceptions to this with much lower ratios (14 % and 11 %). The home ranges of the females with 427–789 km^2 resp. 2090–3431 km^2 (50% and 95 % isopleths) lie between the extreme values obtained for the males. Accordingly, no significant difference of the area due to the sex could be determined (Mann-Whitney U test) for the core area (U: 10, df: 6, p: 0.570) or the 95 % boundary (U: 10, df: 6, p: 0.570).

None of the individuals has a home range (95 % boundary) that exceeds the boundary of the protected area markedly. The highest values were found for Madge, Verity and Mexico, whose 95 % isopleth lie to 3.8 % ± 2.5 %, 2.8 % ± 1.7 % and 2.6 % ± 2.0 % outside the game reserves. Interestingly, the value for the core area of Madge is equally high (2.8 % ± 3.5 %) as for the 95 isopleth (compare Figure 24). However, the second core area at the border is present only in some of the home range estimates. The compactness values are significantly higher for the 95 % than for the 50 % isopleth (U: 8, df: 14, p: 0.0134). They are also higher for the males than for the females (for both isopleths) but are not statistically significant (95 %: U: 2.5, df: 6, p: 0.1745, 50 %: U: 4, df: 6, p: 0.3682). When looking at the areas and compactness values of all 50 % isopleths, there is a strong negative correlation between them that is statistically significant (ρ: -0.838, df: 6, p: 0.0093). Thus, the larger the core area, the less compact it is. The correlation for the 95 % isopleth is moderate but not significant (ρ: -0.482, df: 2, p: 0.2265).
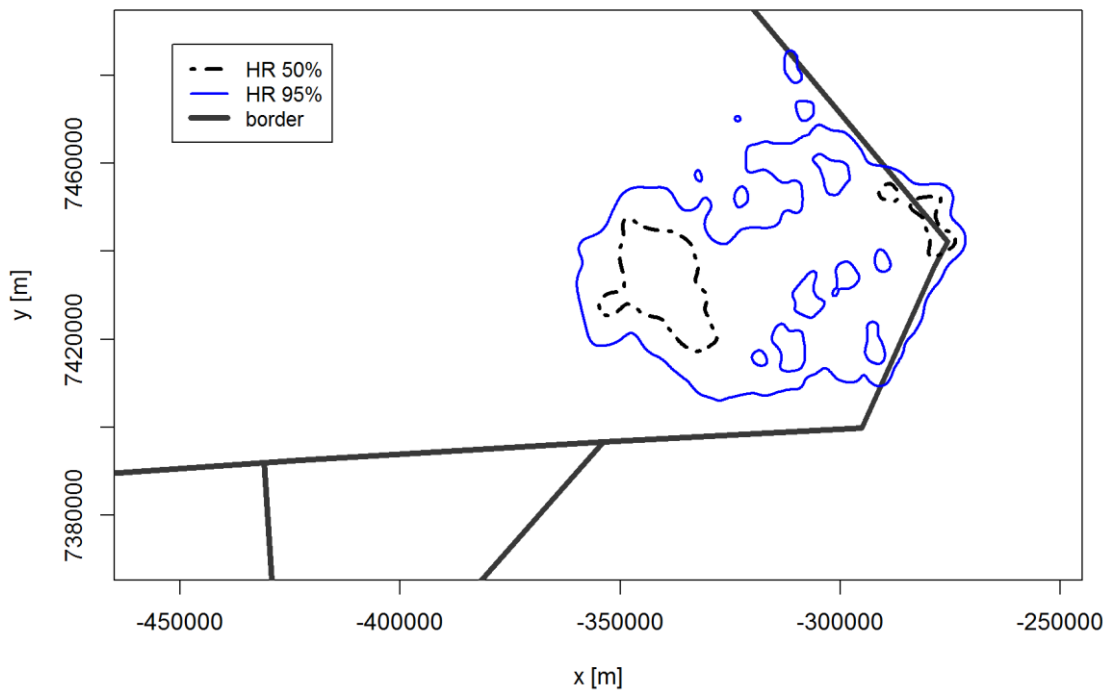
Figure 24. The home range of Madge (biased random bridges result is shown) transgresses the boundary of the game reserves for both the 95 % and 50 % isopleth.

The areas of some home ranges show some abrupt changes over time for both the 95 % and 50 % isopleths (Figure 25). The home range sizes of Ella and Verity both decreased markedly between summer 2011 and winter 2012. While the former was largely stable after the shrinkage, the latter moved in eastern direction afterwards (Figure 27). Two of the male lions (Hitchcock and Mexico) also experienced a pronounced decrease of their home range size between summer 2012 and winter 2013. While the home range of the former has recovered within the following season, it took Mexico three seasons to do likewise. The third male, Orange, increased his home range over time slightly. The strongest increase in area was found for the female Madge (Figure 28). Her territory increased within two years by a factor of 13.5 towards the north and east. Additionally, she had a second disjoint core area west of the old one during summer 2013 that is also visible in the home range over the entire time period (Figure 24). The temporal variation of the compactness values kept mostly within narrow bounds (Figure 26). For three of the lions (Verity, Jane and Orange) the compactness increased during each summer while only one individual (Mexico) showed the opposite pattern.
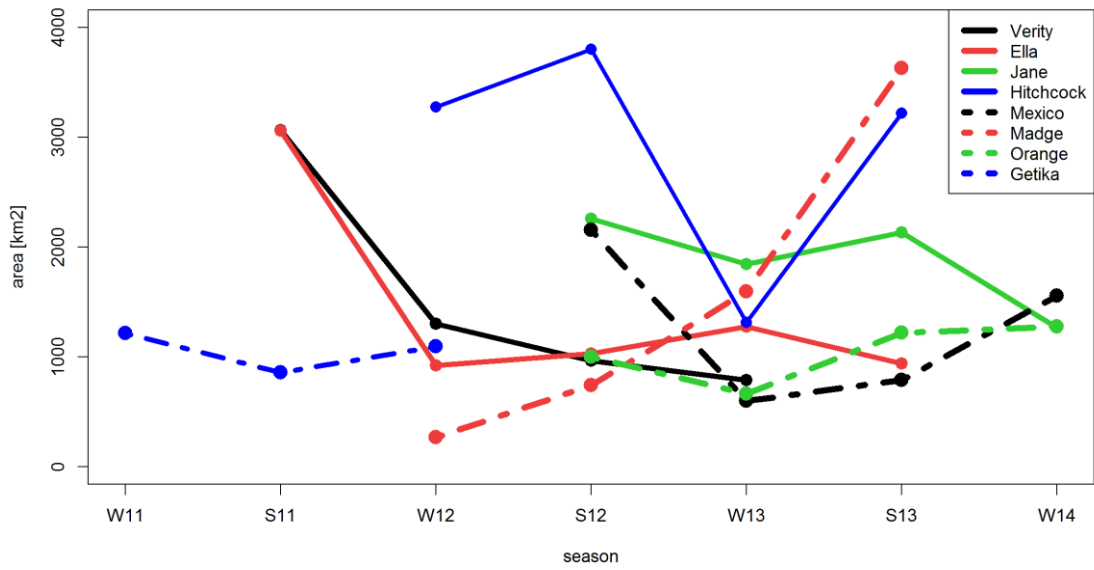
Figure 25. Temporal variability of the 95 % home range size of the lions. W stands for winter season (June–September), S for summer season (November–April). The subsequent number designates the year (2011–2014).
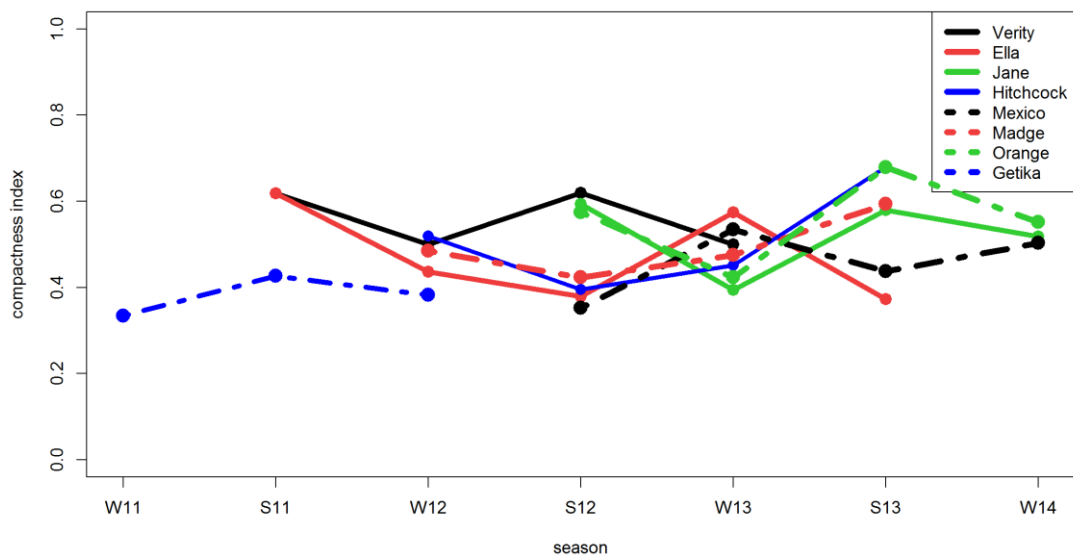
Figure 26. Temporal variability of the 95 % home range compactness of the lions. W stands for winter season (June–September), S for summer season (November–April). The subsequent number designates the year (2011–2014).
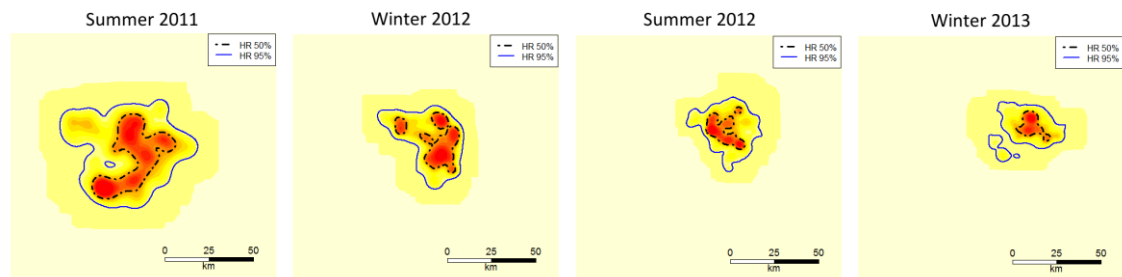
Figure 27. Spatiotemporal variation of Verity's home range. After summer 2011, the home range shrank drastically and subsequently moved towards the east. The same spatial reference frame was used for all of the individual images.
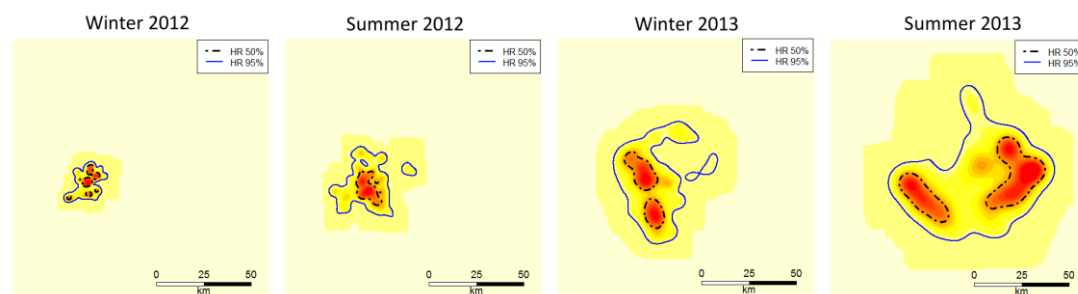
Figure 28. Spatiotemporal variation of the Madge's home range. After winter 2012 a nearly exponential increase in size primarily directed to the northeast could be observed. The same spatial reference frame was used for all of the individual images.

A look at the overlap tables (Table 22, Table 23 and Table 24) as well as Figure 29 and Figure 30 reveals that the home ranges of the males hardly overlap each other for the 95 % and not at all for the 50 % isopleth. Only Hitchcock overlaps the territory of Orange to 16 % at the 95 % boundary, but a VI index value of 4 % indicates that only peripheral regions are affected. Between the females, extensive overlaps are much more common. Strong spatial interactions can be found between Verity, Ella and Getika whereas Ella and Getika have particularly extensive overlaps even for the core area (56 resp. 61 %, VI index of 62 %). The core areas of Verity and Ella as well as Verity and Getika overlap each other by 8–14 %. As observable in Figure 31 a) and Figure 32 a), Verity and Ella stayed together for about half a year before their distance increased again. Jane and Madge, whose distances are shown in Figure 31 b) and Figure 32 b), also show a significant degree of interaction at the 50 % isopleth (16 resp. 31 %). Table 25 gives an overview of the Euclidean distances between the females, which have VI values of at least 20 %. The maximum time lag of the GPS points of the two respective individuals is 60 minutes.
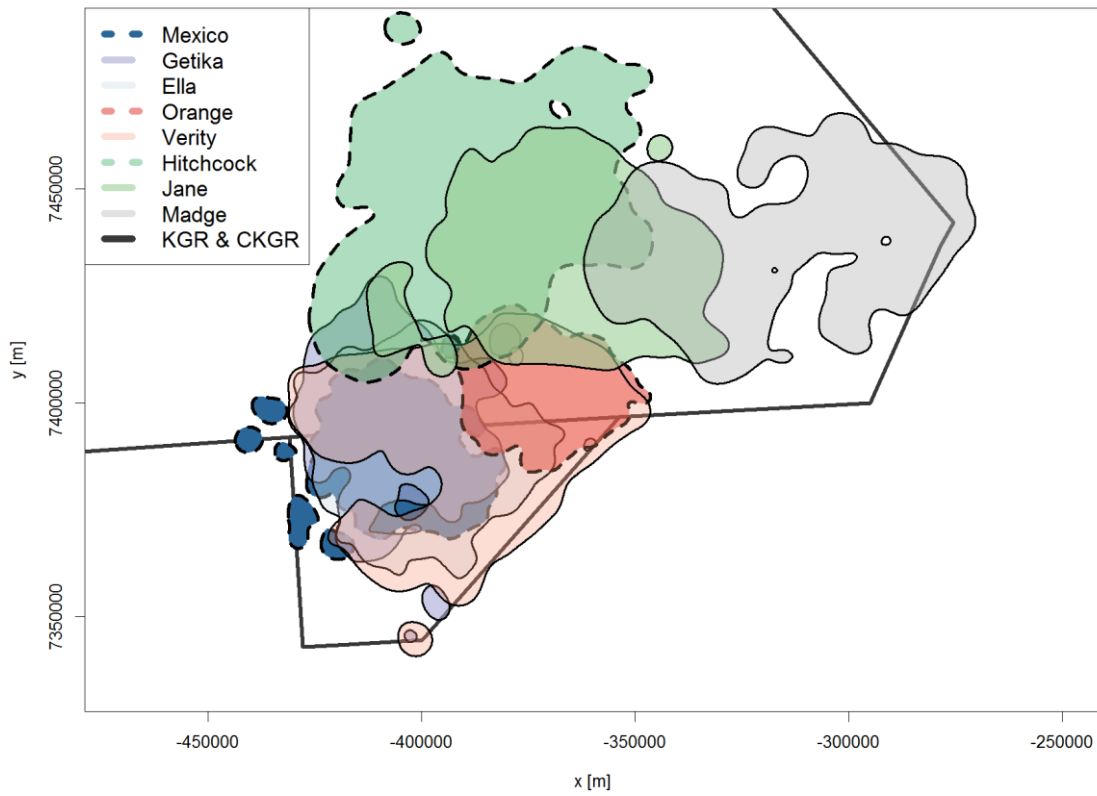
Figure 29. Positions and overlaps of the 95 % home range isopleths of the lions. The home ranges obtained by using KDE and the reference bandwidth are presented. See Figure 3 for the time spans over which data was recorded for each individual.
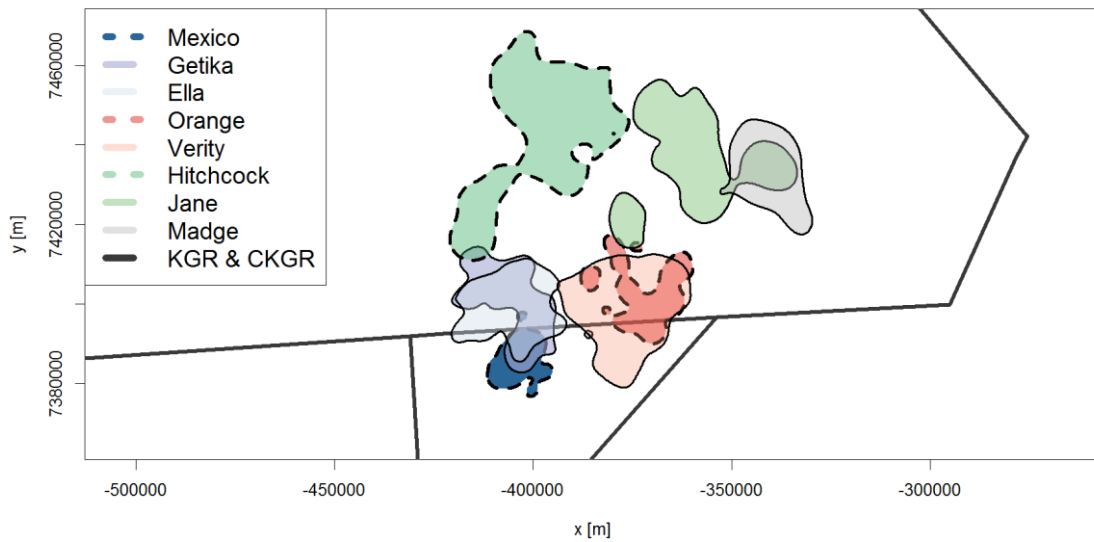
Figure 30. Positions and overlaps of the 50 % home range isopleths of the lions. The home ranges obtained by using KDE and the reference bandwidth are presented. See Figure 3 for the time spans over which data was recorded for each individual.

Table 25. Euclidean distances between lionesses based on the GPS points that are closest in time. Note that different units were used to cover the different granularities. Values with the unit meter are in italics.

Interaction	Minimum	10 % quantile	25 % quantile	50 % quantile
Ella – Getika	*0.0 m*	6.4 km	12.0 km	20.1 km
Verity – Ella	*0.0 m*	*12.0 m*	*56.0 m*	23.2 km
Getika – Verity	*0.0 m*	7.9 km	17.8 km	28.1 km
Jane – Madge	*154.7 m*	16.4 km	23.7 km	36.8 km
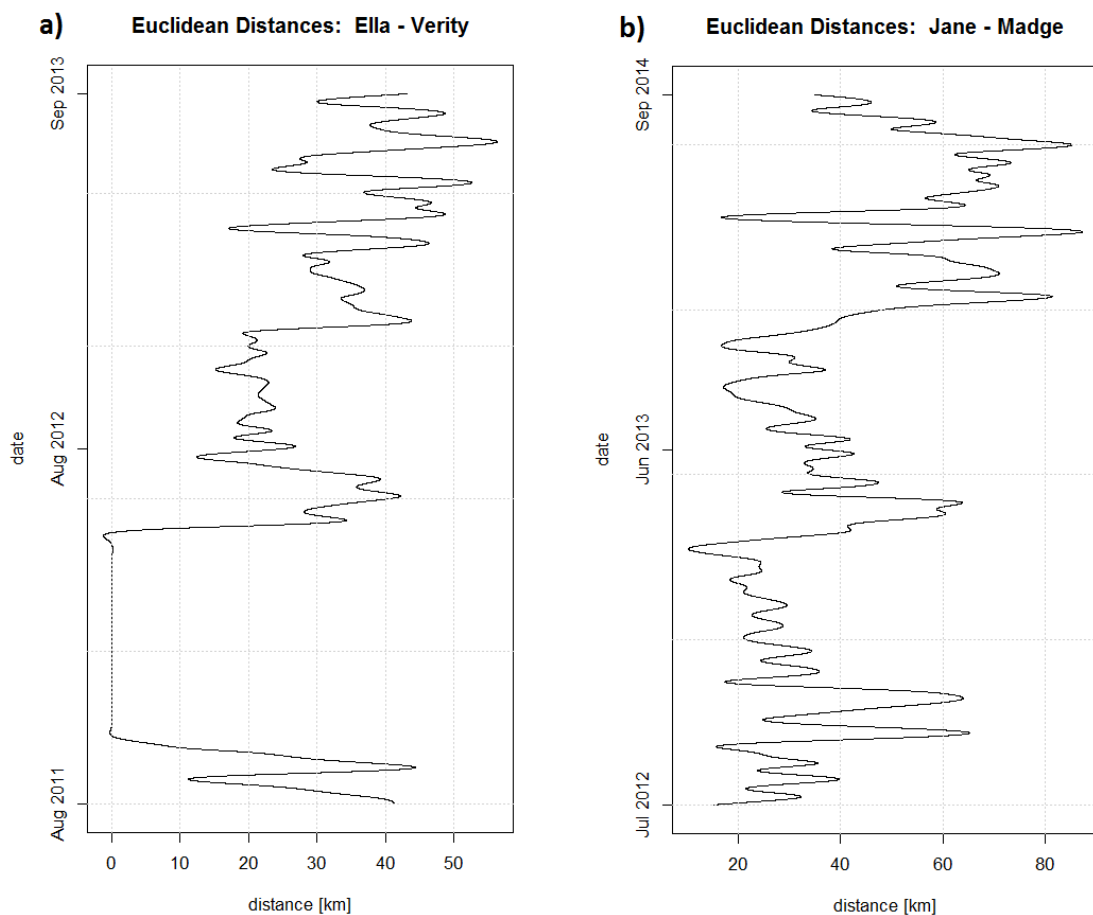
Figure 31. Visualization of the distances between the GPS points recorded at similar times between the females a) Ella and Verity and b) Jane and Madge. Note that the curve of the visualized distances has been smoothed and therefore lacks the actual minima/maxima.
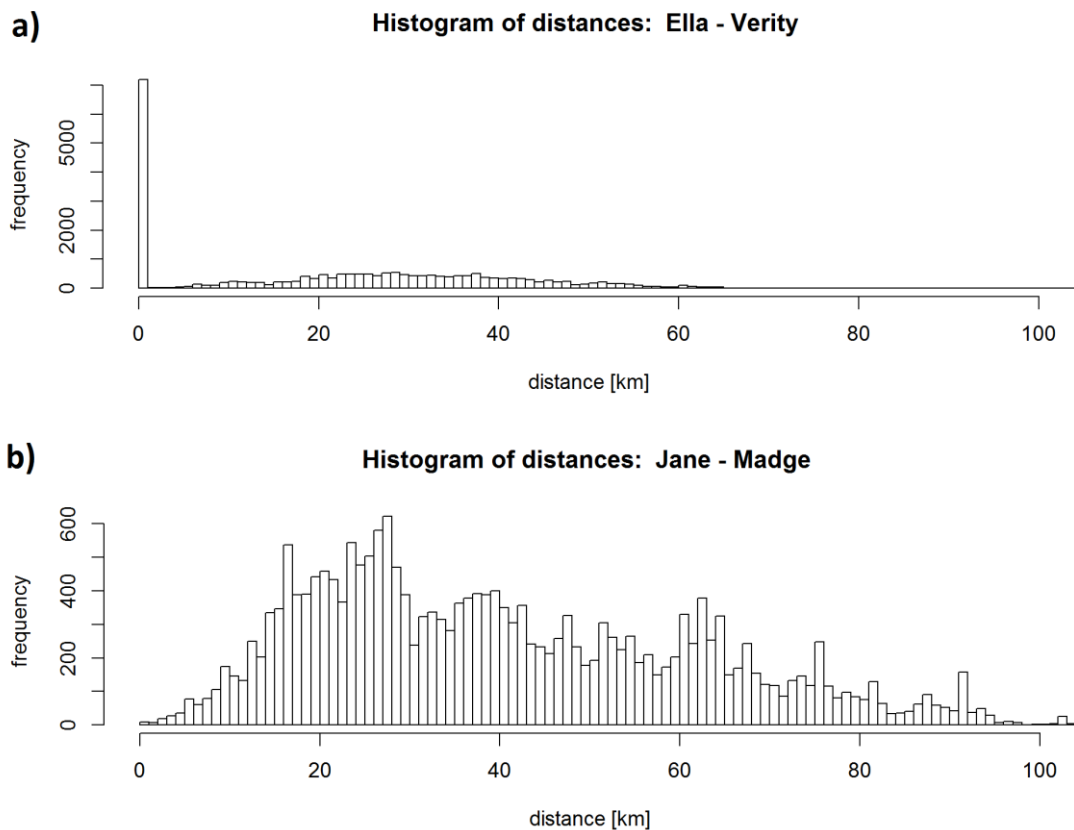
Figure 32. Histograms showing the frequencies of the Euclidean distances between the females a) Ella and Verity, and b) Jane and Madge. The interval length is 1 km. The cut-off value for the histogram is 100 km.

Whereas the home ranges of males do not overlap each other, all of them overlap with at least one female. Mexico covers 61 % of the home ranges of Ella and Getika as well as 38 % of the one of Verity at the 95% boundary (Table 22). He is thus the male with the most spatial overlaps with females. His core area, however, overlaps only those of Getika and Ella markedly (20 % and 13 %). Table 26 and Figure 34 a) support this finding as the minimum distance between Mexico and Verity is with 5.5 km much higher than between Mexico and Ella (0 m) or Getika (666 m). In addition, the distance between him and Verity continuously increased over time (Figure 33 a)). The second male Orange only overlaps significantly with Verity (32 % at the outer boundary, 31 % at the 50 % isopleth and a VI index of 54 %). The low minimum and 10 % quantile of a few meters also indicate a high degree of interaction between them. The last male (Hitchcock) overlaps only one female (Jane) markedly with 59 % at the 95 % isopleth and a VI index of 29 %. Although their core areas hardly overlap (1 %) and they seem to have met only during April 2013 briefly (Figure 33 b)), the distances smaller than 1 km are numerous (Figure 34 b)). Compared to the Euclidean distances of the other individuals that have similarly low minimum distances, the values for the quantiles are much higher.

Table 26. Euclidean distances between male lions based on the GPS points that are closest in time. Note that different units were used to cover the different granularities. Values with the unit meter are in italics.

Interaction	Minimum	10 % quantile	25 % quantile	50 % quantile
Mexico – Verity	5.5 km	19.4 km	25.6 km	35.6 km
Mexico – Ella	*0 m*	*474.6 m*	11.8 km	18.2 km
Mexico – Getika	*666.3 m*	12.4 km	18.9 km	26.2 km
Orange – Verity	*0 m*	*15.5 m*	*295.5 m*	6.9 km
Hitchcock – Jane	*0 m*	12.6 km	23.5 km	36.0 km
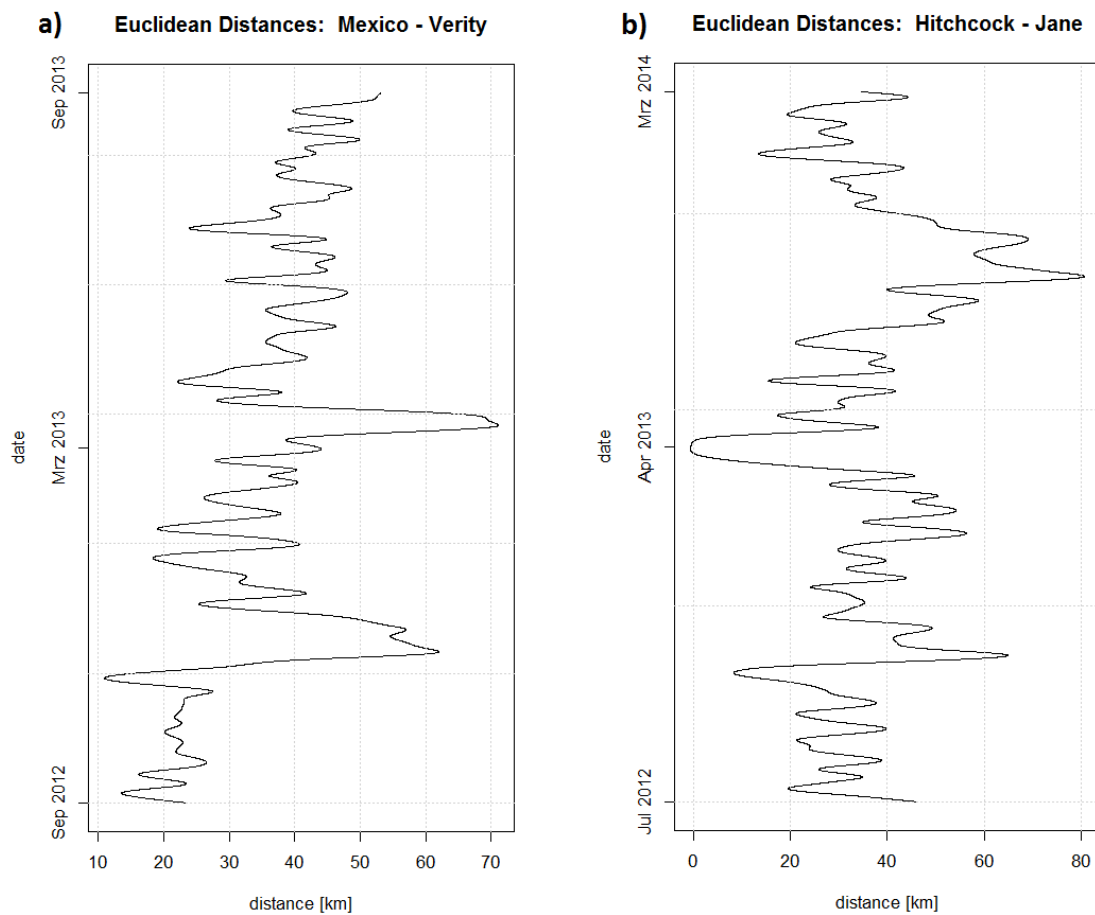
Figure 33. Visualization of the distances between the GPS points recorded at similar times between a) Mexico and Verity and b) Hitchcock and Jane. Note that the curve of the visualized distances has been smoothed and therefore lacks the actual minima/maxima.

a)

Histogram of distances: Mexico - Verity
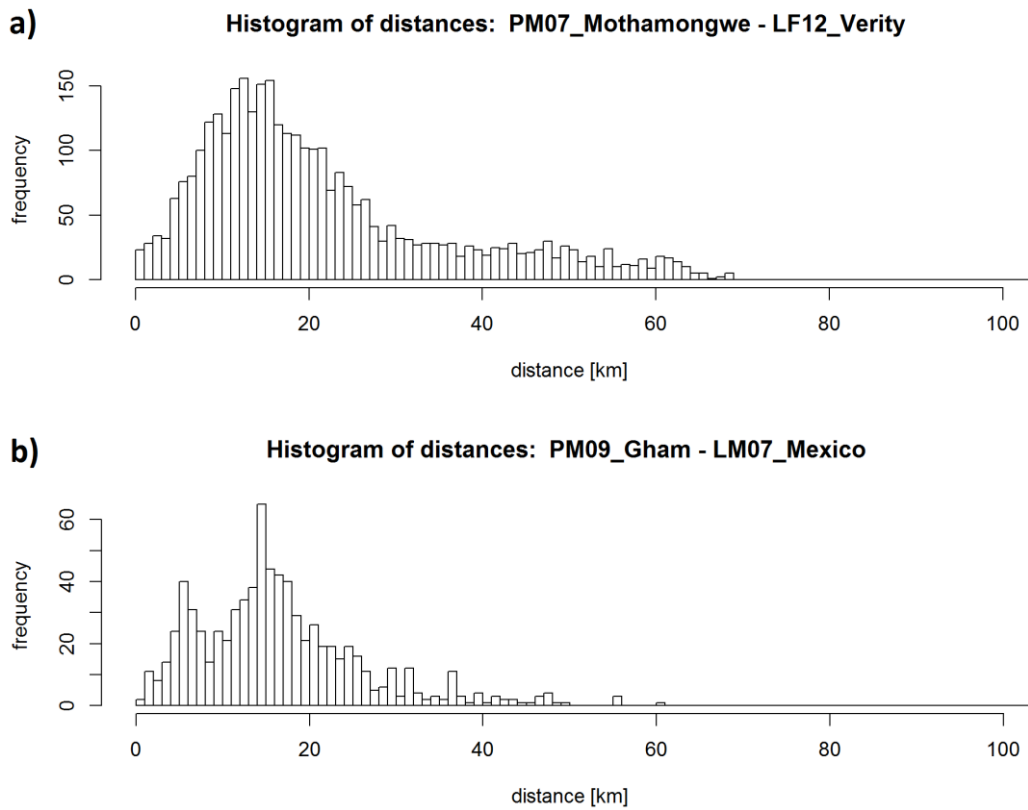
b)

Histogram of distances: Hitchcock - Jane
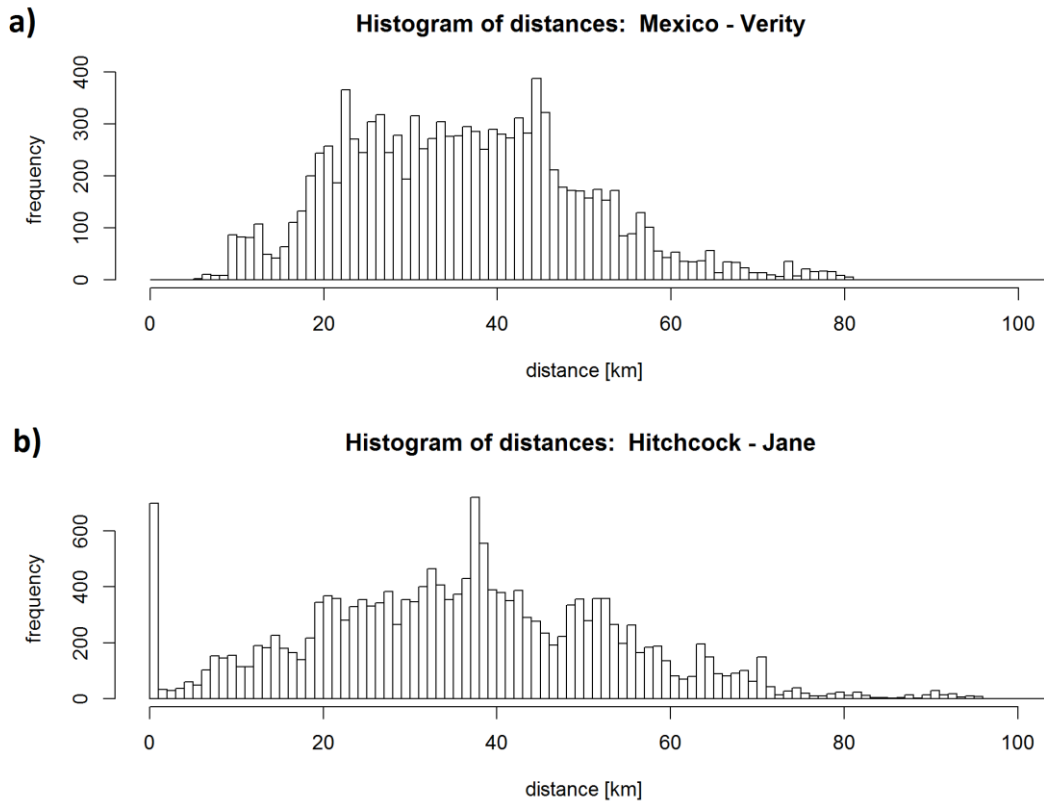
Figure 34 Histograms showing the frequencies of the Euclidean distances between a) Mexico and Verity, and b) Hitchcock and Jane. The interval length is 1 km. The cut-off value for the histogram is 100 km.

9.5.4   Cross-species comparison

The home range sizes of the lions presented in Table 21 are on average larger for both the 50 % ($563.9 \ km^2 \pm 263.4 \ km^2$ vs. $301.1 \ km^2 \pm 114.3 \ km^2$) and the 95 % isopleth ($2682.5 \ km^2 \pm 970.7 \ km^2$ vs. $1318.9 \ km^2 \pm 639.6 \ km^2$). Whereas the differences of the 95 % boundary are statistically significant (U: 24, df: 10, p: 0.0485), those of the 50 % isopleth are not (U: 24, df: 10, p: 0.2140). The mean compactness values of the lions and leopards are identical for the 50 % isopleth (0.38 ± 0.09 vs. 0.38 ± 0.03) and thus statistically not different (U: 13.5, df: 10, p: 0.729). When looking at the 95 % boundary, lions have on average slightly more compact home ranges (0.52 ± 0.06) than the leopards (0.43 ± 0.10) but the difference is not significant (U: 21, df: 10, p: 0.4399).

Table 22–Table 24 display intersections between the home ranges of the leopards and lions. When looking at the 95 % home range isopleth, especially the home range of Bogarigka largely overlaps those of many lions (Table 22). The other three leopards cover the territories of at least one lion each to one third or more. With the exception of Bogarigka, the 95 % and 50 % home range isopleths of the lions overlap a larger proportion of the respective home range boundaries of the

leopards than vice versa. Verity for example overlaps at least 73 % of the home range of each leopard (conversely, the maximum is 57 %). But also Ella, Mexico, Orange and Getika have high overlap values for at least one of the leopards. The home ranges of Jane and Hitchcock hardly intersect those of the leopards whereas no interspecific overlap for Madge can be shown with this data. The VI values in Table 24 display the same pattern, with particular high values between Ronja and Orange, Mothamongwe and Orange as well as Gham and Mexico. Table 23 reveals numerous overlaps between the core areas as well. The territories of the leopards overlap only with those of Mexico, Orange and Getika significantly. From the perspective of the lions, the core areas of Ronja, Mothamongwe and Gham overlap with those of the lions particularly strong. There are no interspecific overlaps of the core areas for Jane, Hitchcock and Madge.

About half of the 32 distance analyses between leopards and lions resulted in minimum values of less than 1 km, with an absolute minimum of 53 m for Mothamongwe and Verity. Table 27 presents an extract of the interspecific distances whose minimum is smaller than 1 km. Note that the maximum allowed time shift was set to 2 h for the computation of the distances. Figure 35 a) shows the histogram of the distances for the individuals with the highest overlap value for the 95 % isopleth (Mothamongwe and Verity, overlap of 97 %), b) presents that for the individuals with the highest overlap value for the 50 % isopleth (Gham and Mexico, overlap of 77 %).

Table 27. Extract of the Euclidean distances between the leopards and lions based on the GPS points that are closest in time. The records are sorted by the 50 % quantile. Mothamongwe is abbreviated as "Motha" and Bogarigka as "Boga". The name of the individual mentioned first refers to a leopard, the other to a lion.

Interaction	Minimum	10 % quantile	25 % quantile	50 % quantile
	[m]	[km]	[km]	[km]
Motha – Orange	408	6.6	10.5	15.0
Gham – Mexico	566	5.5	10.0	15.1
Motha – Verity	53	7.0	11.3	17.3
Ronja – Verity	257	6.3	11.7	18.7
Ronja – Orange	140	6.8	11.9	19.4
Boga – Orange	276	8.6	14.4	21.7
Gham – Ella	106	9.8	15.0	21.9
Gham – Getika	133	10.4	16.6	24.5
Boga – Verity	296	9.4	15.9	25.1
Boga – Ella	186	10.1	16.3	25.3
Boga – Mexico	246	11.0	18.4	26.4
Boga – Getika	360	12.0	19.0	29.0
Ronja – Getika	672	20.8	27.8	35.7
Ronja – Ella	718	15.4	25.5	36.5
Motha – Ella	437	21.0	29.6	40.1

Figure 35. Histograms showing the frequencies of the Euclidean distances between a) Mothamongwe and Verity, and b) Gham and Mexico. The interval length is 1 km. The cut-off value for the histogram is 100 km

10 Discussion

10.1 Effect of parameters

10.1.1 KDE

The fact that no difference between the KDE estimates using PI and SCV exists is not surprising considering their highly similar bandwidth values (see Table 5 and Table 6) and the fact that the bandwidth was the only variable parameter in the computation. The rejection of the null hypothesis for the REF and BCV results on the other hand was unexpected, given their nearly identical mean areas, compactness values and high VI indices. This rejection is probably not based on the differences between the results of REF and BCV but rather a problem arising from the combination of the normalized measures and the working principle of the Kruskal-Wallis test. Since the area and compactness values were divided by the maximum occurring values of the respective HRE to remove the differences due to the individual itself, the largest area (or compactness index) produced by KDE for a specific individual receives the value of 1. Unfortunately, the REF bandwidth estimator resulted in the largest areas and compactness values for all of the 12 individuals and thus always received the value of 1. The Kruskal-Wallis test

builds ranks from the values and checks the regularity of them. Building ranks from a series of exact same values and comparing them against a second variable thus will interfere with the working principle of the test. For this reason and because of the high similarities for all of the descriptive and overlap measures, the results of REF and BCV are regarded as being without any significant difference. As the presence of REF could have also biased the testing for differences for the totality of the KDE estimates, the test was repeated without REF, while only PI, SCV and BCV were included. The results were still significantly different (χ^2: 17.59–71.78, df: 1, p: less than $2.74*10^{-5}$).

Even though it cannot be determined which KDE result is closest to "the truth", those based on REF and BCV seem to be more realistic for most individuals. A core area, which is defined as the most frequently used area where most activities are concentrated (Haas et al. 2005; Hansteen et al. 1997), is unlikely to consist of more than 10 regions, as it is the case for 10 of 12 individuals when using PI or SCV. Considering that only those holes larger than 0.25 km^2 and those regions larger than 1 km^2 have been counted, the fragmentation is in fact even higher. However, PI and SCV did not always lead to as fragmented home ranges as shown in Figure 12 c) and d). Furthermore, REF and BCV tend to oversmooth slightly (compare the home ranges of Ronja or Mothamongwe for example in Appendix A.5), which is in agreement with the literature (Gitzen et al. 2006; Jones et al. 1996; Sain et al. 1994; Seaman & Powell 1996). The extent of these differences is much clearer when looking also at the shape of the resulting home ranges (displayed by the compactness index) instead of considering only their areas. The data do not support the claim of superiority of PI and SCV over REF and BCV mentioned in Gitzen et al. (2006) and Duong & Hazelton (2005). It is possible that PI and SCV do not perform well only for the point densities and distributions of these specific datasets, since these factors can influence bandwidth estimators markedly (Gitzen et al. 2006; Scott & Terrell 1987).

Because of the small computational demand and the seemingly reasonable home range estimates, REF is the most appropriate bandwidth estimator for these datasets. As BCV produces similar results but takes the longest of all methods to calculate the bandwidth (Duong & Hazelton 2005), it is less recommendable. PI and SCV reveal more details and can provide a second perspective for those datasets whose fragmentation stay within limits when using these bandwidth estimators.

10.1.2 t-LCH

The occurrence of (significant) differences between the *a*- and *k*-rule corresponds to a previous comparison of Getz et al. (2007) who already noticed differences when using simulations and real data. Whereas their results indicated a consistently better performance of the *a*-rule (for the 95 % and 100 % isopleth), the same cannot be stated for the leopard and lion data in this study. Here, despite the rejection of the null hypothesis through test statistics, the areas and compactness values can be termed as being similar. For some individuals the *a*-rule yielded slightly larger areas while

for others it produced marginally smaller areas (maximum deviation of 14 % and a mean deviation of 1 %). The highly similar compactness indices and visual analysis support the claim of a comparable performance of the two rules for the 95 % isopleth. For the 50 % home range, the situation looks quite different. Here, the *a*-rule yielded markedly larger (on average 16 %) and more compact (on average 42 %) core areas. Consequently, the core areas are less defined and lack any spatial differentiation. This is contradictory to the statement of Getz et al. (2007: 2) that the *a*-rule produces "[…] more clearly defined isopleths in regions where data are more abundant." Since the functioning of the *a*-rule (see Section 7.3.3) supports the statement of Getz et al. (2007), it is likely that the differing behavior of the *a*-rule is connected to the data used in this study. Extended home ranges of the individuals may hold a substantial range in point density. In order to obtain reasonable and stable results for the low-density isopleths (such as 95 %), quite high *a*-values had to be set. This in return led to the inclusion of a lot of points in the high-density regions (e.g. 50 %) and thus to a lack of spatial detail. As the *k*-rule does not regard spatial distances but assigns a fixed number of points to each hull, the varying density does not affect the choice of its value to the same degree.

The inclusion of time through the time-scaled distance alters the result of the local convex hull approach substantially. While a dot-like pattern similar to that of undersmoothed KDE results is observable for $s = 0$, the regions of the isopleths become more interconnected when 40 % or more of the hulls are time-selected. In addition, they become directed towards the pathways of the animals (Lyons et al. 2013). This leads not only to better defined isopleths, particularly for the *k*-rule, but also bears a substantial added value as it provides a rough estimate of the movement paths.

Since the degree of the inclusion of time (40 %, 60% or 80 %) did not affect the results noticeably (and most of them were statistically significant), it seems to be sufficient to stick to the recommendation of Lyons et al. (2013) and use an *s*-value that time-selects 60 % of the hulls. Due to the lack of spatial detail of the *a*-rule, the usage of the *k*-rule is preferable for this kind of data if one is particularly interested in the spatial dynamics of the core area. If the 95 % home range is of primary interest, the choice has only a minor influence. A potential advantage of the *a*-rule, however, could be the increased reliability that all regions of the home range that are essential for an individual are included in the core area isopleth.

10.1.3 BRB

The mechanistic nature of BRB requires a choice of parameters based on the ecology of the specific individual under investigation and its data (see Sections 7.3.4 and 8.5.4). Thus, there should be actually no need to vary parameter values extensively. However, the smoothing parameter h_{min} seems to be an exception as the model proposed by Benhamou & Cornélis (2010) (the developers of the BRB approach) and Jay et al. (2012) did not lead to reasonable home range

estimates for most of the individuals. One reason for this is the variety of sampling intervals present in a dataset, which requires to choose which one(s) should be included in the computation of h_{min}. Aside from that, the definition of the model exhibits a fundamental problem: While the time span between two position measurements used to calculate the maximum travel velocity does not have a large influence on this velocity (see Section 8.5.4), the subsequent multiplication with the respective time span to obtain the final distance almost exclusively determines h_{min}. The quantification of this time span is not clearly defined and offers scope for interpretation. As a further difficulty the appropriate time span can vary markedly between individuals of the same species in the same habitat. The home range estimate of the leopard Mothamongwe is based on a time span of 90 min for the calculation of h_{min} and seems to be rather oversmoothed (Figure 36 a) and b)). The estimate of the leopard Ronja, which rests on a longer time span of 120 min, seems to be adequate. Other examples are the lions Orange and Madge. The BRB results of both are based on 60 minutes intervals. While the computed bandwidth fits perfectly to Orange, the home range of Madge is severely undersmoothed (Figure 36 c) and d)). Due to these reasons, the usage of several models or a scaling for h_{min} was necessary to obtain reasonable estimates. In addition, the usage of only one constant sampling interval for each dataset may facilitate the modelling of h_{min}.

Similarly to KDE, the influence of the smoothing parameter on the area and compactness is quite strong (compare Figure 14 and Figure 36). Since BRB is approximated through a movement-based KDE, the increase in h_{min} leads to larger kernels and thus necessarily to larger home range areas (because of overshooting) (Getz et al. 2007; Lichti & Swihart 2011). Together with the continuous filling of small holes, this results in an almost constant increase. The compactness mainly changes when disjoint home range areas arise or disappear. This happened mostly for the core areas which therefore show a much more jumpy trend, as confirmed by the high CV.
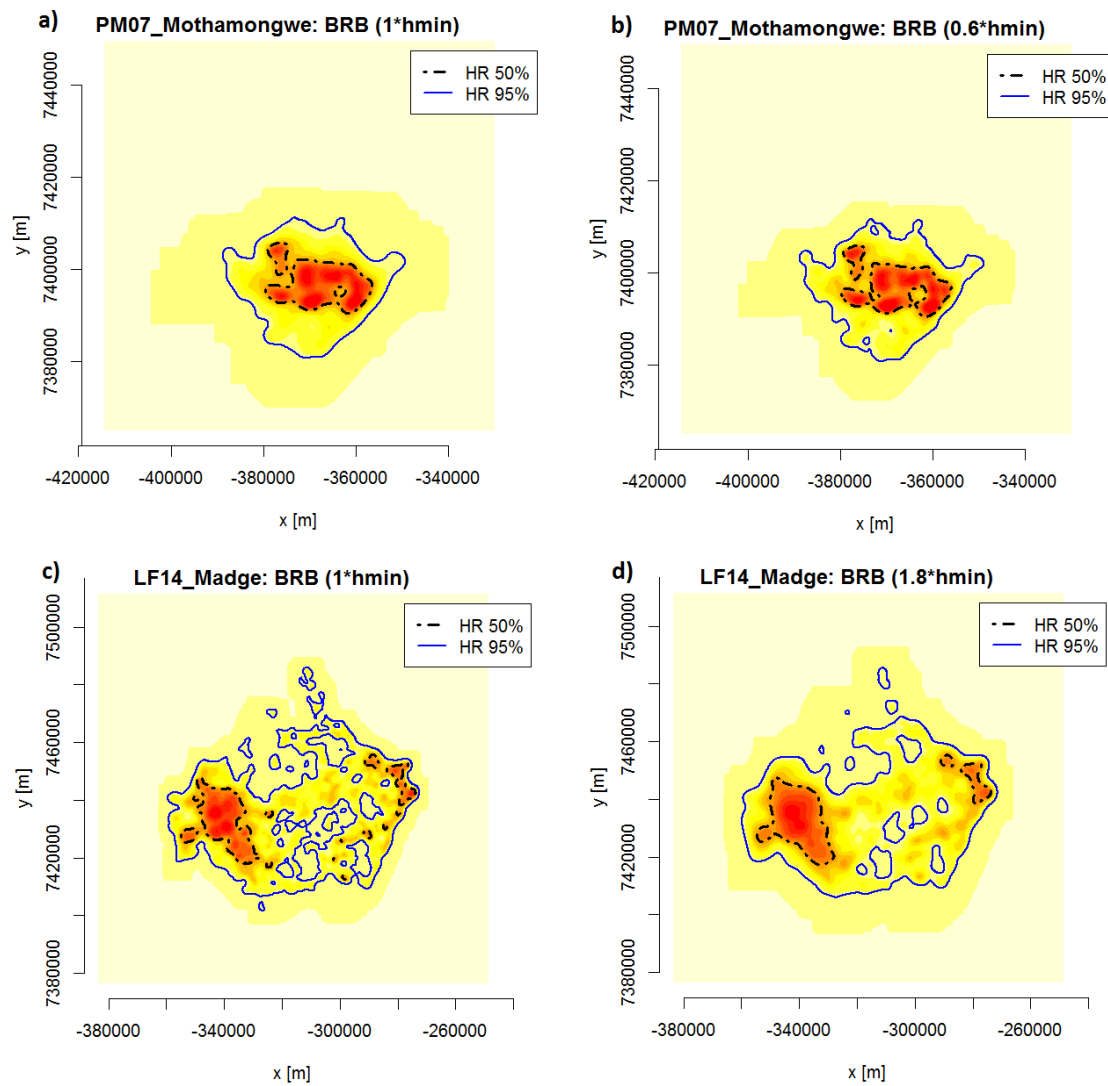
Figure 36. Difficulty in computing an appropriate h_{min}. Image a) and b) belong to the leopard Mothamongwe, c) and d) to the lion Madge. The images on the left (a) and c)) present the reference value for h_{min}, the images on the right side are more sensible appearing suggestions.

10.2 Evaluation of the home range estimators

10.2.1 Performance

The fact that MCP produced the largest home range estimates is in agreement with the general literature (Börger et al. 2006; Huck et al. 2008; Hull et al. 2015).The often-mentioned dependence of the area on the sample size could not be observed (Börger et al. 2006; Downs & Horner 2008; Seaman et al. 1999). Otherwise the difference between MCP and the other methods would be larger for the lions than for the leopards, which have markedly smaller sample sizes. This is not the case here and in agreement with Nilsen et al. (2008) and Hull et al. (2015), who could not find a systematic relationship between the sample size and the area of MCP when using data of free-

ranging animals. It is more plausible that the strong dependency of this HRE on the spatial distribution of the samples caused its larger area estimates (Downs & Horner 2008; Seaman et al. 1999). This is supported by the fact that the difference between the home range estimators is smaller when high compactness indices were obtained for KDE, t-LCH and BRB (compare the area and compactness of the 50 % and 95 % isopleths in Table 19) and thus MCP's assumption of convexity becomes more realistic (Börger et al. 2006). However, despite its largest area estimates, it is dangerous to take the results of MCP as a conservative estimate for purposes such as the protection of species, as suggested by Huck et al. (2008). Particularly the core area of MCP overlaps the core areas of the other HRE only to 40–65 % (25- and 75-percentile, 54 % on average) with extreme values of down to 21 % for one individual. This means that although a sufficiently large area would be protected, it may not be the most important area for the animal. For the 95 % isopleth, the situation is less critical, with overlaps of 70–90 % (mean: 72 %, extreme value: 58 %) but still far away from a full coverage.

On average, the area sizes of the 95 % isopleths of KDE, t-LCH and BRB can be considered as being the same. The same is true for the 50 % isopleth, although only the areas of KDE and BRB as well as BRB and t-LCH are similar enough to be statistically significant. This is surprising as various simulations claimed the superiority of the one or other approach (Getz & Wilmers 2004; Getz et al. 2007; Lichti & Swihart 2011). Keeping in mind that these findings are partially contradictory and are only valid for their respective simulated dataset (Seaman et al. 1999), the high similarity of the estimators confers some reliability to the results. That KDE usually generated the smallest areas is contradictory to the findings in the literature. In fact, various analyses with simulated and real data indicated that KDE tends to oversmooth and result in higher area estimates than e.g. t-LCH, whose estimates were consistently larger in this study (Downs & Horner 2008; Huck et al. 2008; Getz et al. 2007; Lichti & Swihart 2011; Seaman & Powell 1996). Of course, the results refer to averaged values and the parameter range obtained for KDE is large. But since two of its parameters led to oversmoothing and the other two to undersmoothing, the average is assumed to represent a realistic estimate.

When looking at the shape of the home ranges the differences become more pronounced (compare Table 19). Whereas MCP produces consistently the most compact estimates, KDE is at the other extreme, with values that are only 30–50 % as high. Keeping in mind that MCP is based on the assumption of convexity, the large discrepancies to the remaining HRE is evident (Börger et al. 2006). However, while the 95 % isopleth resembles the results of the other HRE, the almost circular core area lacks any spatial detail (see Figure 15 a)). The kernel-based approaches KDE and BRB have markedly lower compactness values than t-LCH (or MCP), especially regarding the core area. This is due to their fragmented home ranges, which contain much more disjoint regions than the geometrically-based approaches. Since the compactness index is a ratio of the total area of the isopleth and the area of the smallest circumscribing circle encompassing all its

disjoint regions, the latter ones markedly influence the compactness value. The number of holes on the other hand does not affect the index, as their areas are not subtracted from the total area. Therefore, despite the much higher number of holes of BRB for the core area (compare Table 19), its compactness is on average the same as the one of KDE. As t-LCH tends to generate interconnected isopleths as soon as time-scaled distances are used, its estimates are more compact and less fragmented (Getz et al. 2007). In addition, the estimates of t-LCH are much more consistent than those of the kernel-based approaches (Lichti & Swihart 2011). It is likely, however, that this is mainly the consequence of the different methodologies. Whereas the home range estimates of t-LCH are in the end selected from a range of candidates to get "reasonable" results, no such preselection is done for KDE and only to a lesser extent for BRB (choice of scaling factors).

10.2.2 Practical application

Irrespective of its performance, MCP allows to estimate home ranges with a minimum effort and expert or prior knowledge. Although being only an extension of this simple HRE, t-LCH turned out to be the most time-consuming and computationally troublesome approach (Getz & Wilmers 2004). In order to obtain a representative range of potential results to select from, about 30–40 different *a*- and *k*-values had to be computed for each individual and level of time inclusion. Apart from the expenditure of time, the availability of memory proved to be the major issue. Even after the inevitable reduction of the lion datasets to approximately 10'000 points, the required memory often exceeded 16 gigabytes for the above-mentioned number of *a*-/*k*-values when using time-scaled distances. Another issue with t-LCH relates to the choice of its parameters (Getz & Wilmers 2004). Although guidelines and methods exist to select the parameters *a* and *k*, none of them worked for these datasets. While the MSHC rule (see Section 7.3.3) could not be applied due to a lack of sufficiently large regions (or objects) that are inaccessible or avoided by the leopards and lions in the study area, the rules of thumb to select *a* and *k* either led to very fragmented and unstable or to massively oversmoothed home ranges. Despite its disadvantages, of all methods t-LCH allows the deepest insights into the data. Although the choice of an "appropriate" result from a range of candidates is subjective, it requires to engage oneself with the data and its behavior when using different parameters. As the choice of the exact value for both the neighborhood rule and the time parameter *s* turned out to be not as critical as for KDE, the disadvantages are considered as being counterbalanced by the benefits.

KDE is comparably simple to use as MCP but requires, depending on the method used to estimate the smoothing parameter, much more computing time for large datasets. As the bandwidth is usually the only adjustable parameter with a significant impact, it is recommended to use as many different methods for bandwidth estimation as possible. Ideally, a package like *ks* is selected to compute KDE that uses the full bandwidth matrix instead of reducing the constrained matrix to a single value, as it has been necessary for *adehabitatHR* (see Duong & Hazelton (2005) for further

details). Since *ks* does not support the same data structures as the other HRE, spatial comparisons are impeded severely. Therefore, the computation of KDE was performed using *adehabitatHR*. When only KDE is used for the analysis of data, this restriction does not matter and *ks* would be the favoured choice.

BRB also uses a smoothing parameter like KDE, but its estimation is materially different. Instead of estimating h_{min} from the data itself, it must be deduced from ecological models. The difficulty is to find a model that works reliably for all individuals of a species irrespectively of their underlying data. In order to adjust a given model or develop a new one, substantial ecological expert knowledge is necessary. Thus, to obtain sensible results using BRB is time-consuming, even though the computational part itself is carried out much faster than e.g. for t-LCH.

10.3 Home ranges of individuals and their interactions

10.3.1 Leopards

The observed home ranges of leopards in the Khutse Game Reserve and the Central Kalahari Game Reserve are among the largest worldwide (Marker & Dickman 2005). Similarly high values could only be found for males in the Kgalagadi Transfrontier Park with home range sizes of 769–2182 km^2 (Bothma et al. 1997; Hayward et al. 2009; Marker & Dickman 2005) and, at a lower level, in the Cederberg Mountains, with areas of 100-910 km^2 (Martins & Harris 2013). The Kgalagadi Transfrontier Park is situated at the border of Botswana and South Africa and thus is also part of the (semi-) arid Kalahari region (Bothma & Bothma 2012) whereas the Cederberg Mountains lie 200 km north of Cape Town in South Africa with a highly variable annual rainfall of 179–669 mm (Martins & Harris 2013). Other reported home range sizes are around 179–451 km^2 in Namibia (with the exception of the Waterberg Plateau for which home ranges of 40–119 km^2 have been estimated), 12–38 km^2 in Kenya or 15–76 km^2 in the northeastern region of South Africa (Kruger National Park) (Hayward et al. 2009; Marker & Dickman 2005; Mizutani & Jewell 1998; Stein et al. 2011). The exact numeric values exhibit a high degree of uncertainty due to differing home range estimators, parameterizations and definition used in the respective studies. Even when the same methodology was used for two studies, different spatial distributions of the GPS fixes of the respective animals also affect the performance of HRE ((Downs & Horner 2008; Getz & Wilmers 2004; Horne & Garton 2006; Lichti & Swihart 2011). Nevertheless, the differences in magnitude are evident and indicate significant differences.

Although it is hardly possible to statistically relate the home range size directly to individual climatic factors, numerous studies investigating the ecology of leopards found a correlation between the quality of the habitat and the home range area (Bothma & Bothma 2012; Marker & Dickman 2005; Mizutani & Jewell 1998; Stein & Hayssen 2013). An arid habitat is usually characterized by a scarcity of prey for the leopards, requiring them to expand their home area to meet their requirements. However, among other factors, the presence and density of inter- and

intraspecific competitors also influences the quality of a habitat for a leopard and thus its home range markedly (Bothma et al. 1997; Hayward et al. 2009; Marker & Dickman 2005). Intraspecific competition may be a reason for the increase of the home range area of the male Bogarigka (see Figure 20). Although its expansion might have been at the cost of the male Mothamongwe, it seems to be too strong compared to the decrease of the latter. Thus, it is quite possible that another unobserved (male) leopard moved away or died and thus created a vacancy, or that Bogarigka took over the home range of another unobserved male. The home range shift of Ronja during the summer 2013 (see Figure 21) is more likely to be related to raising her offspring since she has shown similar shifts before the period investigated in this study[3]. In this summer, Ronja raised a cub that left her to find an own home range in April or June. One reason for her shift towards the south might have been a lower density of other carnivores, which may endanger the life of cubs (Hunter & Hinde 2005; Stein & Hayssen 2013). Since it has been shown previously that even extensive overlaps of leopards of the same sex may occur (Table 24), it is unlikely that the shift of Ronja's home range is related to intraspecific competition.

The extent of the observed overlaps (compare Figure 16) is surprising since leopards are known to be solitary and to maintain a largely exclusive home range towards individuals of the same species and particularly of their own sex (Bailey 1993; Hagen et al. 1995; Hunter & Hinde 2005; Mizutani & Jewell 1998). Although the large home ranges in arid habitats are known to exhibit considerable overlaps of the peripheral regions, at least the core area is thought to be used exclusively (Hunter & Hinde 2005; Marker & Dickman 2005; Stein & Hayssen 2013). However, the two male leopards Bogarigka and Gham had even for the core area overlaps of 53 % resp. 34 % (Table 23). Even though the analysis of their Euclidean distance revealed that they were usually separated by 5 to 30 km (with a minimum of about half a kilometer), this is a remarkable degree of overlap and an indicator of a pronounced active avoidance behavior (Hunter & Hinde 2005; Marker & Dickman 2005; Mizutani & Jewell 1998). This may be an inevitable adaptation since home ranges of several hundred or thousand square kilometers are barely defendable.

The spatial interactions of Ronja with Mothamongwe (and to a minor extent with Bogarigka and Gham) correspond to the literature as home ranges of males usually overlap those of several females in order to have access to as many of them as possible (Bailey 1993; Bothma & Bothma 2012; Mizutani & Jewell 1998). The latter is also the reason why home ranges of males are in general much larger than those of females. In addition, it was assumed that this also leads to lower compactness values. Both, however, could not be observed in this study (Table 21): The only female leopard has the second largest home range that is about twice the size of that of the males Gham and Mothamongwe and of a markedly lower compactness. Without the second core area of Ronja in the south during summer 2013 her home range would be of course considerably

---

[3] Personal communication with Monika Schiess-Meier on July 29, 2015. Monika Schiess-Meier is the founder and managing director of LEC.

smaller (and its compactness higher). Nevertheless it was important enough to belong to the 50 % isopleth of that season and to the 95 % isopleth when looking at the whole timespan. As it is unknown whether that second center of activity should be regarded as an occasional sally or as an indispensable part of the home range, it is safer to assume the latter one from a conservational point of view. The number of individuals is of course insufficient to draw conclusions for the whole leopard population of the Kalahari region. Still, a lack of sex-specific differences has also been stated by Marker & Dickman (2005) who investigated leopards in the northern part of Namibia. According to them, the home range sizes of females may be too large in poor habitats for males to encompass several of them. The presence of significant differences due to sex for leopards in the Kgalagadi Transfrontier Park stated by Bothma et al. (1997), however, questions the generality of this reasoning. The presence of unobserved male and female individuals may alter the interpretation of the observed interactions.

Neither the area nor the compactness of the home ranges showed a clear seasonal variation. While the seasonal differences of precipitation in the study area potentially could lead to corresponding adaptations of the individuals, the pronounced diurnal variations provide a sensible justification for their absence. The study of Marker & Dickmann (2005) in the Waterberg Plateau about 2–3° north and 7–8° west of KGR and CKGR also detected no seasonal variations of the home range size. Except for Ronja and Bogarigka, whose home range changed considerably during the observation period, the relatively stable territories of Mothamongwe and Gham are quite compact (see Table 21). Figure 16 shows that the home range of Mothamongwe lies directly at the eastern border of KGR and transgresses it. Thus, the proximity of livestock may compensate the small home range area in terms of prey availability (Schiess-Meier et al. 2007). However, this does not explain the small and compact territory of Gham. Since overlaps seem to be largely tolerated (compare Figure 17) it is not too likely that a subordinate position of these two leopards in the social hierarchy is the cause for their home range area and shape (Hayward et al. 2009). The fact that the home ranges of three leopards transgress the fenced border of the game reserves corresponds with the reported issue of livestock predation (Schiess-Meier et al. 2007).

10.3.2 Lions

The observed home range sizes (95 % isopleth) for the lions of KGR and CKGR range between 1131 and 4317 km^2 (mean: 2682.5 ± 970.7 km^2). They are thus markedly larger than the home range sizes of 604 km^2–1861 km^2 (mean: 838 ± 421 km^2) computed by Ramsauer (2006) in the same study area during the years 2003–2006. It may be that the lions had more stable home ranges during these years, what results in smaller areas. However, home ranges were not analyzed regarding their temporal variability by Ramsauer (2006). The only equally large areas have been found in the dune savanna of the Kgalagadi Transfrontier Park (1500–4500 km^2) that belongs to the Kalahari region as well (Funston 2011; Hayward et al. 2009; Tumenta et al. 2013). Markedly smaller are the home ranges in the more humid regions of the Waza National Park in Cameroon

(537–1534 km^2), the Kunene region in the northwest of Namibia (up to 1628 km^2) or the Makgadigadi Pans National Park northeast of the CKGR in Botswana (up to 1143 km^2) (Bauer & de Iongh 2005; Hayward et al. 2009; Tumenta et al. 2013). For regions with a high prey abundance such as the tropical savanna of the Selous Game Reserve in Tanzania, home ranges are less than 100 km^2 (Hayward et al. 2009; Spong 2002). Due to different methodologies and spatial distributions of the GPS fixes, the same restrictions regarding the comparisons of home ranges are valid as discussed for the leopards in Section 10.3.1. Much less variable than the observed home range sizes are their compactness values (on average 0.38 ± 0.09 at the 50 % and 0.52 ± 0.06 at the 95 % isopleth). Surprisingly, the compactness of the home range is negatively related to the home range size. From an energetic perspective, at least for the 95 % boundary the opposite would be expected. Yet, it needs to be considered that the home ranges of the individuals are constituents of the pride's territory, for which the situation may be different.

The fact that none of the lions has a home range that extensively overshoots the protected area indicates that sufficient resources are available there for the observed lions. This is in agreement with the findings of Bauer et al. (2014) who detected a massive decrease of the lion population between 2005 and 2010 and thus a release of previously occupied areas. Yet, the 95 % isopleths of some of the lions such as Mexico, Verity or Orange are close to the border and therefore to the livestock of the farmers. Particularly Madge may be a habitual livestock raider (Bauer & de Iongh 2005; Tumenta et al. 2013) since even her core area transgressed the boundary of the game reserve slightly. However, occasional sallies are not regarded by the concept of home ranges, meaning that the actual problem of livestock killing may be much more urgent than displayed by the home ranges and their respective overlap values (Schiess-Meier et al. 2007).

Males are often reported to have larger home ranges than females, even though these differences are only rarely statistically significant because of a too low number of individuals and the high variability between them (Hayward et al. 2009; Loveridge et al. 2009; Tumenta et al. 2013). Such a sex-specific disparity could not be found for the lions here. It is rather that the males have the most extreme areas in both directions, whereas those of the females lie in between. Because of that, females have on average even a larger home range for both the 95 % isopleth (2860 ± 581 km^2 vs. 2385 ± 1698 km^2) and the 50 % isopleth (584 ± 170 km^2 vs. 531 ± 466 km^2). Seasonal patterns have only been found for the compactness of the 95 % boundary for some of the lions. The fact that the area did not show any seasonality at all is in agreement with the findings of Ramsauer (2006). Since Loveridge et al. (2009) only found statistically insignificant seasonal differences for a slightly less arid region than the Kalahari, whereas Tumenta et al. (2013) detected pronounced (and significant) differences for a much more humid study area with three distinct seasons, the seasonal changes may be not pronounced enough in KGR and CKGR to result in respective behavioral changes of the lions. Even if the seasonality of the climate is strong enough, other influences seemed to determine the size of the home ranges during the observation period

(at least for Verity, Ella, Hitchcock and Madge). As lions exhibit strong sociality (Haas et al. 2005; Macdonald & Loveridge 2010), the loss of an individual (particularly of a male) can cause a cascade of reactions such as breakings of prides. It is thus likely that intraspecific drivers caused the observed fluctuations[4].

Based on the overlaps presented in Table 22–Table 24 the individuals were assigned to individual prides. The territories of the three males did not overlap each other beyond a few percent for the outer boundary. Since only males that belong to the same pride have extensively overlapping home ranges, the three males are assumed to belong to different prides (Haas et al. 2005; Loveridge et al. 2009). Due to the high VI value of 54 % and distinct overlaps of the core areas, Verity likely belong to the same pride as Orange. The home ranges of Ella and Getika overlap strongly with that of Mexico and thus are assumed to belong to the same pride. The pronounced overlap of the home range of Getika and Ella (VI index of 62 %) and small Euclidean distances between them (Table 25) support this interpretation. It has to be mentioned, though, that Getika died in February 2013, while data for Mexico is only available since September 2012. Because of that, the observed shared timespan is rather short. Interestingly, the 95 % overlap values for Mexico and Verity are rather high with 38 % resp. 72 %. Considering also the VI value of 21 % this potentially reflects a pronounced degree of interaction. Except for the shrinkage of her home range after the summer of 2011, Verity's territory shifted eastward and away from Mexico (compare Figure 27 and Figure 33 a)). However, the distance towards Orange, whose home range lies in the direction of Verity's shift, did not change markedly. Hitchcock, also a male, overlaps a significant part (59 %) of Jane's home range at the 95 % isopleth and therefore is assumed to be in the same pride. When looking at their core areas, a low spatial overlap of 1 % is surprising. The histogram in Figure 34 b) proves that the two lions met frequently, although this is hardly visible in the smoothed distance curve of Figure 33 b). The separated home ranges but highly overlapping 95 % boundaries and frequent encounters indicate that they belong to different subgroups of the same pride (known as fission-fusion) (Funston 2011; Ramsauer 2006).

With the available data in this study, Madge is the only lioness that could not be assigned to a pride. She spatially interacts only with Jane (see Figure 31 b)) who belongs to a pride. Since lionesses are known to be highly territorial against foreign individuals of the same sex, it is possible that they belong to the same pride which encompasses more members than only Jane and Hitchcock and is split into subgroups (Eloff 1998; Funston 2011; Haas et al. 2005; Spong 2002). According to Figure 31 b) and Figure 32 b), Jane and Madge met only rarely and kept usually a distance of more than 10 km. The shift of Madge's home range towards the northeast (Figure 28) resulted in an overall home range that seems to consist of two separate parts (Figure 29). In addition, this shift increased the distances between Madge and Jane and thus reduced the degree

---

[4] Personal communication with Monika Schiess-Meier and Dr. Stephen Henley on September, 1 2015.

of their spatial interaction (Figure 31 b)). Another interesting interaction occurred between Ella and Verity, who wandered around together for about half a year with distances of less than 1 km (Figure 31 a)). According to information from LEC[5] they used to be in the same pride together with Jane and Madge before and separated for an unknown cause. The observed dynamics of their home ranges may therefore correspond to the time period right after the pride disbanded.

Since the data basis of the eight lions covers only a part of the estimated lion population within the study area (Bauer et al. 2014) and was not selected with regard to some known pride structures, it is not possible to draw conclusions about the size of the prides in the study area. Studies on comparable study sites (Winterbach et al. 2014) found that prides contained about 3 to 12 (on average 4.7–7.5) individuals (Eloff 1998; Funston 2011). This probably reflects the pride sizes that could be expected in KGR and CKGR.

10.3.3 Cross-species comparison

On average, the home range areas of the lions are about twice as large as those of the leopards for both isopleths. This also reflects the results of other authors, particularly in comparable habitats (Bothma et al. 1997; Funston 2011; Hayward et al. 2009). For resource-rich habitats with smaller home ranges, factors of three to four were reported (Hayward et al. 2009).

Leopards and lions in the Central Kalahari region show extensive overlaps regarding their home ranges. Particularly the home ranges of Bogarigka, Verity, Ella and Orange intersect up to the core area with the home ranges of numerous individuals of the other species. However, since lions have no reasons to avoid leopards and the home ranges of both species are very large, a lack of interspecific overlaps would have been surprising. The fact that the home ranges of the lions generally overlap a higher proportion of the respective leopard than vice versa is at least partially due to their larger areas. The opposite pattern is only observed for Bogarigka, whose home range is larger than that of the lions Mexico, Orange or Getika.

For the interspecific distances presented in Table 27 it is likely that the respective individuals encountered several times. At velocities of 50–60 km/h (Haas et al. 2005; Hunter & Hinde 2005), the observed minima of less than 1 km but also some of the 10 % quantiles can easily be covered within a sampling interval of at least 30 min. Thus, such encounters may often remain undetected but had no serious consequences for any of the observed leopards. Since leopards are physically inferior to lions they have an interest in avoiding encounters as often as possible (Hagen et al. 1995; Hunter & Hinde 2005). Such an active avoidance behavior is indicated by the histograms shown in Figure 35. Considering the high overlap values between the respective leopards and lions, distances of less than 5 km make up only a small fraction of all recorded distances.

---

[5] Personal communication with Monika-Schiess Meier and Stephen Henley on September 1, 2015.

IV   Kill site detection

11   Related work

The investigation of kill sites provides information usable for numerous purposes, such as the conservation of carnivores, dietary compositions, and the interactions between carnivores and prey populations (Bacon et al. 2011; Merrill et al. 2010; Pitman et al. 2014). Although continuous observation provides the most accurate kill site estimates, it is restricted by its high time consumption and accordingly small sample sizes (Sand et al. 2005; Tambling & Belton 2009). Particularly for studies of reclusive species living in barely accessible terrain or roaming over large areas, the increasing availability of affordable GPS collars provides a cost-efficient alternative to collect data on kill-sites (Anderson & Lindzey 2003; Pitman et al. 2012).

Spatiotemporal clustering algorithms have been often applied to GPS data in order to detect kill sites. Such clustering approaches are based on the fact that consuming prey requires a predator to stay longer at a location than most other activities (Merrill et al. 2010). Comparisons of kills located though GPS clusters with scat analyses for different predator species revealed that clustering approaches are generally biased towards large prey (Bacon et al. 2011; Pitman et al. 2014; Tambling et al. 2012). For lions, Tambling et al. (2012) found that the number of killed prey weighing less than 100 kg are underestimated by as much as 50 %. Since small prey account only for a small proportion of the total biomass intake (Bacon et al. 2011; Tambling et al. 2012), GPS clusters are nevertheless suitable for the investigation of kill rates and feeding behavior, as being shown in Pitman et al. (2013) and Sand et al. (2005).

Another application of spatiotemporal clustering is to indicate potential kill sites, for which information on additional variables (e.g. vegetation density) are recorded that can be used for building predictive models of kill sites. One of the first studies of this kind, by Anderson & Lindzey (2003), used several spatial and ecological variables determined at GPS clusters of cougars (*Puma concolor*) as input for a logistic regression model. This model suggested the timespan of a GPS cluster, particularly during the night, as a main predictor. Tambling et al. (2010) and Pitman et al. (2012) expanded the list of predictor variables and used general linear models to predict kill sites of lions and leopards, respectively. Among other variables, both studies found the ratio of distance moved before and after a cluster to be an important contributor to the prediction model.

The kill site detection rates and appropriate methodology of clustering algorithms depend on many factors, such as the prey size (Pitman et al. 2012; Tambling et al. 2010), anthropogenic pressure (Pitman et al. 2013; Smith et al. 2015) and the social structure of the predator (Merrill et al. 2010; Tambling & Belton 2009). For example, Pitman et al. (2014) analyzed kill sites of

leopards by defining clusters as two or more subsequent points (sampling interval of 2 h) within 50 m, whereby clusters being closer than 100 m and 8 h (closest point to closest point) were merged. Of the validated clusters obtained by this methodology, 37 % proved to be actual kill sites (Pitman et al. 2014). For lions, on the other hand, which kill noticeably larger prey than leopards (Haas et al. 2005; Hunter & Hinde 2005; Macdonald & Loveridge 2010) only 16 % of the clusters were found to be actual kill sites (Tambling et al. 2012). Although the less refined clustering rules (two or more consecutive points [sampling interval of 1 h] within 100 m) might be partially responsible for the lower success rate, the fact that lions often feed on prey in groups (Haas et al. 2005) is likely to influence the success rate as well, since it leads to lower handling times and thus shorter clusters (Merrill et al. 2010).

12 Methodology

12.1 Analysis procedure

A successful detection of kill sites depends, among other factors, largely on the selected rules for the clustering approach. In order to evaluate the effect of different variables (in this approach) and to determine the rule yielding the lowest error rates, the results of different sets of variables were compared in a first step. The clustering rule that led to the lowest overall error was then used to estimate the ratio of kill sites inside the 50 % and 95 % home range boundaries as well as inside the protected area of the game reserves.

12.2 Effect of the clustering rule

12.2.1 Building clusters

As proposed by various authors (Anderson & Lindzey 2003; Tambling et al. 2010; Tambling et al. 2012), a cluster must consist of at least two consecutive GPS fixes that are closer in space than the maximum observed GPS error plus a buffer for translocations of the individual (and its prey). Although the data of all four lions was predominantly sampled at 30 min and 60 min intervals short periods of coarser sampling intervals occurred. Since it is questionable whether two successive fixes being close in space but far away in time belong to the same cluster, a temporal threshold was incorporated as well. A value of 65 min was set for all individuals. The whole workflow is shown in Figure 37.

12.2.2 Merging and filtering clusters

Since lions consume prey often in prides (Haas et al. 2005; Macdonald & Loveridge 2010), it is likely that individuals do not stay by a carcass permanently but return to it repeatedly (Tambling et al. 2010). By merging clusters that are spatially nearly identical but temporally separated, it can be avoided that such behavior results in several single clusters and, thus, in overestimation of their number. Pitman et al. (2012), who analyzed kill sites of leopards, merged clusters having their

closest points within 8 h. As lions prefer larger prey (Hunter & Hinde 2005) handling times of small prides or individually hunting lions can be longer than those of leopards. Based on this information and observations made by LEC[6], the time threshold for merging clusters was set to 10 h (for the temporally closest points of the respective clusters). Finally, as in Tambling et al. (2010), all clusters lasting less than 2 h were deleted (see Figure 37). Due to the irregular sampling interval, clusters were also deleted, if they consisted of too few GPS fixes. For datasets with 60 min SI, 2 fixes were the minimum and for those having 30 min as their coarsest SI, 4 fixes were required. The clusters obtained after the merging step were considered as potential kill sites and from the data basis for the subsequent weighting.
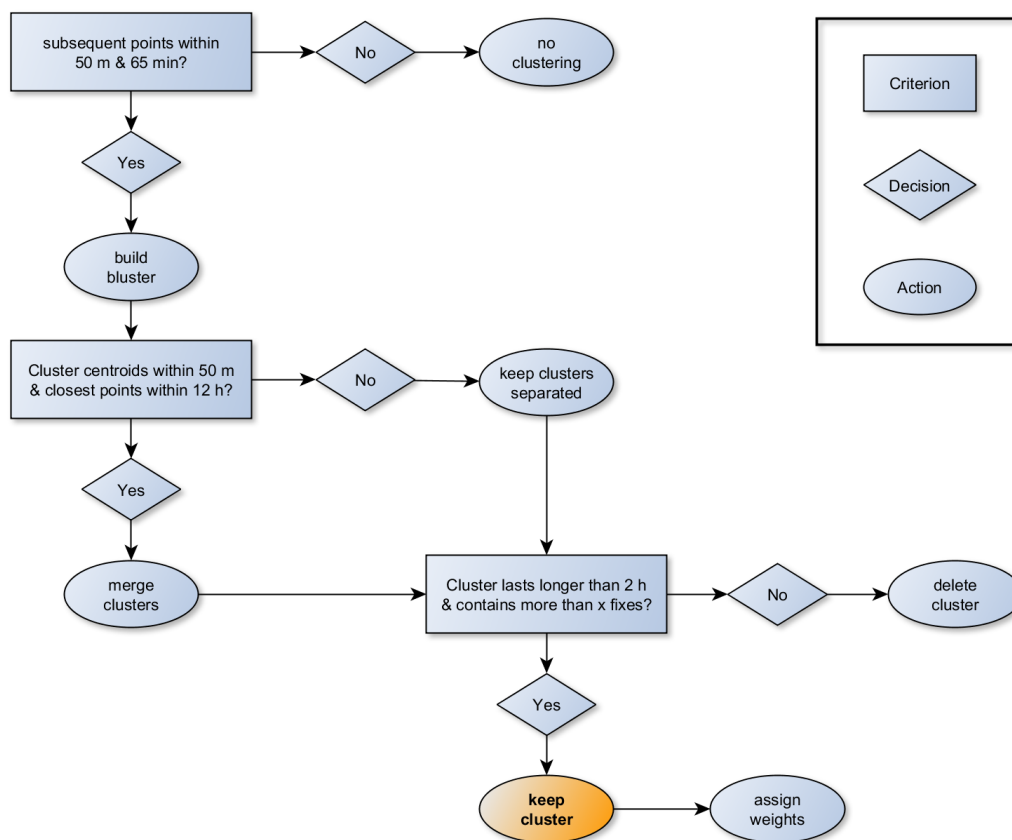
Figure 37. Illustration of the clustering rules applied to the lion datasets. The orange colored ellipse represents the final clusters, which were then weighted according to the variables mentioned in Section 12.2.3.

---

[6] Personal communication with Dr. Stephen Henley and Monika Schiess-Meier on September 1, 2015

12.2.3 Assigning weights

Previous studies that built predictive models of kill sites for felids found that the detection rate could be significantly improved by including additional variables. Except for the duration of a cluster (*Dur*) (Anderson & Lindzey 2003; Pitman et al. 2012), the ratio of distance moved before and after a cluster (*DistR*) (Pitman et al. 2012; Tambling et al. 2010) and the time of day (*ToD*) (Anderson & Lindzey 2003) proved to be the strongest contributors. These variables were incorporated in the clustering approach as weights, expressing the probability of a cluster being an actual kill site. In a first step, the clusters were weighted according to their value for each variable separately.

For the variable *Dur*, the time period of each cluster (defined by the temporal difference between the first and last GPS fix belonging to the same cluster) was computed and divided by the longest time period of all clusters to obtain normalized values. For *DistR*, the ratio of the sum of distances moved between all fixes within 24 h before the start of a cluster and 24 h after the end of a cluster was computed. Thus, the larger the distance travelled during the 24 hours before a cluster and the smaller it is during the 24 hours after a cluster, the higher is the resulting value. The ecological signification of *DistR* is that carnivores are supposed to range farther when being hungry and reduce their activity afterwards (Pitman et al. 2012). Again, the variable values were normalized. The last weighting variable, *ToD*, is based on the fact that many predators prefer to hunt between dusk and dawn due to their reduced visibility (Anderson & Lindzey 2003; Haas et al. 2005; Martins & Harris 2013; Patterson et al. 2004). As lions in KGR and CKGR are also nocturnal (Ramsauer 2006), each GPS fix that belongs to a cluster and was recorded between dusk and dawn was assigned the value 1. Fixes belonging to a cluster and being recorded during the day received a value of 0. Dusk was defined as 5 p.m. and dawn as 8 a.m. If the mean of the assigned values was larger than 0.33, the cluster received a value of 1 for the *ToD* variable. If the mean was smaller than 0.33, a value of 0.5 was set. Since resting occurs mainly during the day, when hunting success is reduced and high air temperatures potentially restrict high physical efforts (Patterson et al. 2004; Ramsauer 2006), corresponding clusters receive lower weights.

12.2.4 Sets of variables

The combinations of the three variables *Dur* (duration of a cluster), *DistR* (ratio of distance travelled before and after a cluster) and *ToD* (time of day) were used to build four different sets of variables to assign weights, which are presented in Table 28. For comparison, the clustering approach used in Tambling & Belton (2009), Tambling et al. (2010), and Tambling et al. (2012) was included as a fifth variable set (set$_{TA}$). Its rules were adapted to the data in this study and are as follows: Consecutive fixes must be within 50 m and 65 min and a cluster must last 2 h or longer. The adaptations were necessary due to the different and heterogeneous sampling interval occurring in our data.

Table 28. Combinations of the three variables used for weighting of clusters. *Dur* corresponds to the number 1, *DistR* to 2 and *ToD* to 3. Set_{12} therefore used the variables *Dur* and *DistR*. Set_{TA} stands for the clustering approach used (among others) in Tambling et al. (2010) and does not use any weights. *norm* stands for "normalized".

Variable set name	Involved variables	Weighting formula
Set_{12}	*Dur*, *DistR*	norm(*Dur* + *DistR*)
Set_{13}	*Dur*, *ToD*	*Dur* * *ToD*
Set_{23}	*DistR*, *ToD*	*DistR* * *ToD*
Set_{123}	*Dur*, *DistR*, *ToD*	norm (*Dur* + *DistR*) * *ToD*
Set_{TA}	-	-

12.2.5 Validation

To validate the results of the different sets of variables, a small amount of validated kill sites and non-kill sites was available, as presented in Table 3 on page 15. According to comparisons with the literature, all of the totally 91 validated kill sites involved large prey above 100 kg (Bauer et al. 2014; Hayward et al. 2006; Schiess-Meier et al. 2007; Winterbach et al. 2014). The validated kill sites were used to compute the type II errors, which show the proportion of undetected validated kill sites. Each cluster was buffered by 50 m and then spatially intersected with each validated kill site belonging to the respective lion. If a match was found, it was tested whether they intersected temporally as well. For the temporal intersection, the kill date estimated by spoor trackers was buffered according to the time difference between the estimated kill date and the observation date. Based on preliminary analyses and information from LEC[7], the buffer values listed in Table 29 were defined. The sum of clusters that spatially and temporally intersected with validated kill sites was divided by the number of validation records for the respective animal, transformed into percentages (values higher than 100 % were set to 100 %) and subtracted from 100 %. Thus, high values indicate high percentages of erroneously not identified kill sites.

Table 29. Time buffers used for the intersection of clusters and validation data.

Time difference*	Time buffer
Up to 1 day	± 1 day
2 to 7 days	± 2 days
8 to 14 days	± 3 days
15 to 21 days	± 4 days
22 to 30 days	± 5 days
more than 30 days	± 10 days
*The timespan between the date of observation and the estimated non-/kill date.	

---

[7] Personal communication with Dr. Stephen Henley on September 3, 2015.

The validated non-kill sites (only available for Madge) were used to determine the type I errors, which show the proportion of detected kill sites that are known to be none. Each cluster was buffered by 50 m and tested for intersection with the validation data. Dates of a non-kill site were buffered by ± 3 days to account for potential inaccuracies that may have occurred during the process of manually determining the date and coordinates of a cluster. The sum of intersections was divided by the number of validation records for the respective animal and transformed into percentages. Again, values higher than 100 % were set to 100 %. The higher the type I error, the higher the percentage of erroneously detected "kill sites".

The resulting errors were measured at different weights (0.1–0.5, in steps of 0.1) and the average of the errors for the weights from 0 to 0.5 was computed for all individuals. Only weights between 0 and 0.5 were considered for the mean error because most error type I and II values are identical beyond this weight, which would reduce the differences between the sets. For Madge, these measures refer to the total error, which is the sum of the type I and type II errors. For Getika, Verity and Ella, these measures refer to the type II error only (due to insufficient validated non-kill sites). The minimum error and its associated weight were determined only for the total error of Madge. Since type II errors always increase with increasing weights, their minimum is always 0 and occurs at weight 0.

12.3   Estimated kill sites

According to the results of Section 13.1, set_{12} and set_{123} achieve the lowest errors. As set_{12} requires less information to compute, it was selected for the subsequent analyses.

12.3.1 Criteria to select weight thresholds

The minimum total error is the most appropriate criterion to select the weight threshold in many situations. It ensures that the sum of overestimation and underestimation of kill sites is minimal according to the available validation data and thus was one of the criteria (denoted as *Error$_{min}$*) used in this study. However, the total error could only be determined for one of the four individuals (Madge). In order to apply the criterion to the other lions, the error type II for the weight yielding the minimum total error was determined for Madge. The weight threshold for the other individuals was selected by inspecting at what weight value the difference of their type II errors was closest to the reference of Madge. This procedure, however, implicitly assumes that there are no significant differences between the individuals regarding the ability to locate their kill sites. Given that no validation data about non-kill sites were available for the other individuals, it was nevertheless the only possible procedure. The resulting weight thresholds for this criterion are shown in Table 34.

A maximum allowed error type II of 10 % was selected as a second criterion (denoted as *Error II₁₀*) to define the weight threshold. It is defined as the maximum weight which results in a type II error less than or equal to 10 % (see Table 34). *Error II₁₀* ensures a reasonable degree of underestimation but ignores potentially resulting overestimation. Information on the error type II was available for all individuals.

A final criterion is based on ecological information rather than on observed error rates of the data by setting the weight threshold according to the resulting mean kill rates. The kill rate denotes the time that passes between two successive kills of an individual or pride (Merrill et al. 2010; Sand et al. 2005). It was determined by using the *time to kill* (*TK*) definition of Merrill et al. (2010) that starts to count the time between kills at the first fix being no longer part of a cluster, and ends to count at the first fix belonging to the consecutive cluster. Because kill rates depend on many factors such as climate, vegetation, sex and prey abundance (Funston et al. 1998; Rapson & Bernard 2007), values from the literature were used to roughly set a lower and upper boundary of the ecologically reasonable *TK* values. Lionesses in Kruger National Park and Karongwe Game Reserve in South Africa were found to have quite high kill rates of 1.7–2.6 days (Funston et al. 1998; Lehmann et al. 2008). Other studies in Madjuma and Shamwari Game Reserve (South Africa), that did not distinguish between males and females, found that lions killed on average every 4 to 5 days (Power 2002; Rapson & Bernard 2007). Accordingly, *TK* thresholds of 2 and 5 days were defined. The respective weights were found by calculating the resulting mean *TK* values at different weight thresholds (Figure 38). The weights being closest to the lower (*TK*_low) as well as to the upper *TK* boundary (*TK*_high) were used as criteria to set the thresholds (see Table 34).
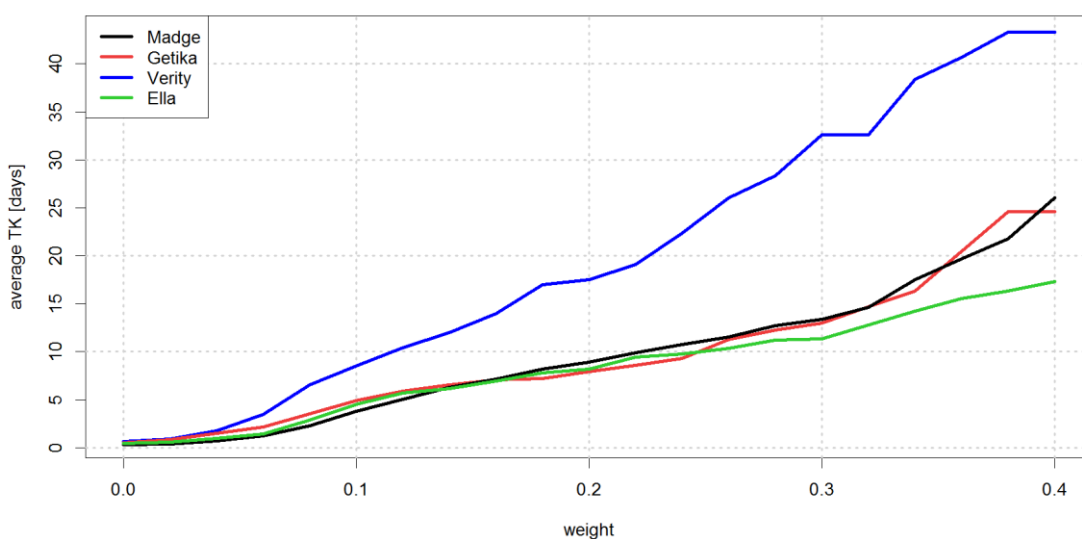
Figure 38. Mean *time to kill* (*TK*) values at different weights. All of the analyzed lions are females.

12.3.2 Spatial distribution of kill sites

The spatial distribution of the kill sites was analyzed according to three ecologically relevant aspects: The ratio of kill sites inside the 50 % home range, inside the 95 % home range, and inside the protected area. The kill sites that matched the respective criteria presented in Section 12.3.1 were intersected with the polygons of the two home range isopleths and the game reserves (KGR and CKGR). The area of the polygons was buffered by 50 m prior to the intersection in order to take the GPS error into account.

13   Results

13.1   Effect of the clustering rule

For all of the four lions, set_{23} results in the strongest decrease of clusters when increasing the weight threshold from 0 (see Figure 39 for Madge and Figure 40 for Getika). Except for Ella, set_{13} shows the flattest curve whereas set_{12} and set_{123} are between the two extremes and almost identical. For Ella, the curves of set_{13}, set_{12} and set_{123} are almost identical and less steep than those of set_{23}. Except for set_{12} and set_{123}, set_{23} and DistR as well as set_{13} and CluDur exhibit curves that are identical or at least very similar for all individuals. The curve of ToD looks different from the other curves because it is a binary factor instead of a continuous normalized number. Verity and Getika (Figure 40) show an almost straight line for ToD, whereas a sharp bend around the weight 0.5 is visible for Ella and Madge (Figure 39). The plots for Verity and Ella can be found in Appendix A.7.
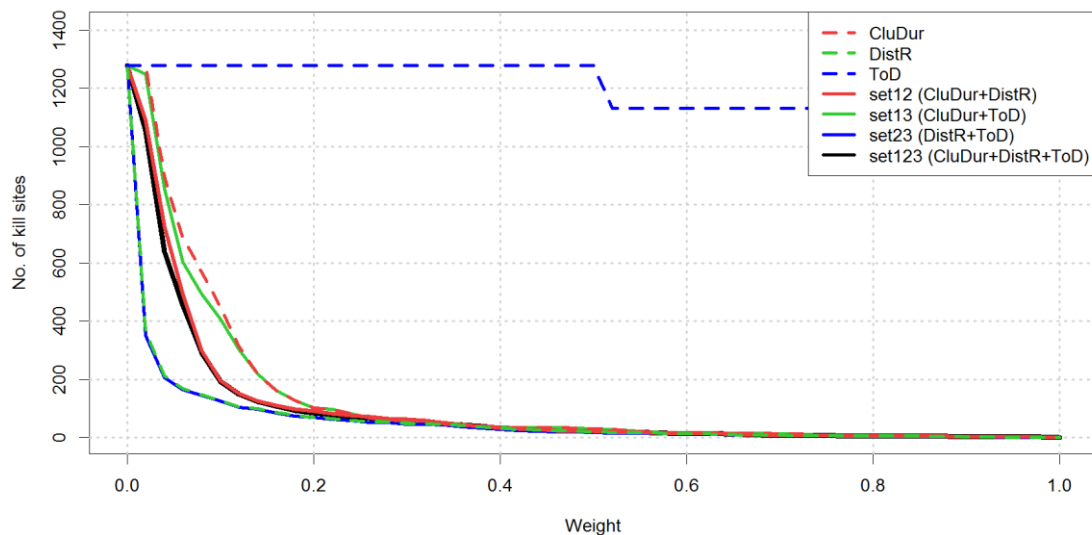
Figure 39. Number of clusters for Madge obtained at different weights. The four sets of variables involving weighting are presented plus the three individual variables for comparison. Set_{TA} resulted in 1409 clusters (not shown).
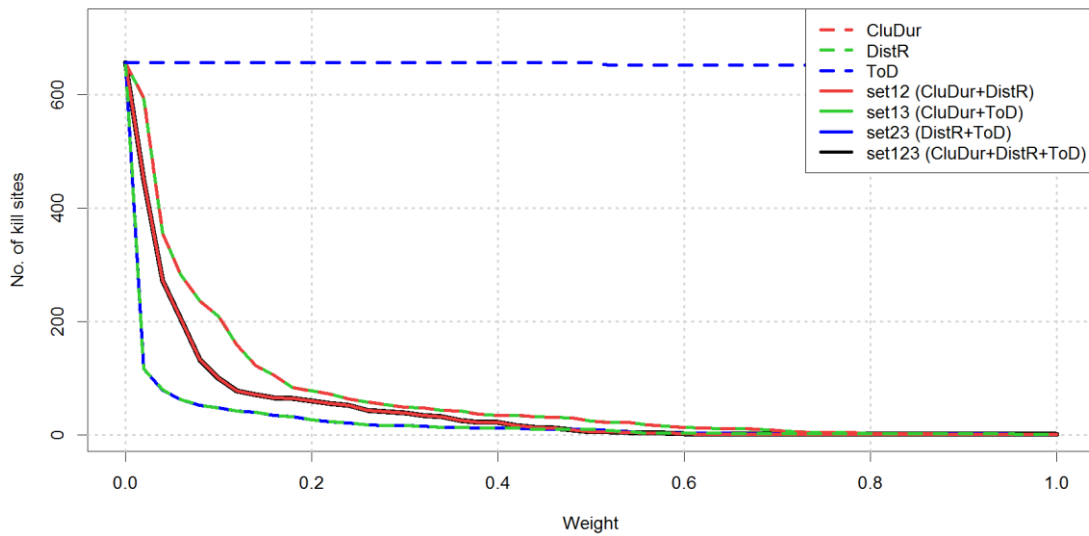
Figure 40. Number of clusters for Getika obtained at different weights. The four sets of variables involving weighting are presented plus the three individual variables for comparison. Set$_{TA}$ resulted in 768 clusters (not shown).

When looking at the errors of the sets of variables, those of type I decrease with increasing weight thresholds whereas those of type II increase (Figure 41 and Figure 42). Since no type I errors could be determined due to an insufficient number of validated non-kill sites, only type II errors are shown for Getika (Figure 42). The errors of the Tambling approach are constant because it does not use weights. For Madge (Figure 41), set$_{23}$ shows the lowest error type I but the highest error type II over all weights. Set$_{13}$ shows the opposite pattern, with the highest errors of type I and the lowest errors of type II for most weights. Both error types are identical for set$_{12}$ and set$_{123}$ and are, except for the weights 0.26–0.34, between the extremes of set$_{23}$ and set$_{13}$. This leads to the lowest minimum total error of 29.4 % (for the weight of 0.14) and the lowest mean total error of 62.2 % of all sets (Table 30). Set$_{13}$ has only a slightly higher mean total error of 63.8 % and often shows the lowest total errors for single weights, but has a markedly higher minimum total error of 40.5 %. The mean total error of set$_{23}$ is higher than the one of the other sets and is only surpassed by set$_{TA}$.

For Getika, the error curves look similar to those of Madge (Figure 42). Again, set$_{23}$ has the highest errors of type II, which is confirmed by Table 31. Although set$_{13}$ has the lowest error for most weights and thus also on average, it is undercut by set$_{12}$ and set$_{123}$ for the weights between 0.14 and 0.26. Set$_{12}$ and set$_{123}$ yield identical type II errors for all weights, which holds true for Verity and Ella, too. The low error type II value (0 %) for set$_{TA}$ indicates that all validated kill sites were detected. For Verity, set$_{12}$, set$_{13}$ and set$_{123}$ have similar errors for most weights and nearly identical ones for the mean errors (Table 32). Only set$_{23}$ consistently yielded higher errors of type II. The lowest mean errors are with 71.2 % markedly higher than those for the other

individuals. For Ella, the lowest errors for most weights and on average were produced by set_{12} and set_{123} (Table 33). Unlike the other lions, set_{13} yielded the highest type II errors here. The error plots for Verity and Ella can be found in Appendix A.7.
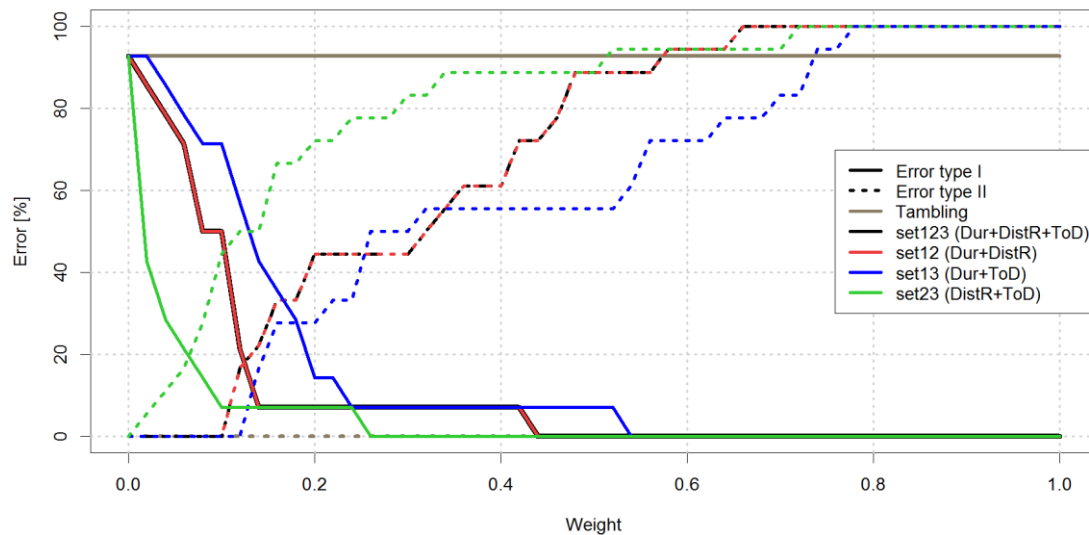
Figure 41. Type I and II error plots for Madge obtained at different weights. The errors of all five sets are shown. Dashed lines represent the rate of missed kill sites, solid lines the rate of erroneously detected ones.
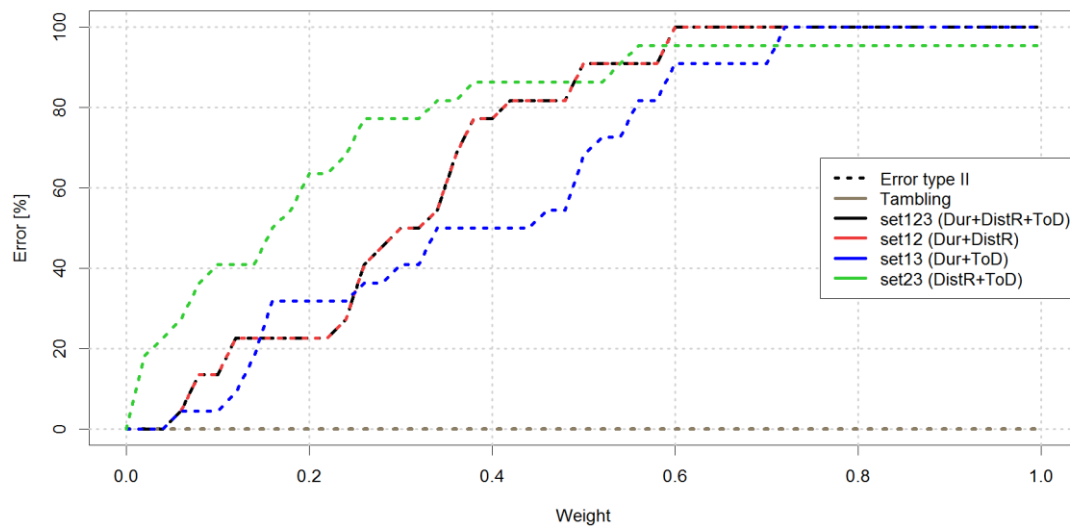
Figure 42. Type II error plots for Getika obtained at different weights. The errors of all five sets are shown. The dashed lines represent the rate of missed kill sites. Insufficient validation data was available to determine type I errors.

Table 30. Validation of the total error (sum of error type I and II) for Madge. The lowest error values per column are underlined.

Variable set	Minimum total error		Total error at different weights [%]					Mean total error
	Value [%]	Weight	0.1	0.2	0.3	0.4	0.5	(0.0–0.5) [%]
set_{12}	<u>29.4</u>	0.14	50.0	51.6	<u>51.6</u>	68.3	88.9	<u>62.2</u>
set_{13}	40.5	0.24	71.4	<u>42.1</u>	57.1	<u>62.7</u>	<u>62.7</u>	63.8
set_{23}	38.1	0.06	<u>46.0</u>	73.8	83.3	88.9	88.9	74.5
set_{123}	<u>29.4</u>	0.14	50.0	51.6	<u>51.6</u>	68.3	88.9	<u>62.2</u>
set_{TA}	92.9	-	92.9	92.9	92.9	92.9	92.9	92.9

Table 31. Validation of the error type II for Getika. The lowest error value per column are underlined (considering only sets with weights).

Variable set	Error type II at different weights [%]					Mean error type II
	0.1	0.2	0.3	0.4	0.5	(0.0–0.5) [%]
set_{12}	13.6	<u>22.7</u>	50.0	77.3	91.0	42.1
set_{13}	<u>4.5</u>	31.8	<u>40.9</u>	<u>50.0</u>	<u>68.2</u>	<u>32.0</u>
set_{23}	40.9	63.6	77.3	86.4	86.4	61.7
set_{123}	13.6	<u>22.7</u>	50.0	77.3	91.0	42.1
set_{TA}	0	0	0	0	0	0

Table 32. Validation of the error type II for Verity. The lowest error values per column are underlined (considering only sets with weights).

Variable set	Error type II at different weights [%]					Mean error type II
	0.1	0.2	0.3	0.4	0.5	(0.0–0.5) [%]
set_{12}	<u>56.5</u>	<u>69.6</u>	87.0	<u>91.3</u>	<u>95.7</u>	<u>71.2</u>
set_{13}	69.6	73.9	<u>82.6</u>	<u>91.3</u>	<u>95.7</u>	71.4
set_{23}	60.9	82.6	91.3	95.7	100	76.9
set_{123}	<u>56.5</u>	<u>69.6</u>	87.0	<u>91.3</u>	<u>95.7</u>	<u>71.2</u>
set_{TA}	0	0	0	0	0	0

Table 33. Validation of the error type II for Ella. The lowest error values per column are underlined (considering only sets with weights).

Variable set	Error type II at different weights [%]					Mean error type II
	0.1	0.2	0.3	0.4	0.5	(0.0–0.5) [%]
set_{12}	<u>44.8</u>	<u>58.6</u>	<u>62.1</u>	<u>72.4</u>	<u>86.2</u>	<u>54.4</u>
set_{13}	55.2	75.9	86.2	96.6	100	70.7
set_{23}	48.3	<u>58.6</u>	72.4	82.8	96.6	64.1
set_{123}	<u>44.8</u>	<u>58.6</u>	<u>62.1</u>	<u>72.4</u>	<u>86.2</u>	<u>54.4</u>
set_{TA}	0	0	0	0	0	0

13.2   Estimated kill sites

For all individuals, the range of weight thresholds due to the applied criterion is small (Table 34). The criterion *Error II$_{10}$* yielded in often the lowest threshold value, whereas the highest values were produced either by *Error$_{min}$* or *TK$_{high}$*. The ratio of kill sites within the 50 % home range isopleth is hardly influenced by the selected criterion for Madge and Ella, and only moderately for Getika and Verity. Except for Getika, whose ratio is between 60.9–67.9 %, all individuals have highly similar ratios between 52.1 % and 57.0 %. The differences of the ratio of kill sites within the 95 % isopleth due to the selected criterion do not exceed 2.4 % (Table 34). The ratio lies between 96.2 % and 98.8 % for all of the individuals. Madge is the only lion whose ratio of kill sites inside the game reserves differs from 100 % for all of the criteria, having 6.8–8 % outside (Figure 43). Depending on the criterion, a small percentage of kill sites lie outside the protected area for Verity as well (0.3–0.4 %). All kill sites of Getika and Ella are within the game reserves.

Table 34. Spatial distribution of the kill sites of all individuals. For the home range intersection, the mean value (± sd) of the 5 home range estimations selected in Section 9.5 is shown.

Criterion	Weight threshold	No. of kill sites	Inside 50 % home range [%]	Inside 95 % home range [%]	Inside game reserves [%]
Madge					
Error$_{min}$	0.14	125	54.2 ± 6.8	96.8 ± 3.1	92.8
Error II$_{10}$	0.10	195	54.2 ± 8.3	96.9 ± 3.7	92.3
TK$_{low}$	0.08	295	54.8 ± 7.5	97.1 ± 3.2	93.2
TK$_{high}$	0.12	150	53.7 ± 7.4	96.8 ± 3.7	92.0
Getika					
Error$_{min}$	0.12	78	67.9 ± 3.7	98.7 ± 2.2	100
Error II$_{10}$	0.06	203	60.9 ± 4.1	97.7 ± 1.4	100
TK$_{low}$	0.06	203	60.9 ± 4.1	97.7 ± 1.4	100
TK$_{high}$	0.10	99	67.3 ± 3.7	98.8 ± 1.8	100
Verity					
Error$_{min}$	0.04	308	52.6 ± 3.0	96.2 ± 1.8	99.7
Error II$_{10}$	0.02	520	52.1 ± 3.2	96.5 ± 1.7	99.6
TK$_{low}$	0.04	482	55.7 ± 2.7	96.6 ± 0.9	100
TK$_{high}$	0.08	95	56.6 ± 2.4	98.9 ± 1.5	100
Ella					
Error$_{min}$	0.06	482	55.7 ± 2.7	96.6 ± 0.9	100
Error II$_{10}$	0.04	635	55.7 ± 3.1	96.4 ± 1.1	100
TK$_{low}$	0.06	482	55.7 ± 2.7	96.6 ± 0.9	100
TK$_{high}$	0.10	183	57.0 ± 3.4	97.5 ± 1.6	100
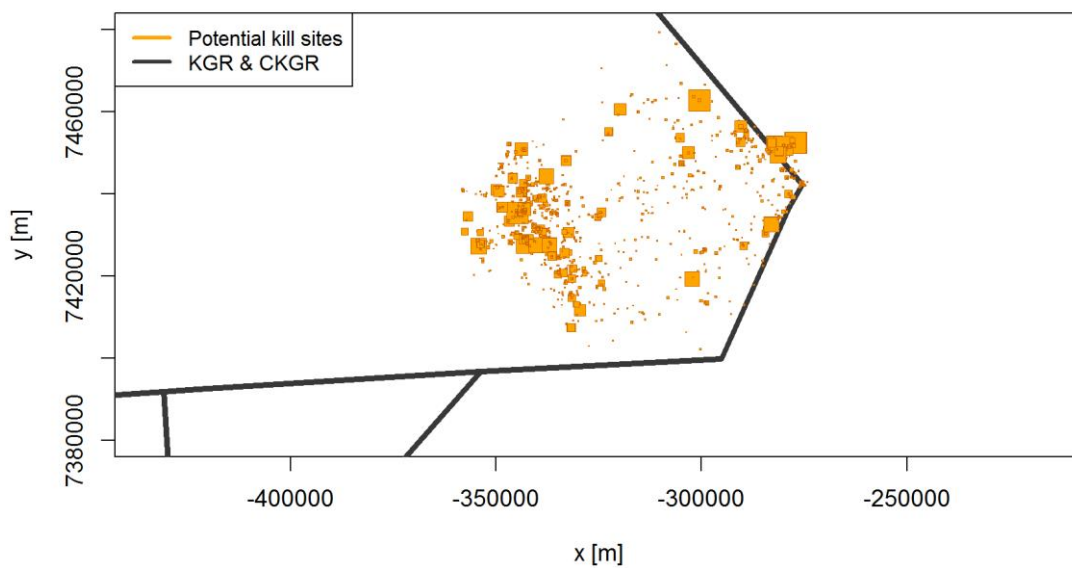
Figure 43. Visualization of Madge's potential kill sites. The size of the cluster marker scales according to its weight: The larger a cluster marker, the higher the probability that it represents an actual kill site. No weight threshold was applied.

14 Discussion

14.1 Effect of the clustering rule

The fact that almost identical results for both the number of clusters as well as for the errors were obtained for set_{12} and set_{123} demonstrates that *ToD* had no effect. The identical numbers of clusters for *Dur* and set_{13} as well as *DistR* and set_{23} (see Figure 39 and Figure 40) support this finding. This is surprising considering that nocturnal predators, such as the investigated lions, usually rest during the day and hunt during the rest of the day (Anderson & Lindzey 2003; Ramsauer 2006; Tambling et al. 2010). Because of that, clusters (referring to kill and resting sites) are expected to occur at any time of day and thus require being differentiated by *ToD*. For set_{23}, *ToD* may have no effect because the distance ratio already differentiates clearly between resting and kill sites. Halving the weight of clusters that already have very low values may result in changes too small to detect. However, this is less likely for set_{13} because resting can result in equally long clusters as consuming prey. Therefore, another possible explanation is that the binary classification used for *ToD* is too coarse and thus confuses resting and kill sites (Tambling et al. 2010). The lack of a sharp bend in the curve of *ToD* for Verity and Getika (Figure 40) is due to a low number of clusters classified as diurnal. This either confirms an inadequate classification or indicates an unusual resting behavior of those individuals (Haas et al. 2005; Macdonald & Loveridge 2010; Ramsauer 2006; Schiess-Meier et al. 2007).

Figure 39 and Figure 40 show that *DistR* (and thus set_{23}) leads to a clear separation between the majority of clusters having a low weight and the minority having a high weight. This is caused by the large value range that can occur when dividing the sum of Euclidean distances. As soon as there is at least one particularly large ratio, most other clusters receive small weights for this variable, which reduces their differentiability. The duration of a cluster (*Dur*, set_{13}), on the other hand, allows for a better differentiability of a larger proportion of clusters due to a narrower range of values and therefore seems to be preferable over set_{23} and *DistR*, respectively. The lower errors of set_{13} compared to set_{23} found in three of four error plots support this conclusion. Since set_{12} and set_{123} include both variables, their influences cancel each other out. This effect leads to a total error for Madge that is slightly smaller than that of set_{13} and significantly smaller than that of set_{23}. The fact that set_{12} and set_{123} also produced the lowest mean type II errors for Verity and Ella supports the finding that they are the most appropriate sets of variables (that have been investigated here) for the detection of clusters.

Although set_{12} and set_{123} yielded the lowest total errors and markedly lower type I errors for Madge, their type II errors can compete with those of set_{TA} only for low weights. If it is critical not to miss any potential kill site, a weight threshold of 0 ensures the same low rate of type II errors as set_{TA}. By using a low threshold such as 0.1 (for Madge), however, a type II error of 0 % and a type I error of 50 % yields half as many unnecessary field visits compared to set_{TA}. The inclusion of variables to assign weights that mark the probability of a cluster being a kill site has no disadvantages compared to the approach of Tambling & Belton (2009). Applying weights is thus a sensible extension that allows reducing significantly the workload for visiting potential kill sites to validate them, e.g. to gather data for the construction of a predictive model.

14.2 Estimated kill sites

Although the number of kill sites varies significantly depending on the weight threshold criterion, the ratios are quite stable. This indicates that the importance of different regions can be estimated reliably, even though the absolute number of kill sites might massively under- or overestimate the actual number. Since the TK_{low} and TK_{high} criteria predetermine the number of kill sites by using the kill rate for its computation, they are not recommendable to estimate absolute kill site numbers. Regarding the estimation of the ratios, however, they produce comparable results as the other criteria. A potential advantage of them over $Error_{min}$ and $Error\,II_{10}$ is that the performance of the latter heavily depends on the amount of available validation data.

Interestingly, the 50 % home range isopleths for three of four lions contain almost the same percentage of kill sites. As an exception, Getika not only has a significantly higher ratio of kill sites within the 50 % boundary (Table 34), but also the smallest (static) home range of all individuals (Table 21). Since Getika's home range widely overlaps with those of Ella and Verity, who have lower ratios and larger core areas, it is unlikely that this area has particularly high prey

abundances (Winterbach et al. 2014). Rather, Getika spends more time in the core area and thus hunts predominantly there. The fact that the ratios of kill sites within the 95 % home range isopleth are close to 100 % supports the claim, that this area contains all resources required by the individual (Burt 1943).

As already indicated by the overlap analysis of the home ranges (compare Section 9.5.3), Verity and Madge are the only individuals with kill sites outside the protected area. Since the kill sites outside the game reserves intersect grazing areas of cattle, it is likely that they represent livestock predation (Mills & Schiess-Meier 2009; Mishra et al. 2015; Schiess-Meier et al. 2007). The fact that both lions were labeled as problem animals and finally shot[8] supports this assumption. Cattle killed by lions weigh more than 100 kg in most cases and thus should be easily detectable by using clustering approaches (Ramsauer 2006; Tambling et al. 2010). Nevertheless, the observed ratios of kill sites outside the protected area seem to be, particularly for Verity, too low to justify their classification as problem animals. It is thus likely that lions show different killing and feeding behavior when being close to human settlements (e.g. shorter cluster durations and lower distance ratios) due to potential disturbances, which reduces the detection rate of such kill sites (Pitman et al. 2012). The existence of such impacts due to anthropogenic disturbances has already been observed for cougars by Smith et al. (2015).

14.3 Final remarks

The amount of validation data available for the individual lions was quite small. Particularly validated non-kill sites were sparse and within a reasonable range only for one individual (Madge). The computed errors of Section 13.1 exhibit therefore a high level of uncertainty.

Preliminary analyses (see Appendix A.8) have shown that the inclusion of the accelerometer data, which were partially available for the lions, can improve the accuracy of the clustering approach. However, the accelerometer data cannot be downloaded remotely but can only be obtained when changing the GPS collar (store-on-board), which is typically done every 1–1.5 years. As a consequence, the clustering approach could not be used to locate recent potential kill sites to visit and validate them. Thus, data from the accelerometers was not included in the final clustering algorithm.

---

[8] Personal communication with Dr. Stephen Henley and Monika Schiess-Meier on September 1, 2015.

V   Conclusion

15   Achievements

The first step of the home range analysis concerned the effect of the parameterization of the home range estimators selected for this study. The obtained results differed considerably from the results found in the literature. For KDE, it was shown that the reference bandwidth produced more realistic home range estimates than the more sophisticated cross-validation (except for BCV) and plug-in approaches. For t-LCH, simulations claimed consistently lower errors when using the *a*-rule instead of the *k*-rule. However, using data from this study, the former yielded markedly larger core areas that lack any spatial detail. The *a*-rule was therefore found to be less appropriate. A possible explanation for that may be the large span of point density in the data, which led to the inclusion of too many points during the construction of the hulls when using the *a*-rule. The analyses revealed that the inclusion of the time parameter *s* significantly affects the home range estimates of t-LCH by forming the isopleths according to the pathways of the individual. In addition, it was found that the model proposed by Benhamou & Cornélis (2010) and Jay et al. (2012) to determine the smoothing parameter of the approximated version of BRB has some unresolved issues. One of them proved to be the presence of several different sampling intervals in a dataset. Another issue was the strong dependence on the selected timespan associated with the maximum travel velocity.

By averaging the results of the individual sets of parameters for each HRE and individual, MCP proved to compute areas that are significantly larger than those of the other methods. Unlike results from literature, KDE produced home ranges whose areas are the smallest of all methods. When considering only the area, KDE, t-LCH and BRB were found to be statistically identical regarding the 95 % isopleth and almost identical regarding the core area. However, the compactness index, which represents the shape of the home ranges, showed more distinctive differences than the area. It revealed that the estimates of KDE and BRB are equally fragmented and undersmoothed, whereas those of t-LCH tend to be much more cohesive. A drawback of t-LCH proved to be the lack of functioning guidelines to set its parameters for the data used here.

A comparison of the obtained home range estimates with those from the literature revealed that the lions and leopards in the Khutse Game Reserve and the Central Kalahari Game Reserve have home ranges that are among the largest worldwide. This is at least partially explained by the observed temporal variability of the home range area and shape which lead to larger home ranges. Because most other authors did not investigate the temporal variability of their estimates and partially used different home range definitions and estimators, comparisons of home range estimates incorporates a high level of uncertainty. It is likely that the observed home range shifts over time masked differences due to sex and season that might have existed otherwise. The spatial

overlaps of the home ranges were analyzed and used to reconstruct pride structures of the lions. As none of the males showed intersecting home ranges, they were assumed to belong to different prides. For the leopards, an unexpectedly high degree of overlaps was found between individuals of the same sex. An analysis of their Euclidean distances at similar times revealed that they rarely encountered each other and thus demonstrate a strong active avoidance behavior. It was found that, except for Ronja's trip towards the south during one season, all leopards and lions had their home ranges predominantly within the protected area. However, even small percentages being outside indicate potential livestock predation. Regarding interspecific interactions, it was found that extensive overlaps occurred between the home ranges of leopards and lions. The small Euclidean distances obtained for several interspecific comparisons indicate that direct encounters were not unusual but ended for none of the leopards lethal. Since the vast majority of distances are larger than 5 km and lions have no reasons to avoid encounters with leopards, the latter are assumed to actively avoid lions.

The effect of different variables and their combinations, which were found to be particularly useful for locating kill sites in previous studies, was analyzed by incorporating several variables as weighting criteria. It was found that the combination of the duration of a cluster and the ratio of distances moved 24 h before and after a cluster yielded the lowest overall error and moderate type II errors. The time of day of a cluster, on the other hand, had no effect on the result. It is possible that the respective classification was too coarse and therefore minimized the impact of the variable. It was concluded that the incorporation of weights to quantify the probability of a cluster being a kill site entails no disadvantages. On the contrary, selecting an appropriate weight threshold value can save a considerable amount of time when visiting potential kill sites, e.g. to collect validation data to train predictive models. The set of weighting parameters that performed best was applied to four of the lions to estimate the spatial distribution of their kill sites and the extent of livestock predation. Irrespectively of the selected criteria to determine the weight threshold, the ratios of kill sites within the 50 % and 95 % home range isopleths were quite stable. This indicates that, although the absolute number of kill sites vary considerably, their spatial distribution is quite stable on large scales. The fact that almost all kill sites are within the 95 % home range boundary supports its ecological relevance. Those lions that were marked as problem animals and shot by the government were also found to have small percentages of their kill sites outside the protected area. The low extent of potential livestock predation suggests that those clusters could not be located reliably by using spatiotemporal clustering. It is supposed that lions change their feeding behavior when being close to humans so that clusters are shorter and harder to detect, which results in an underestimation of the extent of livestock predation.

16   Implications

The deviations of the results from the literature concerning the choice of the home range estimator and its parameterization emphasizes the differences between real, imperfect data and simulated data. The latter has therefore only a limited validity for analyses of free-ranging animals. Due to a lack of studies that applied t-LCH to comparable datasets, it remained unclear whether the poor performance of the *a*-rule is, as assumed, a result of the extreme range of spatial densities or eventually a programming issue of the *R* package *T-LoCoH*. Further studies are needed to provide clarification. The moderate differences of the areas computed by the different HRE (except for MCP) indicate that their choice is not critical when home range sizes are the only goal. The observed differences of 10–20 % are within the (high) level of uncertainty arising through the comparison of results that used different parameterizations, methodologies and data sources. The incorporation of the shape and spatial position of a home range, however, reveals larger differences between the HRE. Particularly the shape of home ranges produced by MCP proved to be markedly different from those of all other HRE. It is therefore recommended to include shape measures in home range analyses so that comparisons between studies are based on more than a single criterion. This, however, requires using the same measures for all studies. Due to the large differences between MCP and the other HRE regarding the size, shape and position of the home ranges, the result of MCP should not be regarded as a conservative estimate of ecologically important areas for an individual.

The observed variability of home ranges over time questions, at least for lions, the suitability of the conventional static home range analysis. By computing home ranges based on data from a single year, some of the observed shifts may not be visible or might be misinterpreted. Using data from several years, as it is the case here, helps detecting such shifts but can lead to seemingly disjoint core areas and overestimated areas. A key finding of the home range analysis part is the strong dependence of the home range estimate on the temporal aggregation level used. It is therefore suggested to analyze home ranges at different temporal aggregation levels to detect potential shifts. In addition, using several home range estimators provides a more comprehensive view of home ranges and allows to quantitatively estimate their level of uncertainty. The observed extents of the core areas and their intersections for some of the leopards indicate that they should not be understood in the sense of defended territories but only as regions of increased utilization density. This is supported by the fact that the 95 % home range isopleths were much more compact than the core areas for most individuals.

The findings of the kill site analysis highlight the potential advantages of ranking clusters according to their probability of being kill sites. The application of the developed clustering approach was found to reliably display the spatial distribution of kill sites on large scales. Although the accuracy of the approach is limited, it allows for rough estimates at very low

expenses, particularly in combination with the *time to kill* (*TK*) criterion. However, spatio-temporal clustering approaches cannot be recommended to quantify livestock predation as they are suspected to underestimate such kill sites to a considerable degree.

17   Future work

Incorporating the shape of a home range was found to support more comprehensive differentiations of home ranges. In order to serve as an additional criterion for comparisons between studies, however, the same shape measures must be used. Further research is required to analyze the effects of various characteristics of home ranges (e.g. the level of disjointedness in the case of several polygons) and find measures that optimally represent them, so that they can be established as standards. In addition, the home range analysis raised many questions concerning the observed spatiotemporal shifts. It is therefore suggested to conduct analyses that investigate the reasons for those shifts in order to consider them appropriately in conservation strategies. Although the analysis of home ranges in terms of individual seasons revealed many shifts over time, they may look different when using different temporal aggregations. Accordingly, future work should expand the analysis of spatiotemporal shifts, e.g. by using moving windows of varying width for temporal aggregation and comparing their results.

A major limitation of the kill site detection consisted in the insufficient validation data to evaluate the performance of the different sets of variables properly. It is suggested to collect large numbers of validated kill and non-kill sites, e.g. by using the presented clustering approach, to assess its performance in a statistically significant manner. It was concluded that the investigated clustering approaches are likely to underestimate the absolute number and proportion of livestock predation. In order to verify this hypothesis, it is suggested to check the GPS positions of a known problem animal as soon as it leaves the protected area and moves towards rangeland. By comparing the number of clusters with the number of validated livestock predation events, the adequacy of the clustering approaches for this purpose of use may then be assessed.

VI References

Anderson, C. R., & Lindzey, F. G. (2003). Estimating Cougar Predation Rates from GPS Location Clusters. *The Journal of Wildlife Management*, *67*, 307–316.

Bacon, M. M., Becic, G. M., Epp, M. T., & Boyce, M. S. (2011). Do GPS Clusters Really Work? Carnivore Diet From Scat Analysis and GPS Telemetry Methods. *Wildlife Society Bulletin*, *35*, 409–415.

Bailey, T. N. (1993). The African Leopard. Ecology and Behavior of a Solitary Felid. New York: Columbia University Press.

Bauer, D., Schiess-Meier, M., Mills, D. R., & Gusset, M. (2014). Using spoor and prey counts to determine temporal and spatial variation in lion (*Panthera leo*) density. *Canadian Journal of Zoology*, *92*, 97–104.

Bauer, H., & de Iongh, H. H. (2005). Lion (*Panthera leo*) home ranges and livestock conflicts in Waza National Park, Cameroon. *African Journal of Ecology*, *43*, 208–214.

Bauer, H., Nowell, K., & Packer, C. (2012). *Panthera leo.* The IUCN Red List of Threatened Species. <http://www.iucnredlist.org/details/15951/0>.

Bauer, H., & Van Der Merwe, S. (2004). Inventory of free-ranging lions *Panthera leo* in Africa. *Oryx*, *38*, 26–31.

Benhamou, S. (2011). Dynamic Approach to Space and Habitat Use Based on Biased Random Bridges. *PloS one*, *6*, 1–8.

Benhamou, S., & Cornélis, D. (2010). Incorporating Movement Behavior and Barriers to Improve Kernel Home Range Space Use Estimates. *Journal of Wildlife Management*, *74*, 1353–1360.

Börger, L., Dalziel, B. D., & Fryxell, J. M. (2008). Are there general mechanisms of animal home range behaviour? A review and prospects for future research. *Ecology letters*, *11*, 637–650.

Börger, L., Franconi, N., De Michele, G., Gantz, A., Meschi, F., Manica, A., Lovari, S., & Coulson, T. (2006). Effects of sampling regime on the mean and variance of home range size estimates. *Journal of Animal Ecology*, *75*, 1393–1405.

Bothma, J. d. P., & Bothma, M. D. (2012). Leopard range size and conservation area size in the southern Kalahari. *Koedoe*, *54*, 1–4.

Bothma, J. d. P., Knight, M. H., Le Riche, E. A. N., & van Hensbergen, H. J. (1997). Range size of southern Kalahari leopards. *South African Journal of Wildlife Research*, *27*, 94–99.

Bullard, F. (1991). Estimating the Home Range of an Animal: A Brownian Bridge Approach. Master thesis. Department of Statistics. Chapel Hill, North Carolina, USA.

Burgman, M. A., & Fox, J. C. (2003). Bias in species range estimates from minimum convex polygons: implications for conservation and options for improved planning. *Animal Conservation*, *6*, 19–28.

Burt, W. H. (1943). Territoriality and Home Range Concepts as Applied to Mammals. *Journal of Mammalogy*, *24*, 346–352.

Byrne, M. E., Clint McCoy, J., Hinton, J. W., Chamberlain, M. J., & Collier, B. A. (2014). Using dynamic Brownian bridge movement modelling to measure temporal patterns of habitat selection. *Journal of Animal Ecology*, 1234–1243.

Calenge, C. (2006). The package "adehabitat" for the R software: A tool for the analysis of space and habitat use by animals. *Ecological Modelling*, *197*, 516–519.

Calenge, C., Dray, S., & Royer-Carenzi, M. (2009). The concept of animals' trajectories from a data analysis perspective. *Ecological Informatics*, *4*, 34–41.

Codling, E. A., Plank, M. J., & Benhamou, S. (2008). Random walk models in biology. *Journal of the Royal Society Interface*, *5*, 813–834.

De Solla, S. R., Bonduriansky, R., & Brooks, R. J. (1999). Eliminating autocorrelation reduces biological relevance of home range estimates. *Journal of Animal Ecology*, *68*, 221–234.

Department of Meteorological Services. Botswana Climate. Ministry of Environment, Wildlife and Tourism. <http://www.mewt.gov.bw/DMS/article.php?id_mnu=91>.

Downs, J. A., & Horner, M. W. (2008). Effects of Point Pattern Shape on Home-Range Estimates. *Journal of Wildlife Management*, *72*, 1813–1818.

Downs, J. A., & Horner, M. W. (2012). Analysing infrequently sampled animal tracking data by incorporating generalized movement trajectories with kernel density estimation. *Computers, Environment and Urban Systems*, *36*, 302–310.

Downs, J. A., Horner, M. W., & Tucker, A. D. (2011). Time-geographic density estimation for home range analysis. *Annals of GIS*, *17*, 163–171.

Duong, T., & Hazelton, M. L. (2005). Cross-validation Bandwidth Matrices for Multivariate Kernel Density Estimation. *Scandinavian Journal of Statistics*, *32*, 485–506.

Dürr, S., & Ward, M. P. (2014). Roaming behaviour and home range estimation of domestic dogs in Aboriginal and Torres Strait Islander communities in northern Australia using four different methods. *Preventive Veterinary Medicine*, *117*, 340–357.

Ebdon, D. (1985). Statistics In Geography: A Practical Approach. Oxford, New York, USA: Wiley-Blackwell.

Eloff, F. C. (1998). The Life of the Kalahari Lion (*Panthera leo vernayi*). *Transactions of the Royal Society of South Africa*, *53*, 267–269.

Fieberg, J., & Börger, L. (2012). Could you please phrase "home range" as a question? *Journal of Mammalogy*, *93*, 890–902.

Fieberg, J., & Kochanny, C. O. (2005). Quantifying Home-Range Overlap: The Importance of the Utilization Distribution. *The Journal of Wildlife Management*, *69*, 1346–1359.

Fontúrbel, F. E., & Simonetti, J. A. (2011). Translocations and human-carnivore conflicts: problem solving or problem creating? *Wildlife Biology*, *17*, 217–224.

Food and Agriculture Organization of the United Nations (FAO). Botswana. Natural Resources Management and Environment Department. <www.fao.org/docrep/005/x9751e/x9751e05.htm>.

Frair, J. L., Fieberg, J., Hebblewhite, M., Cagnacci, F., DeCesare, N. J., & Pedrotti, L. (2010). Resolving Issues of Imprecise and Habitat-Biased Locations in Ecological Analyses Using GPS Telemetry Data. *Philosophical Transactions of the Royal Society B: Biological Sciences*, *365*, 2187–2200.

Funston, P. J. (2011). Population Characteristics of Lions (*Panthera leo*) in the Kgalagadi Transfrontier Park. *South African Journal of Wildlife Research*, *41*, 1–10.

Funston, P. J., Mills, M. G., Biggs, H. C., & Richardson, P. R. (1998). Hunting by male lions: ecological influences and socioecological implications. *Animal Behaviour*, *56*, 1333–1345.

Getz, W. M., Fortmann-Roe, S., Cross, P. C., Lyons, A. J., Ryan, S. J., & Wilmers, C. C. (2007). LoCoH: Nonparameteric Kernel Methods for Constructing Home Ranges and Utilization Distributions. *PloS one*, *2*, 1–11.

Getz, W. M., & Wilmers, C. C. (2004). A local nearest-neighbor convex-hull construction of home ranges and utilization distributions. *Ecography*, *27*, 489–505.

Gitzen, R. A., Millspaugh, J. J., & Kernohan, B. J. (2006). Bandwidth Selection for Fixed-Kernel Analysis of Animal Utilization Distributions. *Journal of Wildlife Management*, *70*, 1334–1344.

Gurarie, E., Andrews, R. D., & Laidre, K. L. (2009). A novel method for identifying behavioural changes in animal movement data. *Ecology letters*, *12*, 395–408.

Haas, S. K., Hayssen, V., & Krausman, P. R. (2005). *Panthera Leo*. *Mammalian Species*, 1–11.

Hagen, W., Hagen, H., & Pölking, F. (1995). Der Leopard. Einblicke in das Leben der grossen geflekten Katze Afrikas. Steinfurt: Tecklenborg Verlag.

Hansteen, T. L., Andreassen, H. P., & Ims, R. A. (1997). Effects of Spatiotemporal Scale on Autocorrelation and Home Range Estimators. *The Journal of Wildlife Management*, *61*, 280–290.

Hayward, M. W., Hayward, G. J., Druce, D. J., & Kerley, G. I. H. (2009). Do fences constrain predator movements on an evolutionary scale? Home range, food intake and movement patterns of large predators reintroduced to Addo Elephant National Park, South Africa. *Biodiversity and Conservation*, *18*, 887–904.

Hayward, M. W., Henschel, P., O'Brien, J., Hofmeyr, M., Balme, G., & Kerley, G. I. H. (2006). Prey preferences of the leopard (*Panthera pardus*). *Journal of Zoology*, *270*, 298–313.

Hebblewhite, M., & Haydon, D. T. (2010). Distinguishing technology from biology: a critical review of the use of GPS telemetry data in ecology. *Philosophical Transactions of the Royal Society B: Biological Sciences*, *365*, 2303–2312.

Henschel, P., Hunter, L., Breitenmoser, U., Purchase, N., Packer, C., Khorocyan, I., Bauer, H., Marker, L. L., Sogbohossou, E., & Breitenmoser-Wursten, C. (2008). *Panthera pardus.* The IUCN Red List of Threatened Species. <http://www.iucnredlist.org/details/15954/0>.

Horne, J. S., & Garton, E. O. (2006). Selecting the Best Home Range Model: An Information-Theoretic Approach. *Ecology*, *87*, 1146–1152.

Horne, J. S., Garton, E. O., Krone, S. M., & Lewis, J. S. (2007). Analyzing Animal Movements Using Brownian Bridges. *Ecology*, *88*, 2354–2363.

Huck, M., Davison, J., & Roper, T. J. (2008). Comparison of two sampling protocols and four home-range estimators using radio-tracking data from urban badgers *Meles meles*. *Wildlife Biology*, *14*, 467–477.

Hull, V., Zhang, J., Zhou, S., Huang, J., Li, R., Liu, D., Xu, W., Huang, Y., Ouyang, Z., Zhang, H., & Liu, J. (2015). Space use by endangered giant pandas. *Journal of Mammalogy*, *96*, 230–236.

Hunter, L., & Hinde, G. (2005). Cats of Africa. Behaviour, Ecology and Conservation. Cape Town: Struik (New Holland).

Jay, C. V., Fischbach, A. S., & Kochnev, A. A. (2012). Walrus areas of use in the Chukchi Sea during sparse sea ice cover. *Marine Ecology Progress Series*, *468*, 1–13.

Jones, M. C., Marron, J. S., & Sheather, S. J. (1996). A Brief Survey of Bandwidth Selection for Density Estimation. *Journal of the American Statistical Association*, *91*, 401–407.

Katajisto, J., & Moilanen, A. (2006). Kernel-based home range method for data with irregular sampling intervals. *Ecological Modelling*, *194*, 405–413.

Keating, K. A., & Cherry, S. (2009). Modeling utilization distributions in space and time. *Ecology*, *90*, 1971–1980.

Kesch, K. M., Bauer, D. T., & Loveridge, A. J. (2014). Undermining game fences: who is digging holes in Kalahari sands? *African Journal of Ecology*, *52*, 144–150.

Kie, J. G., Matthiopoulos, J., Fieberg, J., Powell, R. A., Cagnacci, F., Mitchell, M. S., Gaillard, J.-M., & Moorcroft, P. R. (2010). The home-range concept: are traditional estimators still relevant with modern telemetry technology? *Philosophical Transactions of the Royal Society B: Biological Sciences*, *365*, 2221–2231.

Kranstauber, B., Kays, R., Lapoint, S. D., Wikelski, M., & Safi, K. (2012). A dynamic Brownian bridge movement model to estimate utilization distributions for heterogeneous animal movement. *Journal of Animal Ecology*, *81*, 738–746.

Laver, P. N., & Kelly, M. J. (2008). A Critical Review of Home Range Studies. *The Journal of Wildlife Management*, *72*, 290–298.

Lehmann, M. B., Funston, P. J., Owen, C. R., & Slotow, R. (2008). Feeding behaviour of lions (*Panthera leo*) on a small reserve. *South African Journal of Wildlife Research*, *38*, 66–78.

Leopard Ecology & Conservation (2014). Annual Report 2014. Leopard Ecology & Conservation.

Lewis, J. S., Rachlow, J. L., Garton, E. O., & Vierling, L. A. (2007). Effects of habitat on GPS collar performance: using data screening to reduce location error. *Journal of Applied Ecology*, *44*, 663–671.

Lichti, N. I., & Swihart, R. K. (2011). Estimating Utilization Distributions with Kernel Versus Local Convex Hull Methods. *Journal of Wildlife Management*, *75*, 413–422.

Loveridge, A. J., Valeix, M., Davidson, Z., Murindagomo, F., Fritz, H., & Macdonald, D. W. (2009). Changes in home range size of African lions in relation to pride size and prey biomass in a semi-arid savanna. *Ecography*, *32*, 953–962.

Lyons, A. J., Turner, W. C., & Getz, W. M. (2013). Home range plus: a space-time characterization of movement over real landscapes. *Movement Ecology*, *1*, 1–14.

Macdonald, D. W., & Loveridge, A. J. (Eds.) (2010). Biology and Conservation of Wild Felids. Oxford, New York: Oxford University Press.

Marker, L. L., & Dickman, A. J. (2005). Factors affecting leopard (*Panthera pardus*) spatial ecology, with particular reference to Namibian farmlands. *South African Journal of Wildlife Research*, *35*, 105–115.

Martins, Q., & Harris, S. (2013). Movement, activity and hunting behaviour of leopards in the Cederberg mountains, South Africa. *African Journal of Ecology*, *51*, 571–579.

Merrill, E., Sand, H., Zimmermann, B., McPhee, H., Webb, N., Hebblewhite, M., Wabakken, P., & Frair, J. L. (2010). Building a mechanistic understanding of predation with GPS-based movement data. *Philosophical Transactions of the Royal Society B: Biological Sciences*, *365*, 2279–2288.

Mills, D. R., & Schiess-Meier, M. (2009). Annual Report 2009. Leopard Ecology & Conservation.

Millspaugh, J. J., Gitzen, R. A., Kernohan, B. J., Larson, M. A., & Clay, C. L. (2004). Comparability of three analytical techniques to assess joint space use. *Wildlife Society Bulletin*, *32*, 148–157.

Millspaugh, J. J., & Marzluff, J. M. (2001). Radio tracking and animal populations. San Diego: Academic Press.

Mishra, N., Crews, K., Miller, J., & Meyer, T. (2015). Mapping Vegetation Morphology Types in Southern Africa Savanna Using MODIS Time-Series Metrics: A Case Study of Central Kalahari, Botswana. *Land*, *4*, 197–215.

Mizutani, F., & Jewell, P. A. (1998). Home-range and movements of leopards (*Panthera pardus*) on a livestock ranch in Kenya. *Journal of Zoology*, *244*, 269–286.

Nilsen, E. B., Pedersen, S., & Linnell, J. D. C. (2008). Can minimum convex polygon home ranges be used to draw biologically meaningful conclusions? *Ecological Research*, *23*, 635–639.

Patterson, B. D., Kasiki, S. M., Selempo, E., & Kays, R. W. (2004). Livestock predation by lions (*Panthera leo*) and other carnivores on ranches neighboring Tsavo National Parks, Kenya. *Biological Conservation*, *119*, 507–516.

Perotto-Baldivieso, H. L., Cooper, S. M., Cibils, A. F., Figueroa-Pagán, M., Udaeta, K., & Black-Rubio, C. M. (2012). Detecting autocorrelation problems from GPS collar data in livestock studies. *Applied Animal Behaviour Science*, *136*, 117–125.

Pitman, R. T., Kilian, P. J., Ramsay, P. M., & Swanepoel, L. H. (2013). Foraging and Habitat Specialization by Female Leopards (*Panthera pardus*) in the Waterberg Mountains of South Africa. *South African Journal of Wildlife Research*, *43*, 167–176.

Pitman, R. T., Mulvaney, J., Ramsay, P. M., Jooste, E., & Swanepoel, L. H. (2014). Global Positioning System-located kills and faecal samples: a comparison of leopard dietary estimates. *Journal of Zoology*, *292*, 18–24.

Pitman, R. T., Swanepoel, L. H., & Ramsay, P. M. (2012). Predictive modelling of leopard predation using contextual Global Positioning System cluster analysis. *Journal of Zoology*, *288*, 222–230.

Power, R. J. (2002). Prey selection of lions *Panthera leo* in a small, enclosed reserve. *Koedoe*, *45*, 67–75.

R Core Team (2015). R: A Language and Environment for Statistical Computing. R Foundation for Statistical Computing. <http://www.R-project.org/>.

Ramsauer, S. (2006). Living at Low Density. A Study of Within and Between Pride Dynamics in Kalahari Lions. Dissertation. Mathematisch-naturwissenschaftliche Fakultät. Zürich.

Rapson, J. A., & Bernard, R. T. F. (2007). Interpreting the diet of lions (*Panthera leo*); a comparison of various methods of analysis. *South African Journal of Wildlife Research*, *37*, 179–187.

Sain, S. R., Baggerly, K. A., & Scott, D. W. (1994). Cross-Validation of Multivariate Densities. *Journal of the American Statistical Association*, *89*, 807–817.

Sand, H., Zimmermann, B., Wabakken, P., Andren, H., & Pedersen, H. C. (2005). Using GPS technology and GIS cluster analyses to estimate kill rates in wolf-ungulate ecosystems. *Wildlife Society Bulletin*, *33*, 914–925.

Scheel, D., & Packer, C. (1991). Group hunting behaviour of lions: a search for cooperation. *Animal Behaviour*, *41*, 697–709.

Schiess-Meier, M., Ramsauer, S., Gabanapelo, T., & König, B. (2007). Livestock Predation–Insights From Problem Animal Control Registers in Botswana. *The Journal of Wildlife Management*, *71*, 1267–1274.

Scott, D. W., & Terrell, G. R. (1987). Biased and Unbiased Cross-Validation in Density Estimation. *Journal of the American Statistical Association*, *82*, 1131–1146.

Seaman, D. E., Millspaugh, J. J., Kernohan, B. J., Brundige, G. C., Raedeke, K. J., & Gitzen, R. A. (1999). Effects of Sample Size on Kernel Home Range Estimates. *The Journal of Wildlife Management*, *63*, 739–747.

Seaman, D. E., & Powell, R. A. (1996). An Evaluation of the Accuracy of Kernel Density Estimators for Home Range Analysis. *Ecology*, *77*, 2075–2085.

Smith, J. A., Wang, Y., & Wilmers, C. C. (2015). Top carnivores increase their kill rates on prey as a response to human-induced fear. *Proceedings of the Royal Society B: Biological Sciences*, *282*, 1–6.

Spong, G. (2002). Space use in lions, *Panthera leo*, in the Selous Game Reserve: social and ecological factors. *Behavioral Ecology and Sociobiology*, *52*, 303–307.

Stein, A. B., Fuller, T. K., DeStefano, S., & Marker, L. L. (2011). Leopard population and home range estimates in north-central Namibia. *African Journal of Ecology*, *49*, 383–387.

Stein, A. B., & Hayssen, V. (2013). *Panthera pardus* (Carnivora: Felidae). *Mammalian Species*, *900*, 30–48.

Swanepoel, L. H., Dalerum, F., & van Hoven, W. (2010). Factors Affecting Location Failure of GPS Collars Fitted to African Leopards (*Panthera pardus*). *South African Journal of Wildlife Research*, *40*, 10–15.

Swanepoel, L. H., Lindsey, P., Somers, M. J., van Hoven, W., Dalerum, F., Pettorelli, N., & Penteriani, V. (2013). Extent and fragmentation of suitable leopard habitat in South Africa. *Animal Conservation*, *16*, 41–50.

Swihart, R. K., & Slade, N. A. (1985a). Influence of Sampling Interval on Estimates of Home-Range Size. *The Journal of Wildlife Management*, *49*, 1019–1025.

Swihart, R. K., & Slade, N. A. (1985b). Testing For Independence of Observations in Animal Movements. *Ecology*, *66*, 1176–1184.

Tambling, C. J., & Belton, L. E. (2009). Feasibility of Using Proximity Tags to Locate Female Lion *Panthera leo* Kills. *Wildlife Biology*, *15*, 435–441.

Tambling, C. J., Cameron, E. Z., Du Toit, J. T., & Getz, W. M. (2010). Methods for Locating African Lion Kills Using Global Positioning System Movement Data. *The Journal of Wildlife Management*, *74*, 549–556.

Tambling, C. J., Laurence, S. D., Bellan, S. E., Cameron, E. Z., du Toit, J. T., & Getz, W. M. (2012). Estimating carnivoran diets using a combination of carcass observations and scats from GPS clusters. *Journal of Zoology*, *286*, 102–109.

Tomkiewicz, S. M., Fuller, M. R., Kie, J. G., & Bates, K. K. (2010). Global positioning system and associated technologies in animal behaviour and ecological research. *Philosophical Transactions of the Royal Society B: Biological Sciences*, *365*, 2163–2176.

Tumenta, P. N., van't Zelfde, M., Croes, B. M., Buij, R., Funston, P. J., Udo de Haes, H. A., & De Iongh, H. H. (2013). Changes in lion (*Panthera leo*) home range size in Waza National Park, Cameroon. *Mammalian Biology*, *78*, 461–469.

Wall, J., Wittemyer, G., LeMay, V., Douglas-Hamilton, I., Klinkenberg, B., & Giuggioli, L. (2014). Elliptical Time-Density model to estimate wildlife utilization distributions. *Methods in Ecology and Evolution*, *5*, 780–790.

Weilenmann, M., Gusset, M., Mills, D. R., Gabanapelo, T., & Schiess-Meier, M. (2010). Is translocation of stock-raiding leopards into a protected area with resident conspecifics an effective management tool? *Wildlife Research*, *37*, 702–707.

Winterbach, H. E., Winterbach, C. W., & Somers, M. J. (2014). Landscape Suitability in Botswana for the Conservation of Its Six Large African Carnivores. *PloS one*, *9*, 1–16.

VII Appendix

A.1 KDE: Influence of the sample size on the bandwidth

The average of 10 iterations done for each of the four leopards is shown. The correction factors, which are based on these values, were used for the lions in order to compensate their reduced sample size for the estimation of the bandwidth.

Individual	HPI$_{half}$	HPI$_{full}$	HSCV$_{half}$	HSCV$_{full}$	HBCV$_{half}$	HBCV$_{full}$
PF07_Ronja	1114.03	922.84	1081.28	881.26	2240.62	2022.49
PM07_Mothamongwe	989.59	820.83	1033.86	843.93	1648.11	1488.12
PM08_Bogarigka	1441.89	1183.76	1470.52	1187.32	3205.26	2861.58
PM09_Gham	1192.77	966.72	1211.51	961.44	2171.04	1945.78

A.2 KDE: Influence of the kernel function

The volume of intersection index (95 %) was calculated between the Gaussian and Epanechnikov kernel using the reference bandwidth for all of the 12 leopards and lions. The higher the VI index, the smaller the differences between the kernel functions.

Individual	VI index[1]
PF07_Ronja	0.94
PM07_Mothamongwe	0.95
PM08_Bogarigka	0.94
PM09_Gham	0.93
LF12_Verity	0.94
LF13_Ella	0.94
LF16_Jane	0.93
LM06_Hitchcock	0.94
LM07_Mexico	0.92
LF14_Madge	0.93
LM08_Orange	0.93
LF07_Getika	0.92
[1]between the Gaussian and Epanechnikov kernel function	

A.3   BRB: Influence of tau

Normalized areas of the 50 % and 95 % isopleth when using BRB with different values for the parameter *tau* [seconds].

Individual-isopleth combination	60 sec	180 sec	360 sec	720 sec	900 sec
PF07_Ronja 50 %	1.00000	0.99993	0.99970	0.99953	0.99922
PF07_Ronja 95 %	0.99902	0.99917	0.99938	0.99981	1.00000
PM07_Mothamongwe 50 %	0.99891	0.99905	0.99926	0.99965	1.00000
PM07_Mothamongwe 95 %	0.99859	0.99877	0.99904	0.99923	1.00000
PM08_Bogarigka 50 %	0.98498	0.98698	0.99021	0.99683	1.00000
PM08_Bogarigka 95 %	0.99194	0.99301	0.99478	0.99838	1.00000
PM09_Gham 50 %	0.99691	0.99728	0.99793	0.99937	1.00000
PM09_Gham 95 %	0.99813	0.99839	0.99872	0.99945	1.00000

A.4   Detailed home range results

Area and compactness values of the core area (50 %), separately by individual and HRE. For t-LCH, the average of the lower and upper boundary values k_1 and k_2 is presented. Females are underlined.

Individual	Area [km²] (50 % isopleth)				Compactness (50 % isopleth)			
	MCP	KDE	t-LCH	BRB	MCP	KDE	t-LCH	BRB
<u>Ronja</u>	259.4	211.7	199.8	175.4	0.95	0.34	0.32	0.31
Mothamongwe	230.9	194.6	203.2	180.9	0.96	0.39	0.44	0.38
Bogarigka	578.0	494.8	394.3	480.1	0.94	0.51	0.46	0.24
Gham	325.7	302.4	301.3	284.7	0.96	0.37	0.52	0.32
<u>Verity</u>	852.9	707.2	769.8	656.6	0.97	0.64	0.27	0.19
<u>Ella</u>	568.8	466.3	439.8	418.7	0.98	0.46	0.44	0.20
<u>Jane</u>	987.6	780.4	723.3	663.5	0.98	0.37	0.30	0.31
Hitchcock	1203.5	1040.7	996.9	1004.6	0.97	0.36	0.33	0.23
Mexico	182.1	182.2	166.1	218.3	0.97	0.50	0.52	0.66
<u>Madge</u>	721.1	401.6	309.1	497.3	0.97	0.50	0.19	0.09
Orange	352.6	312.5	383.0	328.3	0.98	0.45	0.42	0.47
<u>Getika</u>	470.7	418.0	387.8	431.8	0.97	0.46	0.31	0.43

Area and compactness of the home range (95 %), separately by individual and HRE. For t-LCH, the average of the lower and upper boundary values k_1 and k_2 is presented. Females are underlined.

Individual	Area [km²] (95 % isopleth)				Compactness (95 % isopleth)			
	MCP	KDE	t-LCH	BRB	MCP	KDE	t-LCH	BRB
Ronja	1629.1	1304.1	1192.2	1134.5	0.70	0.32	0.28	0.28
Mothamongwe	712.0	721.0	667.7	678.1	0.84	0.55	0.50	0.54
Bogarigka	2505.0	2423.6	2221.6	2279.5	0.60	0.37	0.40	0.35
Gham	872.1	987.0	863.0	912.0	0.81	0.56	0.48	0.55
Verity	3601.2	3350.2	3129.6	3030.0	0.76	0.51	0.50	0.48
Ella	2618.3	2386.1	2364.9	2278.0	0.83	0.59	0.60	0.53
Jane	3327.7	3238.0	2872.3	2937.3	0.82	0.53	0.54	0.49
Hitchcock	4897.0	4346.5	3991.9	4034.0	0.86	0.54	0.51	0.52
Mexico	1852.4	1559.8	1591.7	1824.2	0.91	0.48	0.63	0.49
Madge	4417.4	3347.2	2710.6	3247.3	0.77	0.50	0.46	0.54
Orange	1091.9	1150.6	1077.9	1204.1	0.96	0.66	0.61	0.61
Getika	2243.6	2083.9	1985.9	2047.4	0.90	0.36	0.53	0.28

Ratio of the 50 % isopleth to the 95 % isopleth, separately by individual and HRE. The results of the different HRE are shown for each individual. For t-LCH, the average of the lower and upper boundary values k_1 and k_2 is presented. Females are underlined.

Individual	MCP	KDE	t-LCH	BRB
Ronja	0.16	0.16	0.17	0.15
Mothamongwe	0.32	0.27	0.31	0.27
Bogarigka	0.23	0.20	0.18	0.21
Gham	0.37	0.31	0.35	0.31
Verity	0.24	0.21	0.25	0.22
Ella	0.22	0.20	0.19	0.18
Jane	0.30	0.24	0.25	0.23
Hitchcock	0.25	0.24	0.25	0.25
Mexico	0.10	0.12	0.11	0.12
Madge	0.16	0.12	0.12	0.15
Orange	0.32	0.27	0.36	0.27
Getika	0.21	0.20	0.20	0.21

A.5   Selected home range estimates

The selected home range estimates (5) for each individual used for the ecological analyses are shown below.

Ronja
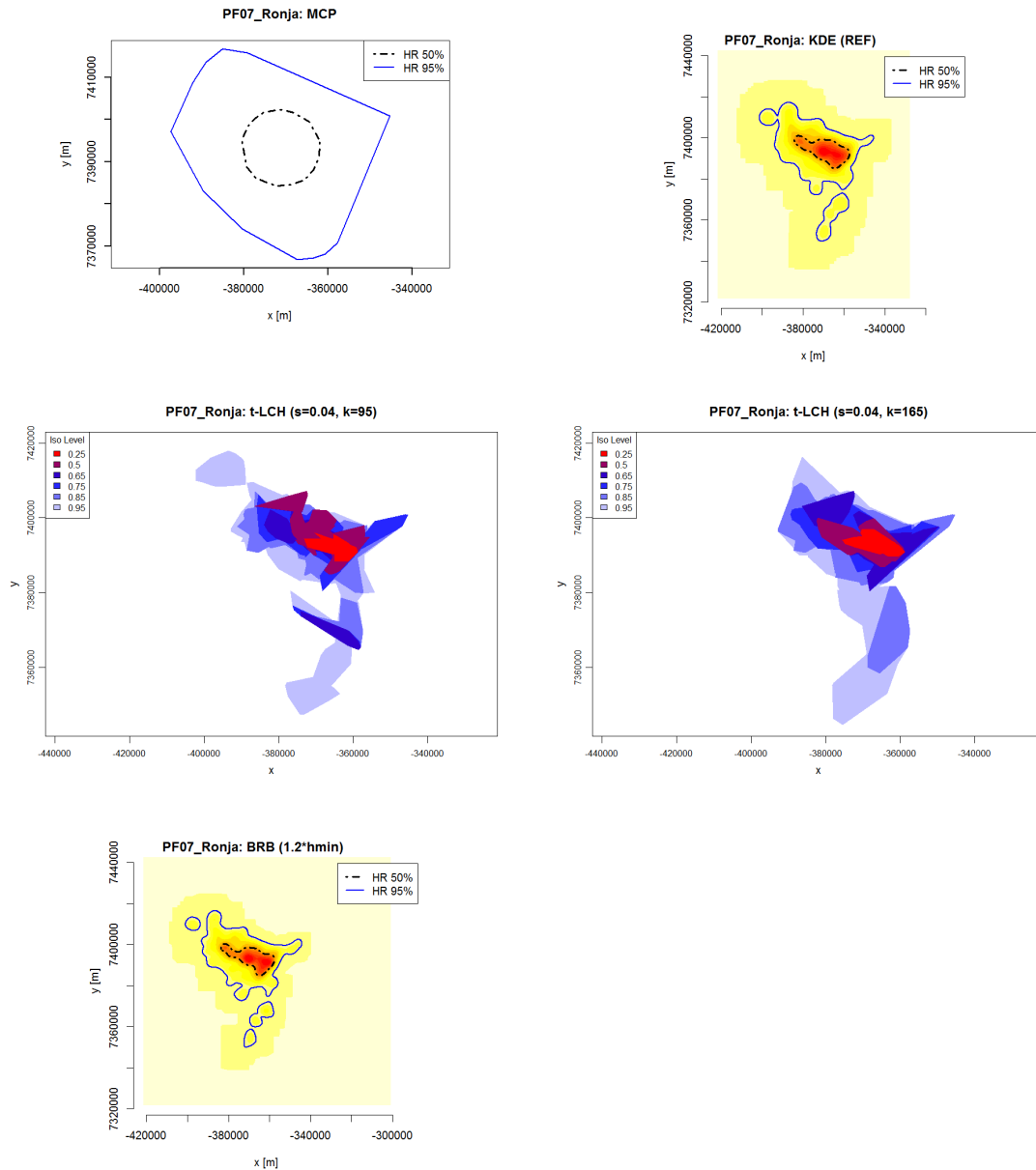
Mothamongwe

PM07_Mothamongwe: MCP
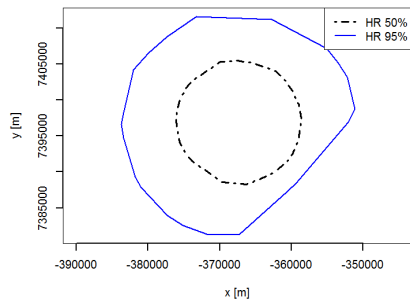
PM07_Mothamongwe: KDE (REF)
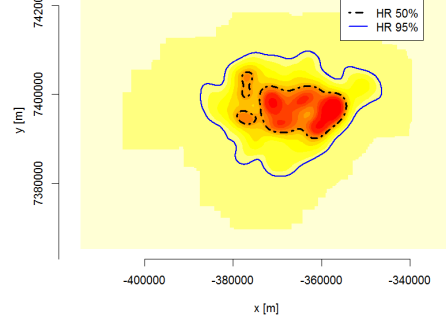
PM07_Mothamongwe: t-LCH (s=0.01, k=90)
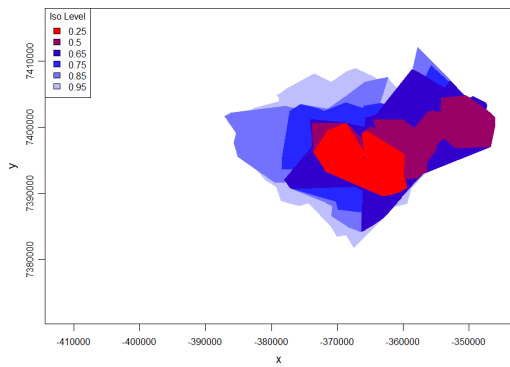
PM07_Mothamongwe: t-LCH (s=0.01, k=140)
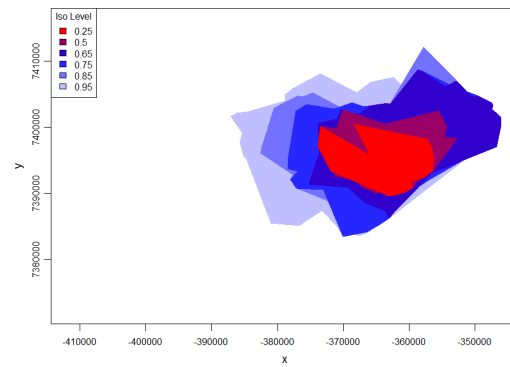
PM07_Mothamongwe: BRB (0.8*hmin)

Bogarigka

PM08_Bogarigka: MCP

PM08_Bogarigka: KDE (REF)

PM08_Bogarigka: t-LCH (s=0.009, k=145)

PM08_Bogarigka: t-LCH (s=0.009, k=205)
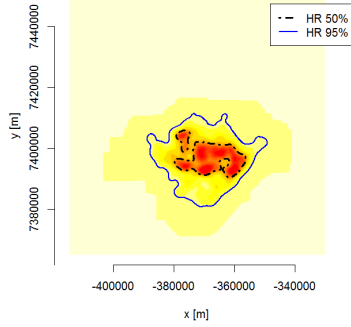
PM08_Bogarigka: BRB (2*hmin)
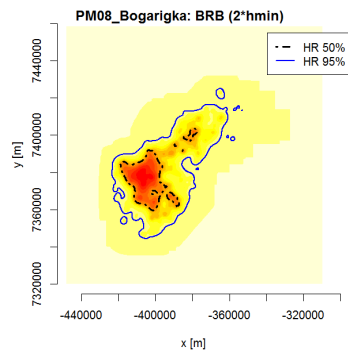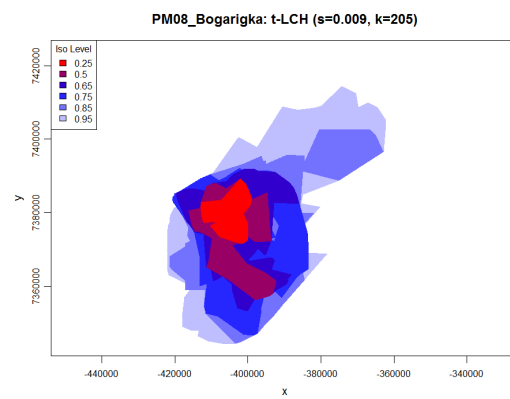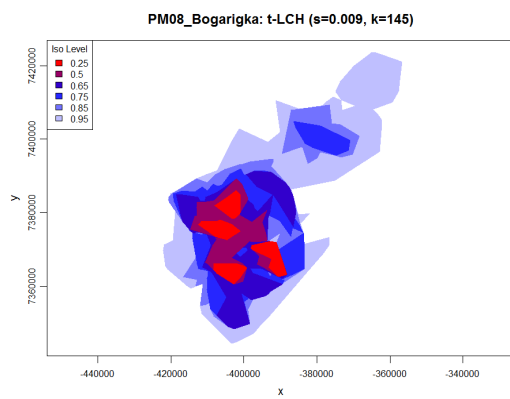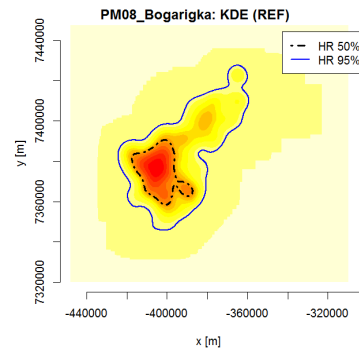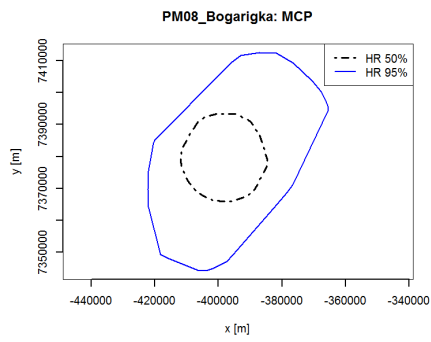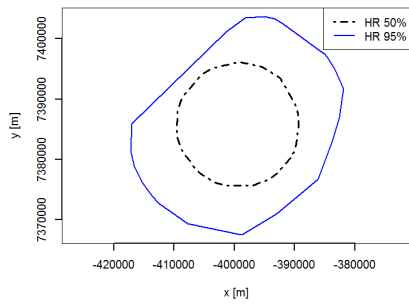
Gham

PM09_Gham: MCP

PM09_Gham: KDE (REF)
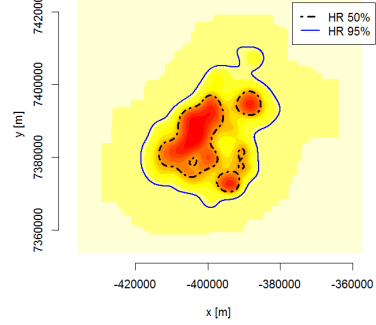
PM09_Gham: t-LCH (s=0.0012, k=135)
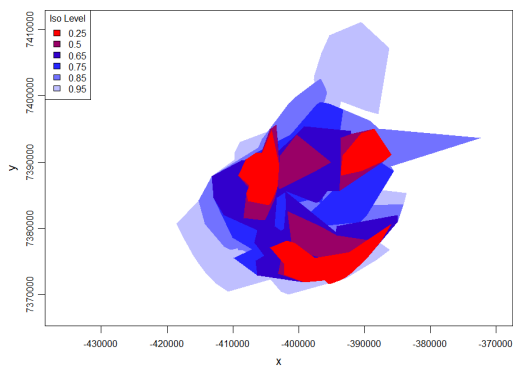
PM09_Gham: t-LCH (s=0.0012, k=170)
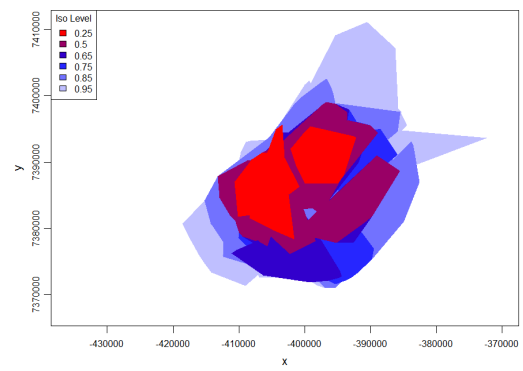
PM09_Gham: BRB (1.4*hmin)
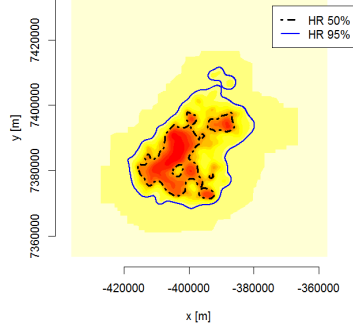
Verity
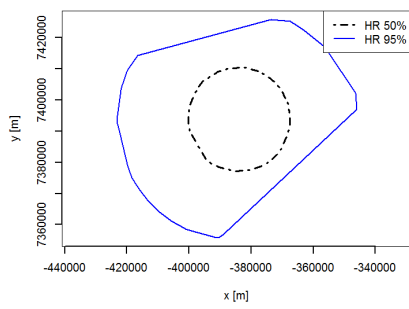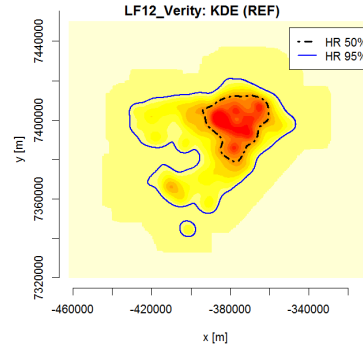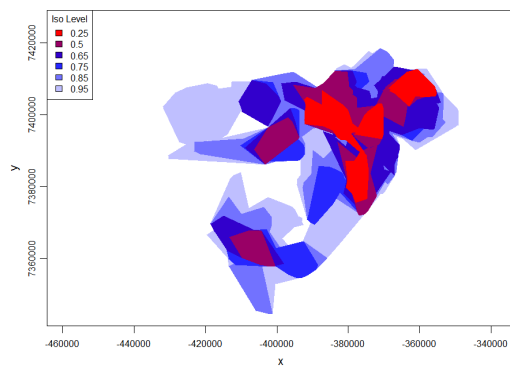
Ella

LF13_Ella: MCP

LF13_Ella: KDE (REF)

LF13_Ella: t-LCH (s=0.005, k=180)

LF13_Ella: t-LCH (s=0.005, k=280)

LF13_Ella: BRB (1.8*hmin)

Jane

Hitchcock

Mexico

Madge

Orange

LM08_Orange: MCP

LM08_Orange: KDE (REF)

LM08_Orange: t-LCH (s=0.01, k=90)

LM08_Orange: t-LCH (s=0.01, k=230)

LM08_Orange: BRB (1.4*hmin)
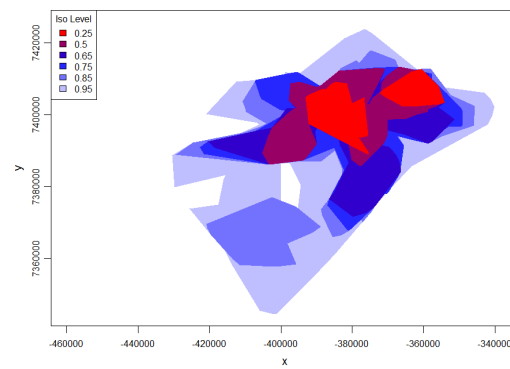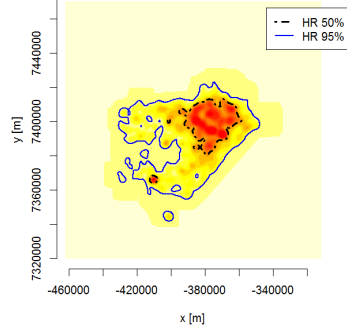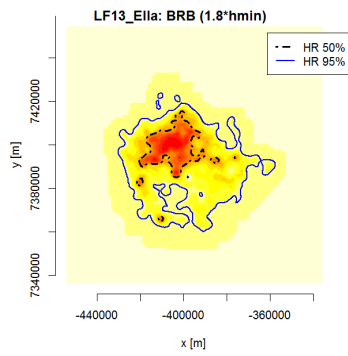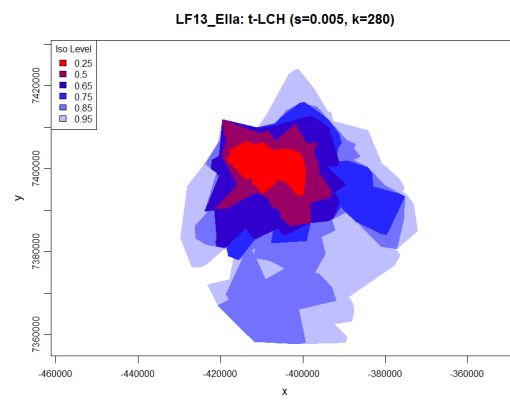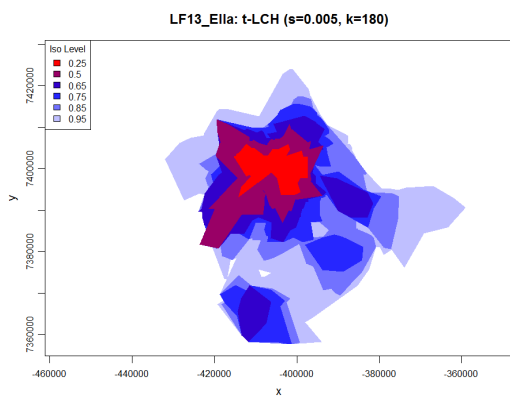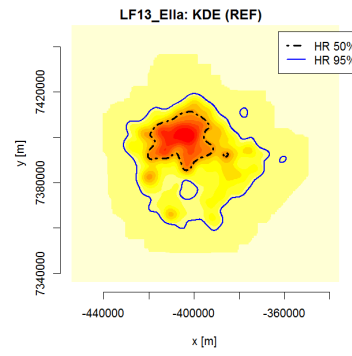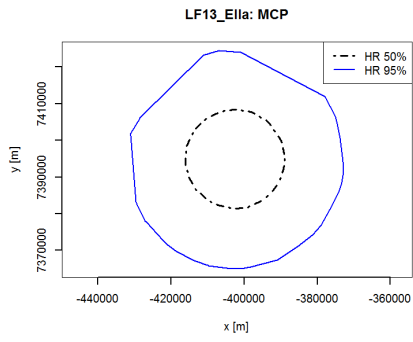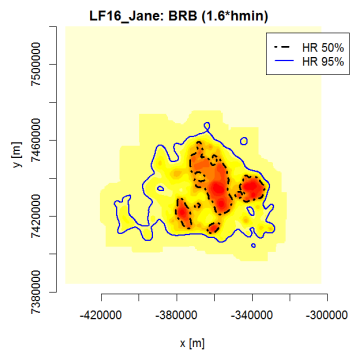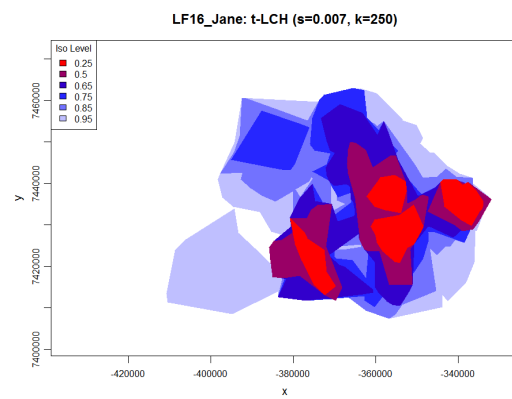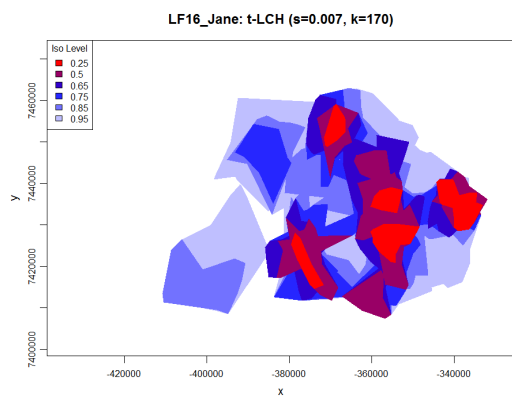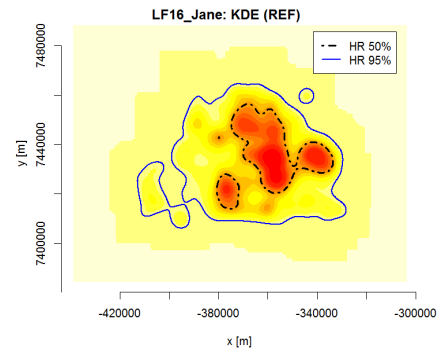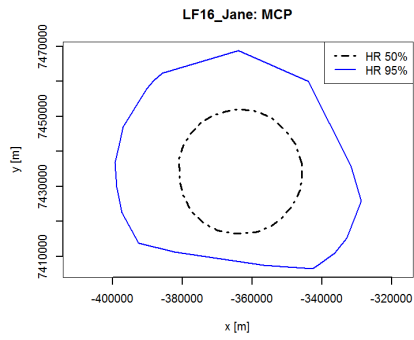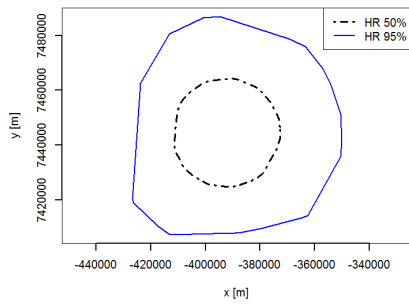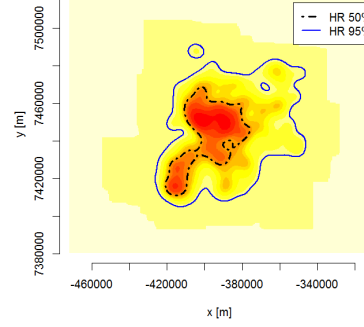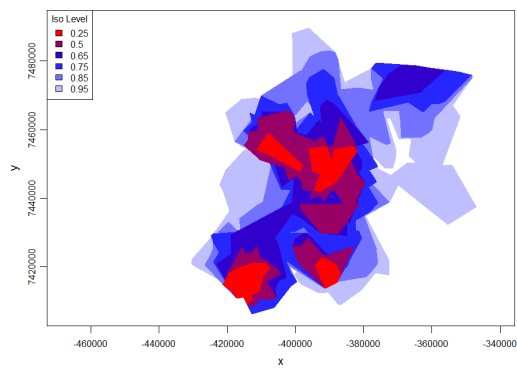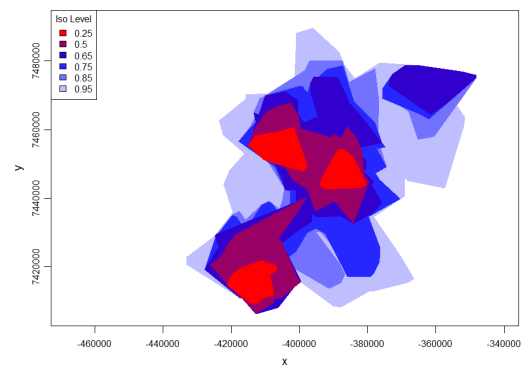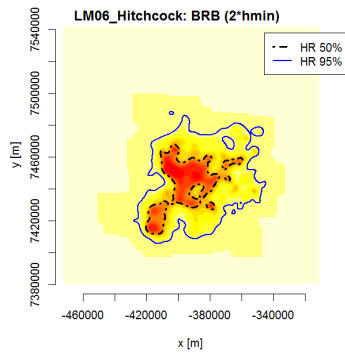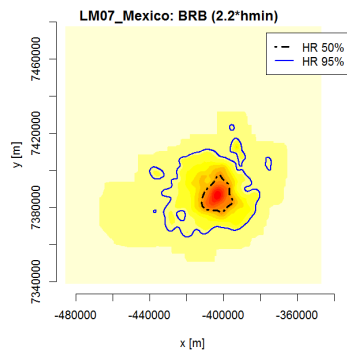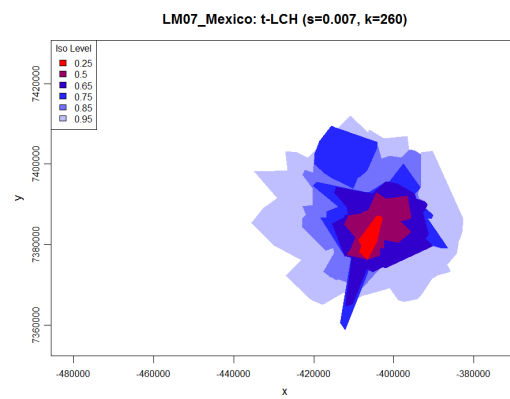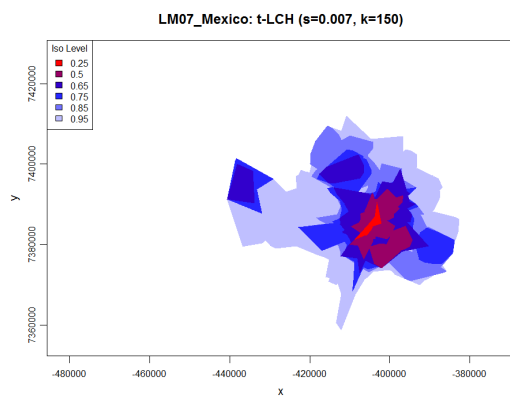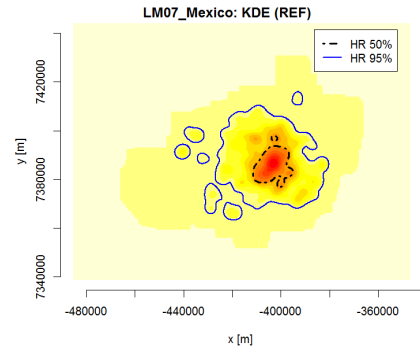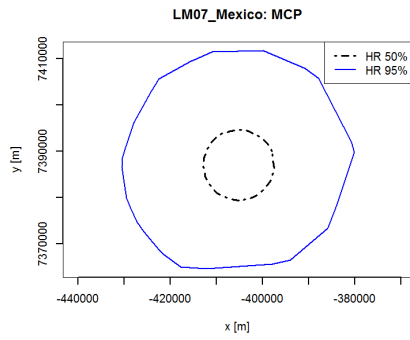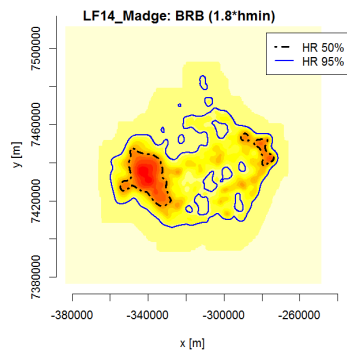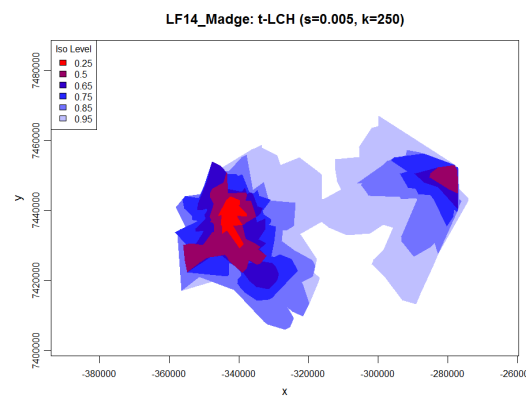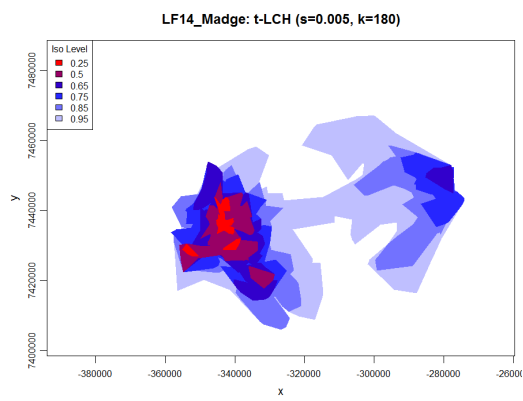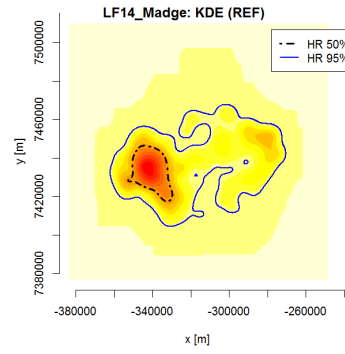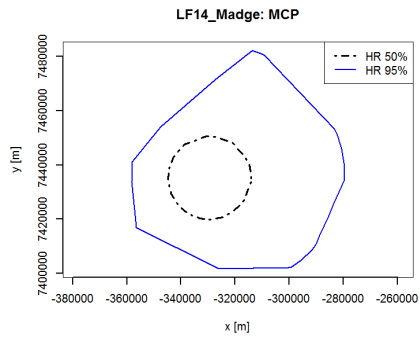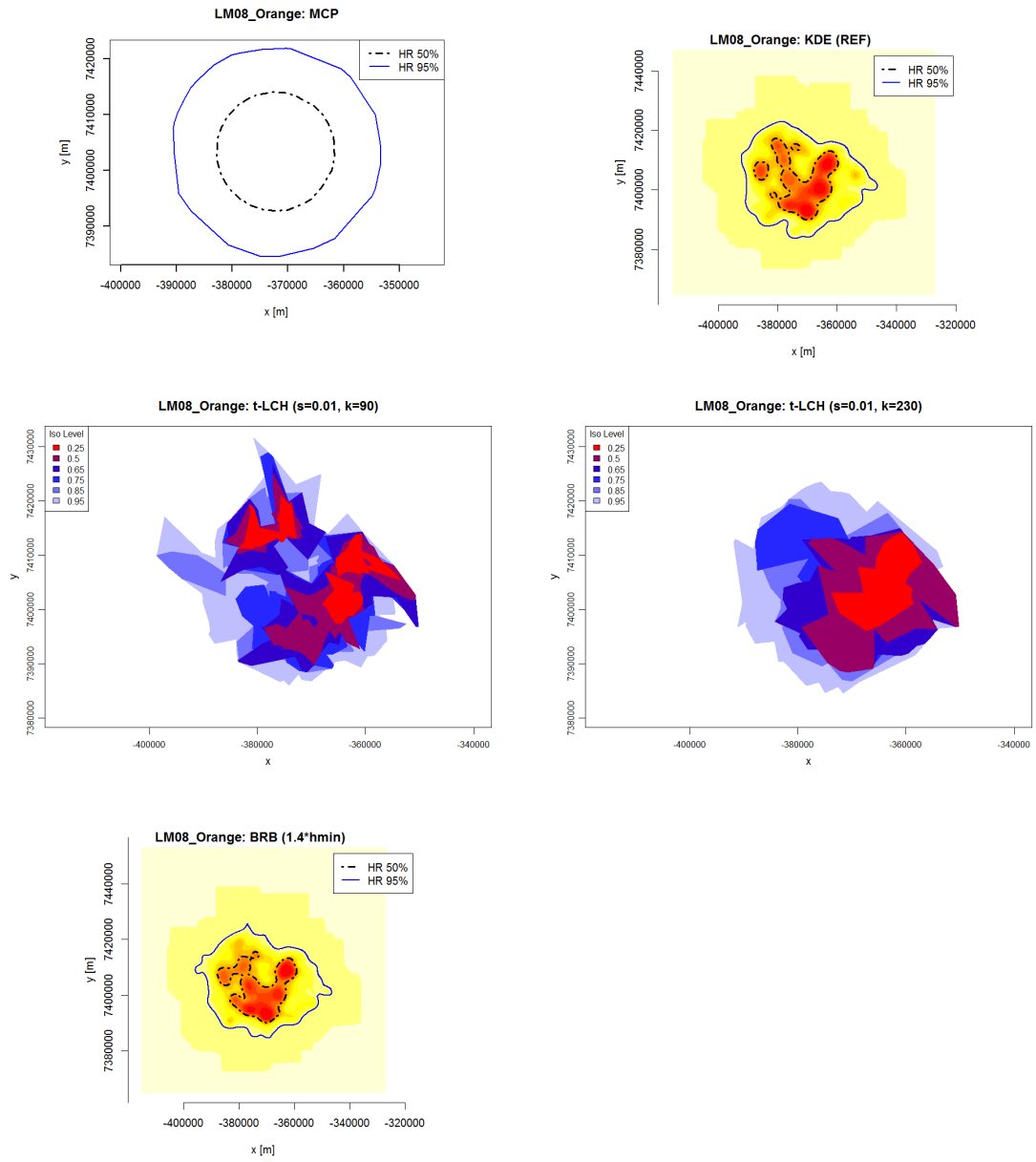
Getika
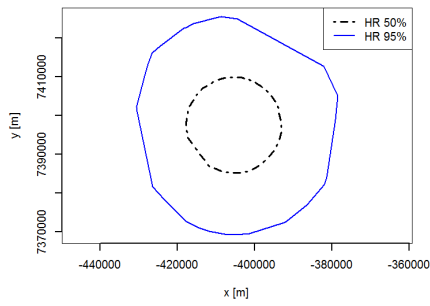
LF07_Getika: MCP

LF07_Getika: KDE (REF)
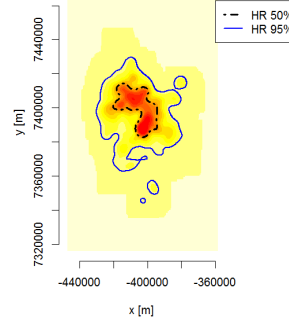
LF07_Getika: t-LCH (s=0.018, k=160)
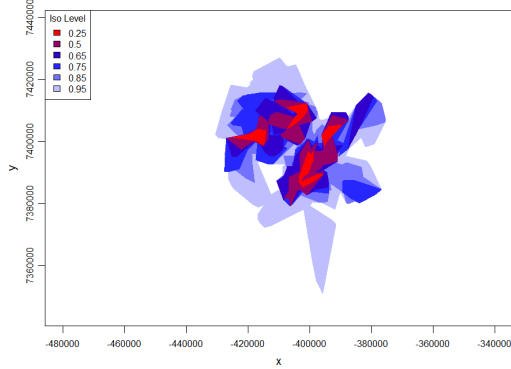
LF07_Getika: t-LCH (s=0.018, k=300)
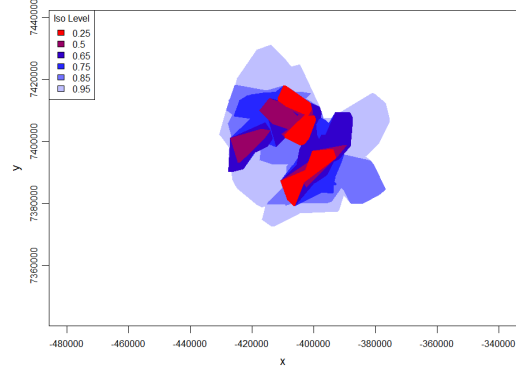
LF07_Getika: BRB (1.8*hmin)
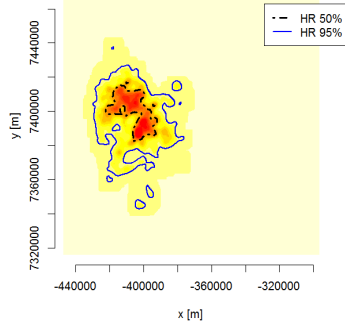
A.6   Temporal variation of all home ranges

The following plots show the temporal variation of the home ranges of all leopards and lions. The home range estimates are based on KDE and the reference bandwidth.

Ronja: Winter 2011–Winter 2014
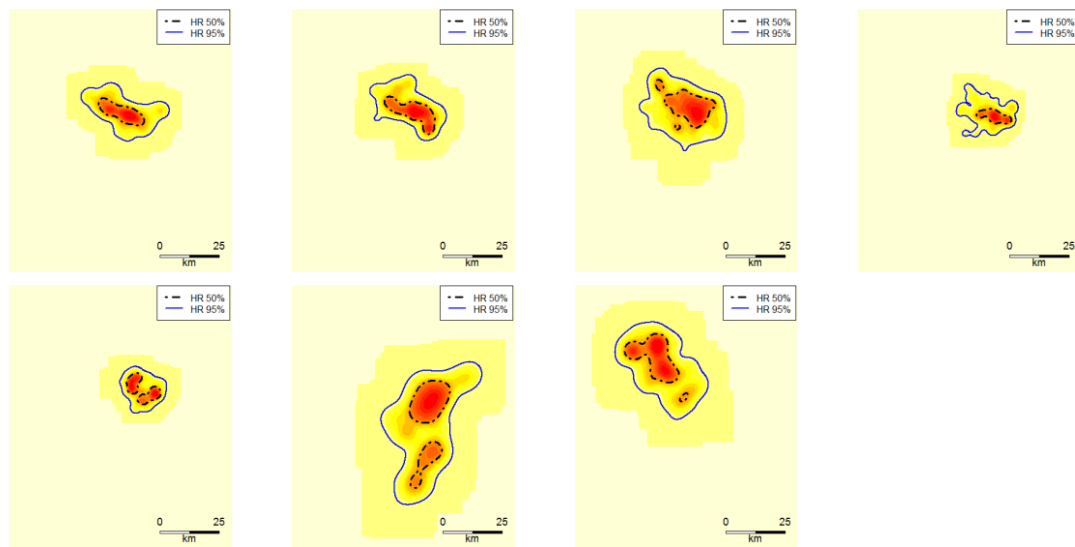
Mothamongwe: Winter 2011–Winter 2013
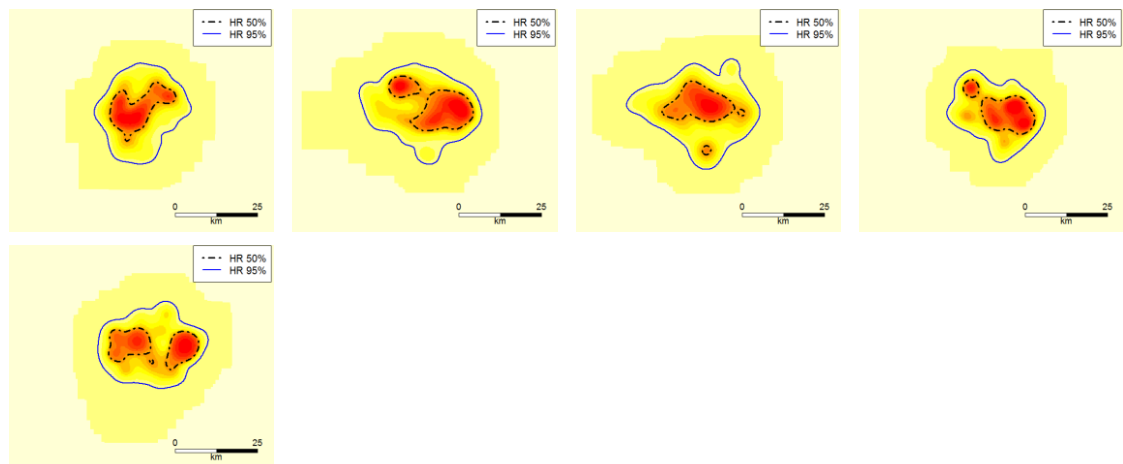
Bogarigka: Summer 2011–Summer 2012
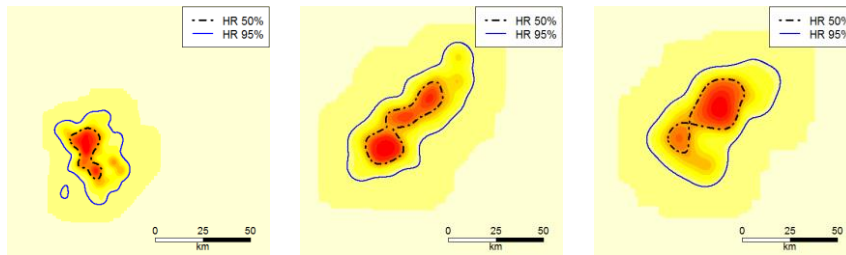
Gham: Winter 2012–Summer 2012
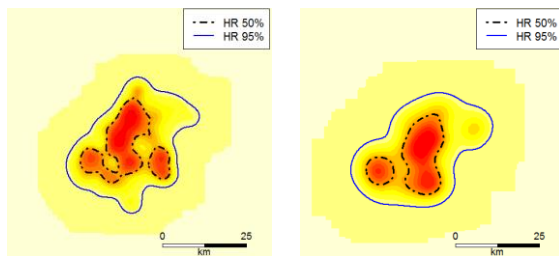
Verity: Summer 2011–Winter 2013
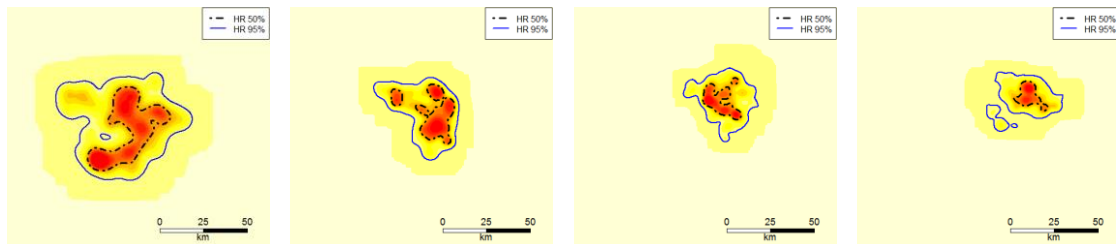
Ella: Summer 2011–Summer 2013
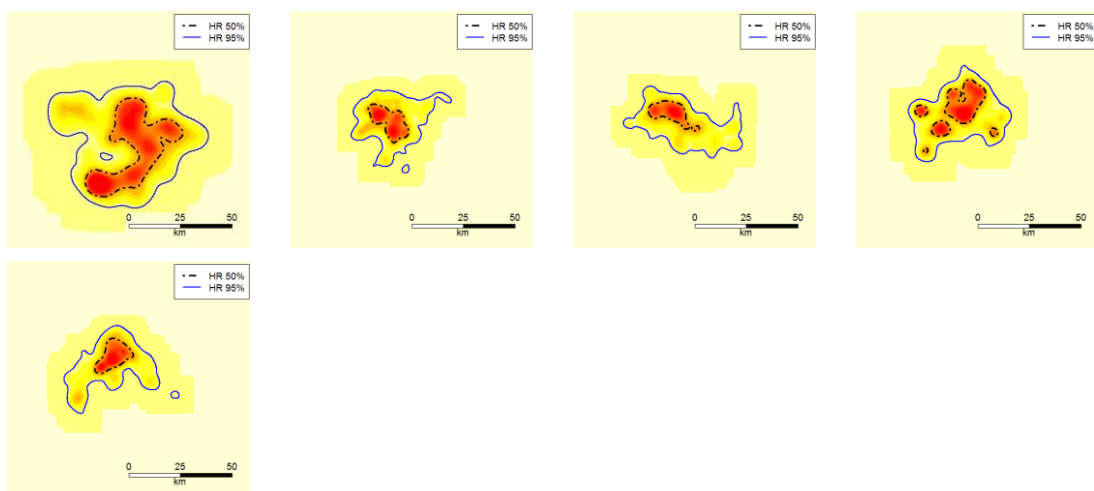
Jane: Summer 2012–Winter 2013
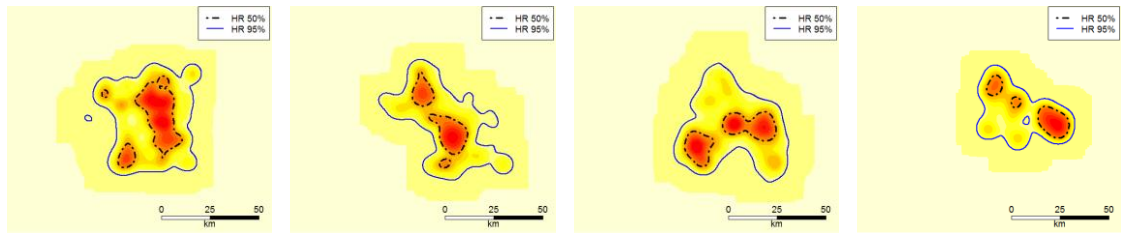
Hitchcock: Winter 2012–Summer 2013
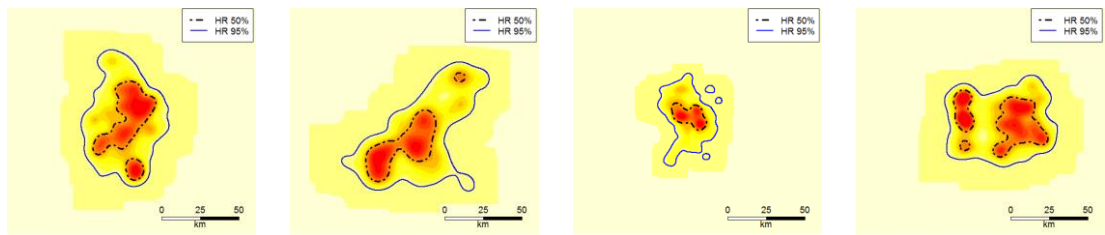
Mexico: Winter 2012–Summer 2013
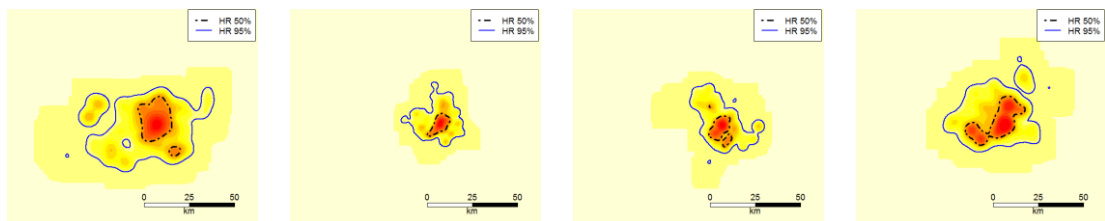
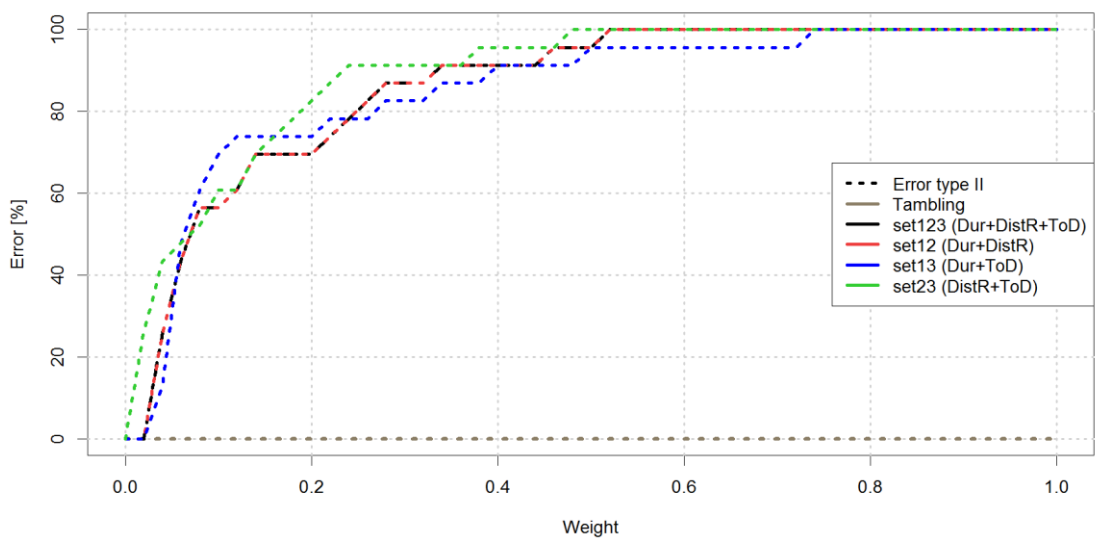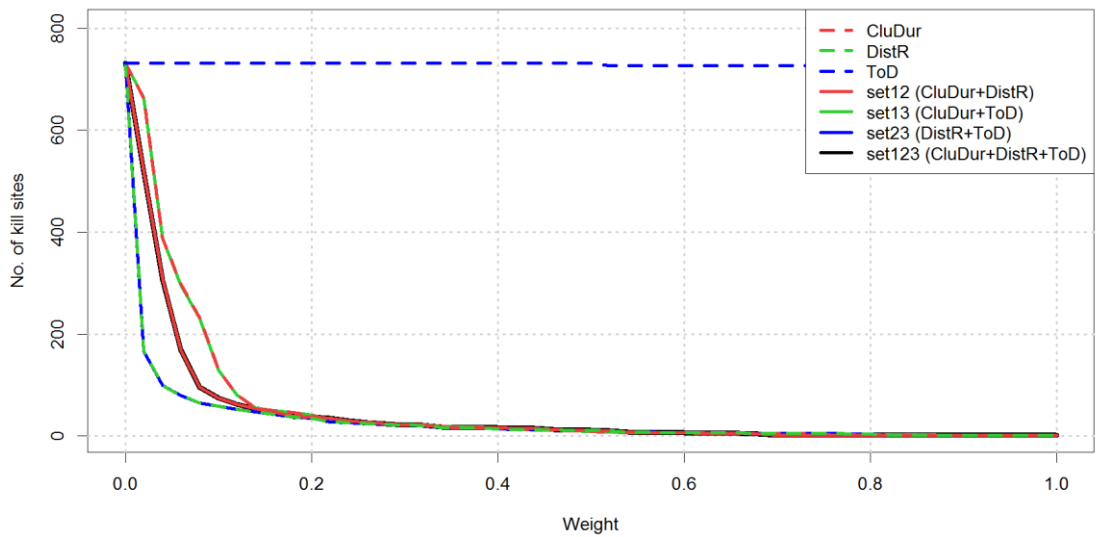**Madge: Summer 2012–Winter 2014**
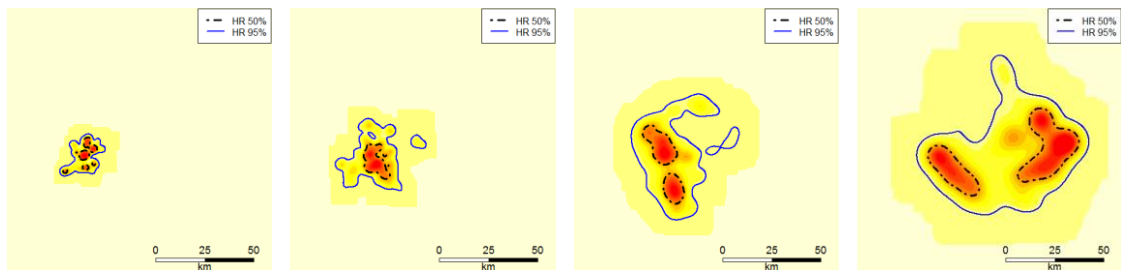
Orange: Summer 2012–Winter 2014
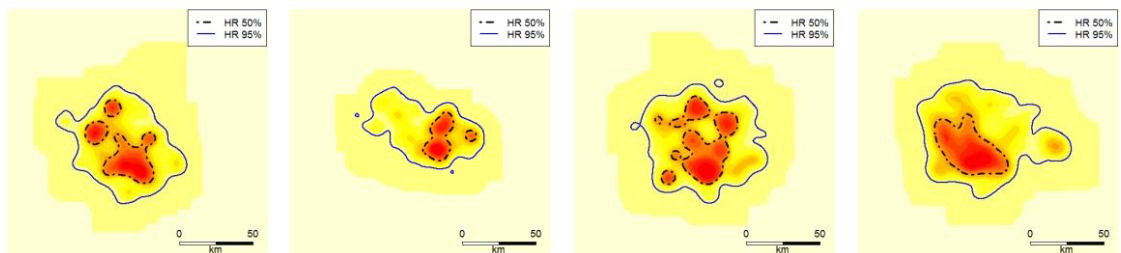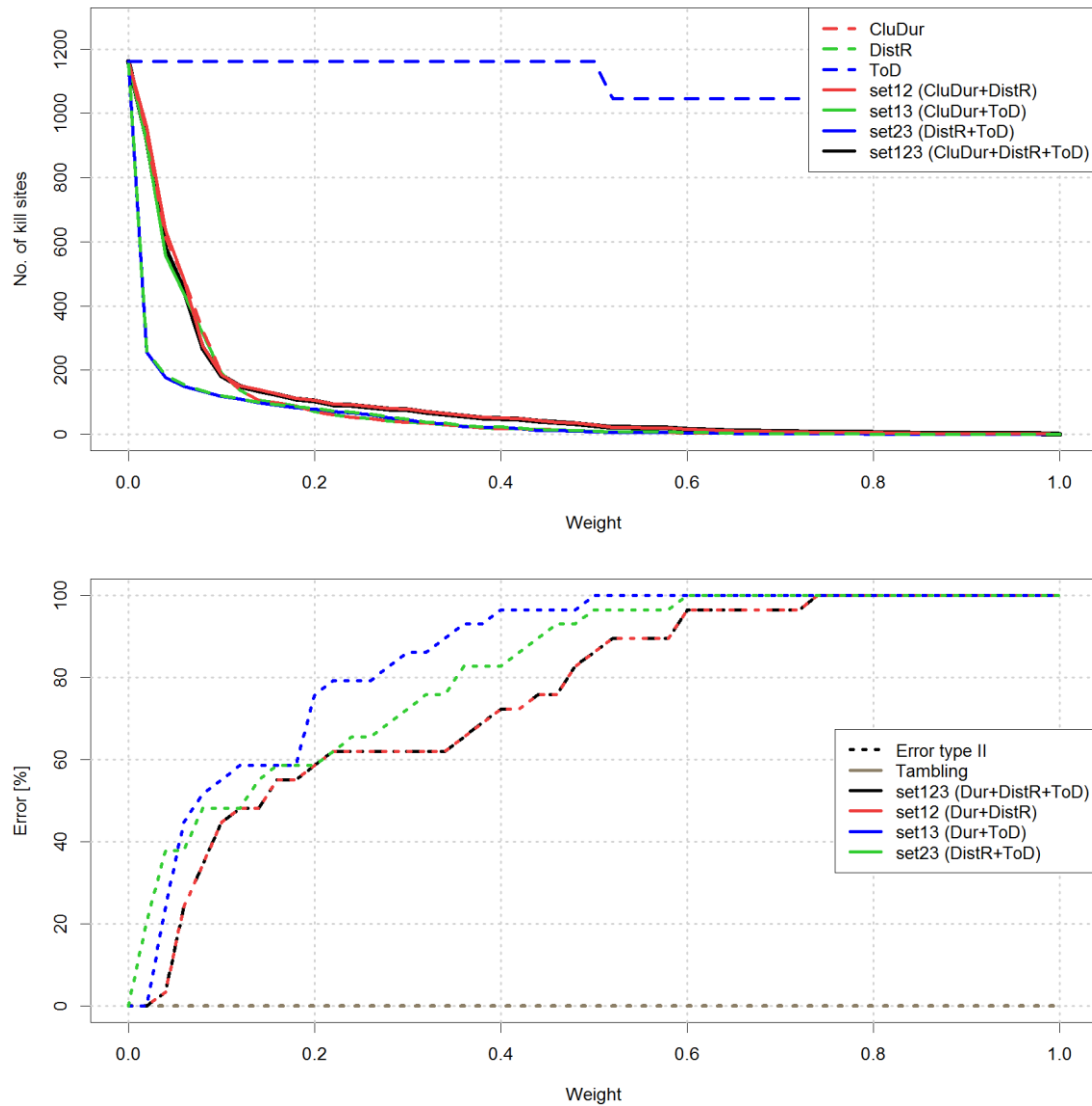
Getika: Winter 2011–Winter 2012
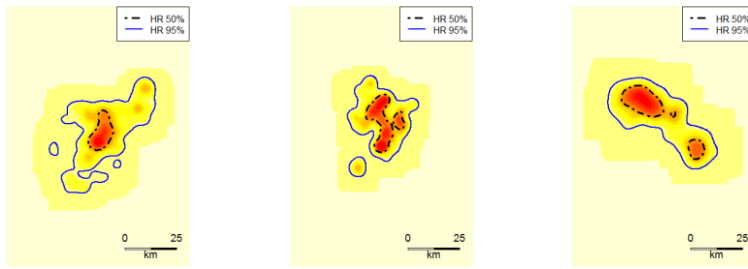
A.7   Effect of the clustering rule

The following plots show the results of the evaluation of the clustering rule (Section 13.1) for Verity and Ella.

Verity

Ella

A.8   Inclusion of activity data

It was investigated whether the inclusion of activity (accelerometer) data could improve the results of the set of variables that yielded the lowest errors in Section 13.1 (set_{12}). Accordingly, the weighting formula of set_{12} presented in Section 12.2.4 was extended to

norm ($Dur + DistR + Act$).

Act was defined as the mean of the 75 %, 85 % and 95 % quantiles of all activity values (in x- and y-direction) within the time span of the respective cluster.
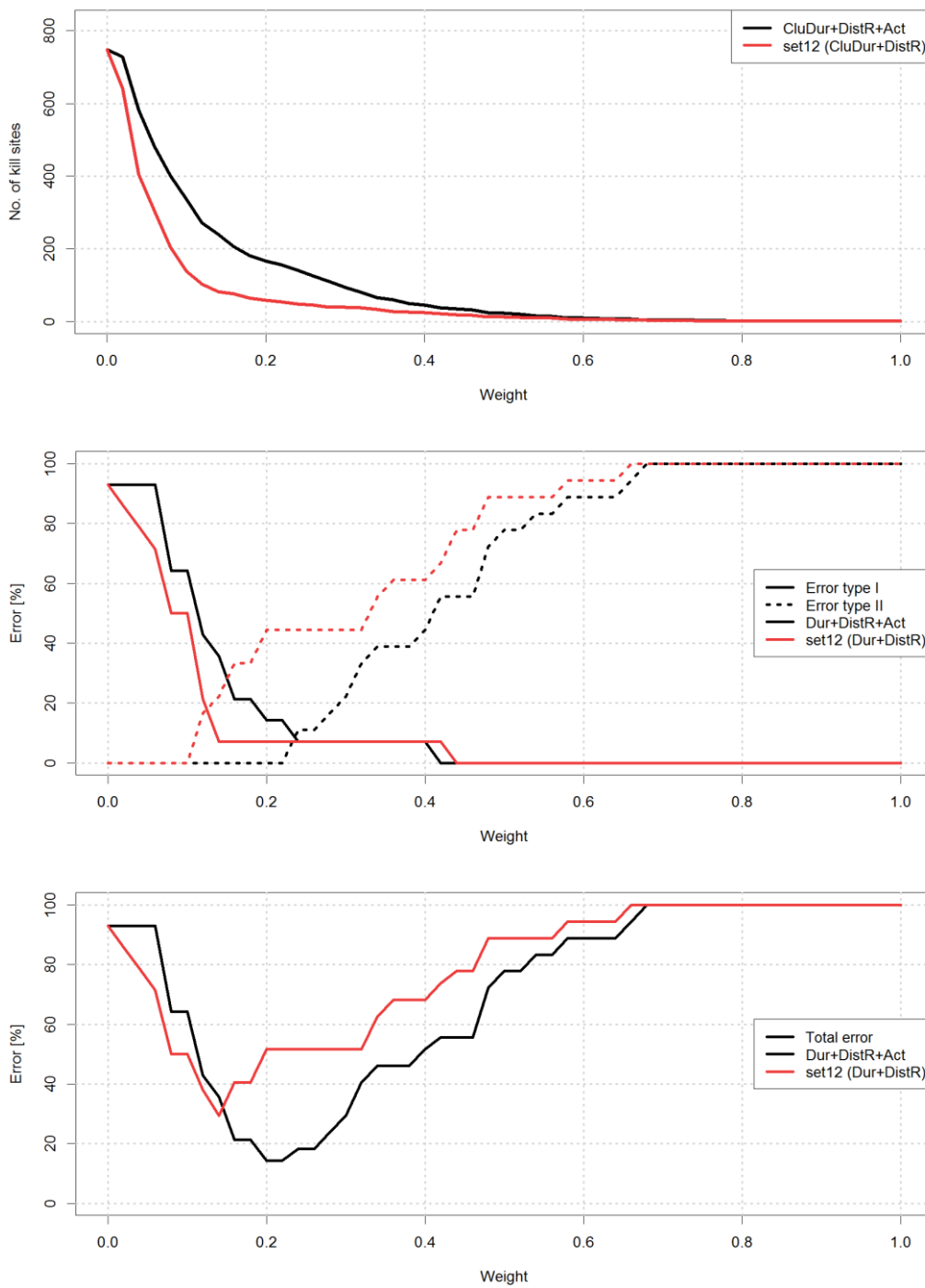
A.9 *R* Code

The code of the most important *R* scripts are provided digitally on the attached CD. Please note that the code was tailored to the author's working environment and expects certain folder directories, input files and *R* packages. It thus will not work on your computer without modifications. The purposes of the *R* scrips are briefly explained in a text document (on the CD).

Personal declaration

I hereby declare that the submitted thesis is the result of my own, independent work. All external sources are explicitly acknowledged in the thesis.

André Zehnder:

_____

Date:

_____